

---

Masters Theses

Student Theses and Dissertations

---

Spring 2011

## The effects select physical parameters have on an explosively formed projectile's performance

Phillip R. Mulligan

Missouri University of Science and Technology, pmulligan@mst.edu

Follow this and additional works at: [https://scholarsmine.mst.edu/masters\\_theses](https://scholarsmine.mst.edu/masters_theses)



Part of the [Explosives Engineering Commons](#)

Department:

---

### Recommended Citation

Mulligan, Phillip R., "The effects select physical parameters have on an explosively formed projectile's performance" (2011). *Masters Theses*. 6795.

[https://scholarsmine.mst.edu/masters\\_theses/6795](https://scholarsmine.mst.edu/masters_theses/6795)

This thesis is brought to you by Scholars' Mine, a service of the Missouri S&T Library and Learning Resources. This work is protected by U. S. Copyright Law. Unauthorized use including reproduction for redistribution requires the permission of the copyright holder. For more information, please contact [scholarsmine@mst.edu](mailto:scholarsmine@mst.edu).



THE EFFECTS SELECT PHYSICAL PARAMETERS HAVE ON AN EXPLOSIVELY  
FORMED PROJECTILE'S PERFORMANCE

By

PHILLIP RUSSELL MULLIGAN

A THESIS

Presented to the Faculty of the Graduate School of the  
MISSOURI UNIVERSITY OF SCIENCE AND TECHNOLOGY  
In Partial Fulfillment of the Requirements for the Degree  
MASTER OF SCIENCE IN EXPLOSIVES ENGINEERING

2011

Approved by  
Dr. Jason Baird, Advisor  
Dr. Paul Worsey  
Dr. Braden Lusk

© 2011

PHILLIP RUSSELL MULLIGAN

ALL RIGHTS RESERVED

## **ABSTRACT**

Identifying how changes in the physical parameters of an Explosively Formed Projectile (EFP) affect its performance is crucial in determining what physical parameters could be changed to achieve a desired performance. This research analyzes five of the physical parameters of an EFP, similar to an Iranian design (Worsey, 2009), and the effects on performance. The five physical parameters selected for this research were charge weight, confining geometry, flyer thickness, flyer curvature, and explosives-type. Eighteen different EFP designs were used to test the penetration, measured velocity, production of a dominant projectile, and kinetic energy of these five physical parameters. Of the physical parameters tested, the charge weight and flyer thickness affected the projectile's performance the most. The author's objective of this work is to use the research information contained herein to design an EFP capable of testing military armor to protect and save lives.

## ACKNOWLEDGMENTS

I would like to offer my sincerest gratitude to my advisor, Dr. Jason Baird, who has supported me throughout my thesis. I could not have completed this without his encouragement and patience. Professor Paul Worsley has been a consistent source of information and support. Without him, the testing and research could not have been completed. I would also like to thank DeWayne Phelps, Jimmie Taylor Sr, Jerry Plunkett, Erin Clark, Alex Hopkins, Drew Blair, Casey Slaughter, Darrell Williams, Buck Hawkins and David Phelps for their assistance during the various testing phases of this research. I would like to acknowledge Dr. Samuel Frimpong and the members of my graduate committee, for believing in my research and for being instrumental in adding the degree for Masters in Explosives Engineering.

Throughout the writing of this thesis, I have drawn on the knowledge and expertise of people who work in the explosives industry, as well as those who teach other students. Braden Lusk, Assistant Professor at the University of Kentucky, has been a mentor and friend throughout this process. His support has been invaluable.

I would also like to thank my family and friends for supporting and encouraging me in my pursuit of this degree. I would like to acknowledge Jerry Plunkett for his contributions to this research. Barb Robertson, Shirley Hall, and Judy Russell have been phenomenal in their assistance of this research.

## TABLE OF CONTENTS

	<b>Page</b>
ABSTRACT.....	iii
ACKNOWLEDGMENTS .....	iv
LIST OF ILLUSTRATIONS .....	ix
LIST OF TABLES.....	xiii
NOMENCLATURE .....	xiv
 SECTION:	
1. INTRODUCTION.....	1
2. LITERATURE REVIEW.....	5
2.1 DEFORMATION OF AN EXPLOSIVELY DRIVEN FLAT METALLIC FLYER DURING PROJECTION, (LIM, 2010).....	5
2.2 IED EFFECTS RESEARCH AT TNO DEFENSE SECURITY AND SAFETY, (VOORT, 2009). .....	7
2.3 EFP ORIGINAL’S DESIGN PROCESS, (BAIRD, 2008) .....	7
2.4 EXPERIMENTAL AND NUMERICAL STUDY ON THE FLIGHT AND PENETRATION PROPERTIES OF EXPLOSIVELY FORMED PROJECTILE, (WU, 2007).....	9
2.5 <i>EXPLOSIVELY FORMED PROJECTILES</i> , (DR. JAMES N. WILLSON; DR. DAVID E. LAMBERT, AND MR. JOEL B. STEWART, 2006).....	11
2.6 STUDY OF THE PENETRATION OF WATER BY AN EXPLOSIVELYFORMED PROJECTILE, (C. LAM; D. MCQUEEN, 1998).....	12
2.7 EXPLOSIVES EFFECTS AND APPLICATIONS, SECTION 10.2, CHRIS A.WEICKERT, 1998) .....	12

2.8	EXPLOSIVELY FORMED PENETRATOR RESEARCH, (HENRY S MCDEVITT, 1997) .....	13
2.9	AN INVESTIGATION INTO AN ALTERNATIVE FRAGMENT PROJECTOR FOR INSENSITIVE MUNITIONS QUALIFICATION, (C. LAM, T. LIERSCH AND D. MCQUEEN, 1997). .....	13
2.10	RESEARCH AND DEVELOPMENT IN THE AREA OF EXPLOSIVELY FORMED PROJECTILES CHARGE TECHNOLOGY, (WEIMANN, 1993).....	14
2.11	A COMPARISON OF THE CTH HYDRODYNAMICS CODE WITH EXPERIMENTAL DATA, (EUGENE S HERTEL, 1992). .....	17
2.12	<i>FUNDAMENTALS OF SHAPED CHARGES</i> , (W. P. WALTERS, J. A. ZUKAS, 1989). .....	17
3.	EFP DESIGN .....	19
3.1	CHARGE WEIGHT DESIGNS .....	23
3.2	CONFINING GEOMETRY DESIGNS .....	29
3.3	FLYER THICKNESS DESIGNS .....	35
3.4	FLYER RADIUS OF CURVATURE DESIGNS .....	38
3.5	EXPLOSIVE TYPE DESIGNS .....	43
4.	TESTING METHODS .....	46
4.1	PENETRATION TEST .....	49
4.2	VELOCITY TEST .....	54
4.3	DOMINANT PROJECTILE TEST .....	58
4.4	TEST SET-UP .....	62
5.	DATA ANALYSIS .....	68
5.1.	CHARGE WEIGHT .....	68
5.1.1.	Charge Weight Velocity.....	69



5.1.2. Charge Weight Dominant Projectile. ....	70
5.1.3. Charge Weight Kinetic Energy .....	74
5.1.4. Charge Weight Penetration. ....	76
5.1.5 Charge Weight Analysis. ....	77
5.2. CONFINING GEOMETRY .....	79
5.2.1. Confining Geometry Velocity. ....	79
5.2.2. Confining Geometry Dominant Projectile .....	81
5.2.3. Confining Geometry Kinetic Energy. ....	83
5.2.4. Confining Geometry Penetration.....	84
5.2.5 Confining Geometry Analysis. ....	85
5.3. FLYER THICKNESS.....	86
5.3.1. Flyer Thickness Velocity.....	86
5.3.2. Flyer Thickness Dominant Projectile. ....	87
5.3.3. Flyer Thickness Kinetic Energy. ....	89
5.3.4. Flyer Thickness Penetration. ....	89
5.3.5 Flyer Thickness Analysis.....	90
5.4. FLYER RADIUS OF CURVATURE .....	93
5.4.1. Flyer Radius of Curvature Velocity. ....	93
5.4.2. Flyer Radius of Curvature Dominant Projectile.....	94
5.4.3. Flyer Radius of Curvature Kinetic Energy.....	95
5.4.4. Flyer Radius of Curvature Penetration. ....	96
5.4.5 Flyer Radius of Curvature Analysis.....	97
5.5. EXPLOSIVE-TYPE .....	99

5.5.1. Explosive-Type Velocity.....	99
5.5.2 Explosive-Type Dominant Projectile.....	100
5.5.3. Explosive-Type Kinetic Energy. ....	103
5.5.4. Explosive-Type Penetration. ....	104
5.5.5 Explosive-Type Analysis.....	104
5.6 EFFECTIVE CHARGE WEIGHT ANALYSIS .....	104
6. CONCLUSIONS AND RECOMMENDATIONS.....	113
6.1 CHARGE WEIGHT.....	115
6.2 CONFINING GEOMETRY.....	116
6.3 FLYER THICKNESS .....	117
6.4 FLYER RADIUS OF CURVATURE.....	118
6.5 EXPLOSIVE-TYPE.....	118
6.6 OVERALL CONCLUSION.....	119
7. FUTURE WORK .....	121
APPENDIX .....	123
BIBLIOGRAPHY.....	142
VITA.....	144

## LIST OF ILLUSTRATIONS

	Page
Figure 1.1 Various EFP Designs (Fong, 2004).....	2
Figure 2.1 Lim's Drawing of Effective Charge Weight.....	6
Figure 2.2 Flyer Fully "Shocked" .....	9
Figure 2.3 Projectile Formation During Flight (Wu, 2007).....	10
Figure 2.4 Penetration of a 2.54 cm Steel Plate (Wu, 2007) .....	10
Figure 2.5 Projectile Modeled (Left) and Projectile Collected (Right) (Wu, 2007).....	10
Figure 2.6 Figure collected during Explosively Formed Projectiles (Dr. James N. Willson; Dr. David E. Lambert, and Mr. Joel B. Stewart, 2006) .....	11
Figure 2.7 EFP Design with Wave Shaper (Weimann, 1993) .....	15
Figure 2.8 Projectile Velocity (VP) and Projectile Formation at Different Charge Lengths (Weimann, 1993) .....	16
Figure 2.9 Projectile Produced with Star Shaped Base (Weimann, 1993). .....	17
Figure 2.10 Projectile Formation during Flight (W. P. Walters, J. A. Zukas, 1989).....	18
Figure 3.1 Original EFP Design.....	20
Figure 3.2 Various Charge Weight Designs .....	23
Figure 3.3 Penetration and Production of a Dominant Projectile .....	28
Figure 3.4 Basic EFP Detonation Wave Expansion .....	30
Figure 3.5 Components of the Confining Geometry Designs.....	31
Figure 3.6 Hypothetical Detonation Wave Expansion .....	32
Figure 3.7 0.318 cm Thick Flyer (Left) and 0.635 Thick Flyer (Right).....	35
Figure 3.8 Charge Weight to Flyer Weight Ratios .....	38

Figure 3.9 Flat Flyer Plate .....	40
Figure 4.1 Above Ground Testing Facility .....	47
Figure 4.2 Layout of the Underground Testing Facility .....	48
Figure 4.3 Target for Penetration Test .....	49
Figure 4.4 Depth Finder Configuration .....	50
Figure 4.5 Depth of Penetration .....	51
Figure 4.6 Impact Cluster .....	53
Figure 4.7 Scale/Reference Board (V-Screen).....	55
Figure 4.8 Open-Faced-Sandwich Gurney Equation Configuration.....	57
Figure 4.9 Dominant Projectile Collected During Testing .....	59
Figure 4.10 Picture from High Speed Video of a Dominant Projectile .....	60
Figure 4.11 Image from High Speed Video of a Non-Dominant Projectile .....	60
Figure 4.12 Dominant Impact Point (Left) and Impact Cluster (Right) .....	61
Figure 4.13 Suspended EFP. Noted are Suspension Wires (blue arrows) and Connection Points (yellow circles). .....	63
Figure 4.14 Above Ground Facility, Penetration and Velocity Tests Set-up .....	64
Figure 4.15 Initial Dominant Projectile Test Set-up.....	65
Figure 4.16 Second Stand Design for Dominant Projectile Test .....	66
Figure 5.1 Charge Weight Velocity Data .....	70
Figure 5.2 Projectile Weight for the Charge Weight Designs .....	72
Figure 5.3 Projectile Produced from EFP Delta .....	73
Figure 5.4 Projectiles Produced From the Alpha EFP Design.....	73
Figure 5.5 Kinetic Energy Data for Charge Weight Designs .....	75

Figure 5.6 Penetration Data for the Charge Weight Designs.....	76
Figure 5.7 Charge Weight Experiment Comparison of Velocity Data and Projectile Weight.....	78
Figure 5.8 Confining Geometry Velocity Data.....	80
Figure 5.9 Impact cluster of EFP Golf (Left) and Hotel (Right) .....	81
Figure 5.10 Impact point from India.....	82
Figure 5.11 High-speed Image of India's Projectile .....	82
Figure 5.12 Projectile Produced from India.....	83
Figure 5.13 Confining Geometry's Penetration Data.....	84
Figure 5.14 Blunt Tipped Projectile Produced from EFP Alpha (Left) and Pointed Tipped Projectile Produced from India (Right).....	85
Figure 5.15 Flyer Thickness Velocity Data .....	87
Figure 5.16 Flyer Thickness Impact Points: Juliet, Kilo, Lima .....	88
Figure 5.17 Lima's Projectile .....	88
Figure 5.18 Flyer Thickness Penetration Data.....	89
Figure 5.19 Kinetic Energy and Penetration Comparison of Alpha and Lima.....	91
Figure 5.20 Penetration and Velocity Comparison of Similar CW:FW Designs; Solid Color Connecting Lines Show Similar CW:FW Ratios .....	92
Figure 5.21 Impact Point of EFP Mike.....	94
Figure 5.22 EFP November's Impact Points.....	95
Figure 5.23 Flyer Radius of Curvature Penetration Data .....	96
Figure 5.24 Flyer Radius of Curvature's Velocity Data.....	97
Figure 5.25 Mike's Impact Point (Left) and Delta's Impact Point (Right).....	98
Figure 5.26 Explosive-Type Velocity Data .....	100

Figure 5.27 Explosive-Type High-Speed Video (Left) and Impact Point (Right) .....	101
Figure 5.28 Flyer Plate (Left), Projectile Produced from EFP Quebec (Middle and Right).....	101
Figure 5.29 Fragment of EFP Oscar's Projectile.....	102
Figure 5.30 Explosive-Type Kinetic Energy Data.....	103
Figure 5.31 Effective Charge Weight .....	106
Figure 5.32 Volume of ECW Volume used in Calculating ECW Angle.....	110

**LIST OF TABLES**

	Page
Table 3.1 Averaged Charge Weight Design Information .....	25
Table 3.2 Averaged Confining Geometry Design Information .....	33
Table 3.3 Averaged Flyer Thickness Design Information.....	36
Table 3.4 Averaged Flyer Curvature Design Information .....	41
Table 3.5 Averaged Unigel Design Information.....	44
Table 5.1 Dominant Projectile Data.....	71
Table 5.2 Effective Charge Weight Angle for Each EFP Design.....	111
Table 6.1 Data Summary .....	114

## NOMENCLATURE

<b>Symbol</b>	<b>Description</b>
<b><math>\Theta</math></b>	Effective charge weight angle in degrees
<b>2R</b>	Liner diameter (2 * Radius)
<b><math>\pi</math></b>	3.14159
<b>°</b>	Degrees
<b>%</b>	Percent
<b>a</b>	Quadratic equation value
<b>b</b>	Quadratic equation value
<b>c</b>	Quadratic equation value
<b>C</b>	Charge Weight (grams)
<b>C-4</b>	Composition 4: 94% RDX, 6% Plasticizer
<b>CD</b>	Charge Diameter
<b>CL</b>	Charge Length
<b>cm</b>	Centimeter
<b>CSC</b>	Conical Shaped Charge
<b>CW</b>	Charge weight
<b>D</b>	Detonation velocity
<b>DOE</b>	Design of experiments
<b>E</b>	Specific explosive kinetic energy or Gurney energy of an explosive at Theoretical Maximum Density
<b>ECW</b>	Effective Charge Weight



<b>EFP</b>	Explosively Formed Projectile
<b>fps</b>	Frames per second
<b>EOD</b>	Explosives Ordinance Disposal
<b>ft</b>	Feet
<b>FW</b>	Flyer weight
<b>g</b>	Grams
<b>h</b>	Maximum height for effective charge weight
<b>HH</b>	Head Height
<b>IEDs</b>	Improvised Explosive Devices
<b>Kbar</b>	Kilobar
<b>KE</b>	Kinetic Energy
<b>km</b>	Kilometer
<b>kg</b>	Kilogram
<b>lb</b>	Pound
<b>lbs</b>	Pounds
<b>M</b>	Initial Mass of the Flyer (grams)
<b>Missouri S&amp;T</b>	Missouri University of Science and Technology
<b>mm</b>	Millimeter
<b>μsec</b>	Microsecond
<b>oz</b>	Ounce
<b>PETN</b>	Pentaerythritol Tetranitrate
<b>psi</b>	Pounds per square inch
<b>PVC</b>	Polyvinyl chloride

<b>R</b>	Radius of flyer
<b>r</b>	Radius of the top of a cone
<b>sec</b>	Seconds
<b>Tan</b>	Tangent
<b>TMD</b>	Theoretical maximum density
<b>TNT</b>	Trinitrotoluene
<b>unk</b>	Unknown
<b>V</b>	Velocity
<b>v</b>	Volume
<b>V-screen</b>	Velocity Screen

## 1. INTRODUCTION

The objective of this research is to identify how changes in select physical parameters affect and contribute to the overall performance of an Explosively Formed Projectile (EFP). This research identifies how changing specific physical parameters within an EFP's design can provide for more efficient, armor-testing devices. It is not the intent of this author to design better weapons or improve current weapons to be used in an offensive role.

Experimental testing was conducted at the Explosive Engineering Research Facilities at the Missouri University of Science and Technology (Missouri S&T). This facility consists of an explosive laboratory, an underground testing facility capable of handling a detonation equivalent to 7.7 kg (17 lbs) of C-4, and an above ground testing facility with an unconfined limit equivalent to 900g (2 lbs) of C-4. The explosive testing limits at Missouri S&T define the upper limit to the design and testing methods used in this research.

EFPs have been studied at Missouri S&T since the late 1980's (Worsey, 2009). The depth and areas of research, in EFPs, have varied over the years. This author was involved in such a research project from May 2008 to February 2009. In this research, an EFP design (Original) was constructed, based on the available material and recommended methods from military specialists, to test armor that is designed to resist projectile penetration (Baird, 2008). The resulting EFP design resembled an Iranian EFP (Worsey, 2009). This design is later referred to as EFP Original and the Original EFP design. This EFP design met the needs of this project. However, it was noted that the performance

varied depending on its detonator depth (cap depth). These variances led to a need to identify how changing the physical parameters of an EFP design affected its performance.

EFPs are effective devices for penetrating a target and creating significant destruction over a large range of distances. EFPs are a Misznay-Schardin device (Baird, 2008) that functions in a similar manner to a conical-shaped charge (CSC). Figure 1.1 shows a simple EFP of various sizes.



**Figure 1.1 Various EFP Designs (Fong, 2004)**

In a CSC, the detonation wave inverts the liner to form its projectile, which consists of a fluid metal jet intended for short-distance penetration. However, the geometry of an EFP is different from a CSC and the result is a slug-like projectile. This projectile has a slower velocity than a CSC jet and is not able to penetrate a target as well as a CSC. However, it is able to travel over long distances accurately (Henry S.

McDevitt, 1997), and still provide a devastating impact, where as a CSC has a maximum standoff of a few centimeters (cm) to work efficiently. The projectile from an EFP can penetrate armor, produce craters, and weaken structures. The design of an EFP is determined by its physical parameters, and thus a desired performance change can be achieved by changing these parameters.

There are currently many EFP designs. The basic concept for each is the same, in that the detonation wave inverts a flyer plate into a solid projectile. However, the overall design and performance differs. Some EFP designs are rather complicated, capable of spinning the projectile and producing fins on the projectile. Others use devices inside the EFP known as “wave shapers,” where a device placed into the explosive, manipulates the detonation wave, thereby causing a projectile not obtainable with cylindrical charge. The simplest and least efficient of these designs is the Original design used in this research (Baird, 2008).

The Original design consists of a cylindrical charge initiated at one end and a concave flyer plate placed at the opposite the end of the charge from the initiation point. Its physical parameters include the type of explosive used, confinement thickness, confinement strength, explosive shape/confining geometry, thickness of the flyer, diameter of the flyer, diameter of the EFP, charge length, flyer’s radius of curvature, flyer material, cap depth, and poundage of explosives used (charge weight) (Chris A. Weickert, 1998). Throughout this research the type of explosive used, confining geometry, thickness of flyer, flyer’s radius of curvature and the charge weights were the physical parameters varied to analyze their affects on performance. The designs for each physical parameter are in Section 3.

There is currently little information available on the affects each physical parameter of an EFP have on an EFP's performance. The objective of this research is to identify how changes in the selected physical parameters affect and contribute to the overall performance of an EFP. This research could lead to a matrix of techniques, enabling a researcher to choose a desired projectile performance need and identify what physical parameters produce the desired results. In addition, this provides an understanding of how changes in the physical parameters of an EFP allows for a design that utilizes each of its physical parameters to achieve a higher performance. This understanding allows Missouri S&T to produce future EFP designs suitable for a wide range of performance needs if required to test armor concepts. In Section 2, the literature review, the physical parameters of an EFP, the projectiles penetration, velocity, shape, kinetic energy and methods used to obtain performance data are identified and discussed.

## **2. LITERATURE REVIEW**

This research tests physical parameters of an EFP and how changing those physical parameters affect an EFP's performance. The following literature was found by searching for "EFPs" and "Explosively Formed Projectiles" through Missouri S&T's library, an internet search, and the International Society of Explosives Engineers' databases. This literature assists in determining what physical parameters are important in an EFP, the performance standards for each EFP design, and the methods used to test an EFP's performance. The EFP literature also identifies the performance parameters that contribute to penetration and assist in establishing a baseline penetration. The discussion of the list of these documents by publication date, from the most current to the oldest follows:

### **2.1 DEFORMATION OF AN EXPLOSIVELY DRIVEN FLAT METALLIC FLYER DURING PROJECTION, (LIM, 2010)**

This research studies the effects effective charge weight has on explosively driven flat metallic flyers. Lim analyzed how the effective charge weight angles of 60° and 40° affect an explosively driven flat metallic flyer. The effective charge weight (ECW) is the amount of explosives that pushes a projectile. The ECW is shown in Figure 2.1.

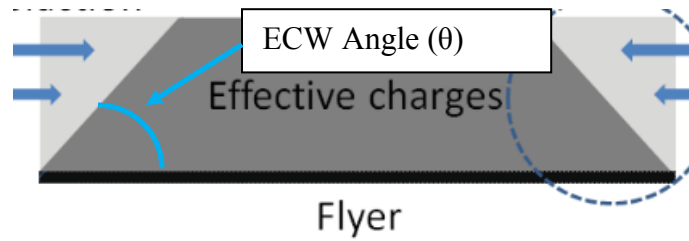


**Figure 2.1 Lim's Drawing of Effective Charge Weight**

The computer models indicate that the ECW angle affects how the rarefaction wave interacts with the explosives by pushing the edges of the 5.0 cm wide by 5.0 cm long, 0.125 cm thick copper flyer plate, faster than the rest of the copper, causing a “U” shaped projectile. Dr. Lim compared the data obtained to the effects predicted by the Open-Faced-Sandwich Gurney equation and made the following modification:

$$V = \sqrt{2E} \left[ \frac{\left( \left( 1 + \frac{2M}{x \tan \theta} \right)^3 + 1 \right)}{6 \left( 1 + \left( \frac{M}{x \tan \theta} \right) \right)} + \frac{M}{x \tan \theta} \right]^{-0.5} \quad \{2.1\}$$

Dr. Lim’s research indicates that the Open-Faced-Sandwich Gurney equation is a good starting place for estimating the velocity of an explosively driven flat metallic flyer. However, the thesis EFP research reported herein uses the Open-Faced-Sandwich Gurney equation to estimate the velocity of a curved metallic flyer, an application for which this Gurney equation was not designed for.



## **2.2 IED EFFECTS RESEARCH AT TNO DEFENSE SECURITY AND SAFETY, (VOORT, 2009)**

In this research, the author examines the physical effects of three common improvised explosive devices (IEDs). One of the IEDs examined is an EFP. The author examines the shape and velocity of the projectile from the designed EFPs. The physical parameters for the three EFP designs are not given. However, the paper does state that one design was hand packed and one made with cast explosives. The author tested the designs for shape formation process, velocity, flight behavior of the projectile, final shape of the projectile, and mass of the projectile. The research states that the desired projectile shape is “cigar shaped.” Voort used flash X-ray to study the projectile formation, flight behavior, and velocity. Firing the projectiles through a PVC pipe filled with sawdust into a pipe filled with water allowed the projectiles to be collected without deformation. This is a method of “soft catching” the projectile. The author concluded that the cast explosive EFP design did not significantly improve the EFP performance over the hand packed EFPs.

The conclusion drawn in Voort’s research supports the decision to hand pack the C-4 in EFPs for this thesis research, rather than using a press to ensure uniform densities.

## **2.3 EFP ORIGINAL’S DESIGN PROCESS, (BAIRD, 2008)**

As no off-the-shelf EFP warheads were available to the University, Dr. Jason Baird’s design, originally created for a contract requiring armor testing, was used as the baseline EFP for this research. The design by Dr. Baird uses several recommended “rules of thumb” (see below), gleaned from several informal source. (Baird, 2008).

Rules of Thumb:

- $2R/CD < 1$
- $HH = 1$  to  $1.5CD$
- $CL/CD = 1.3$  to  $1.8$

Dr. Baird selected an available, inexpensive, 10.16 cm PVC sewer pipe with an inner diameter of 10.64 cm as the casing for EFP Original. This provides a charge diameter of 10.64 cm. The selected flyer diameter was 9.525 cm. The availability of reasonably priced copper sheet less than 10.64 cm wide, contributed to the selection of this flyer diameter. The charge diameter and flyer diameter (2R) selected gives a  $2R/CD = 0.9375$ . The charge diameter and flyer diameter remained constant throughout this research. The head height range was CD (10.16 cm) to 1.5 CD. Dr. Baird adjusted the head height to 8.890 cm. This allows the flyer to be fully “shocked” before any deformation occurs. A fully shocked flyer is one that has been affected by the shock wave prior to its full formation propulsion. See Figure 2.2. Dr. Baird used the detonation velocity of C-4 to calculate the shock velocity through the explosive, assumed the shock was not overdriven, and used the acoustic velocity of copper to calculate the shock velocity through the copper flyer. The estimated shock velocity, through the copper flyer plates based on RDX, is 4.74 mm/ $\mu$ sec (Baird, 2009)

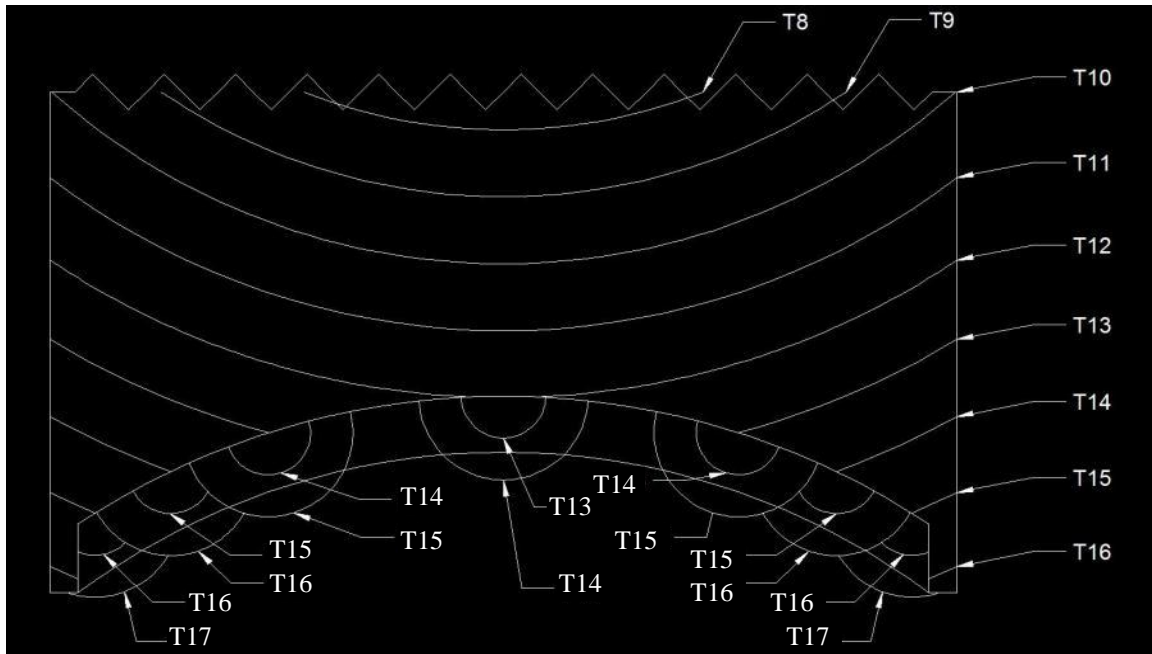


**Figure 2.2 Flyer Fully "Shocked"**

Each "T" in Figure 2.2 is a one-microsecond step in time for the shock wave traveling through the explosive and flyer plate. The total volume the flyer occupies within the cylinder was calculated and subtracted from the overall volume of the cylinder. The resulting volume, multiplied by  $1.58 \text{ g/cm}^3$ , the TMD of C-4 (W. P. Walters, J. A. Zukas, 1989), resulted in a charge weight of 1,389g (3 lbs 1 oz).

#### **2.4 EXPERIMENTAL AND NUMERICAL STUDY ON THE FLIGHT AND PENETRATION PROPERTIES OF *EXPLOSIVELY FORMED PROJECTILE*, (WU, 2007)**

This research studies the penetration capabilities of a 5.0 cm diameter EFP packed with Dynamite, into a 2.54 cm thick steel plate and shot from a distance of 48 meters.

The recorded velocity is 1.56 km/sec. The following Figure 2.3 is a picture taken from a computer model of the projectile formation over time and the air movement around the projectile during flight. The projectile penetrated all the way through the 2.54 cm thick target at 48 meters, Figure 2.4. Figure 2.5 shows the projectile Wu collected.

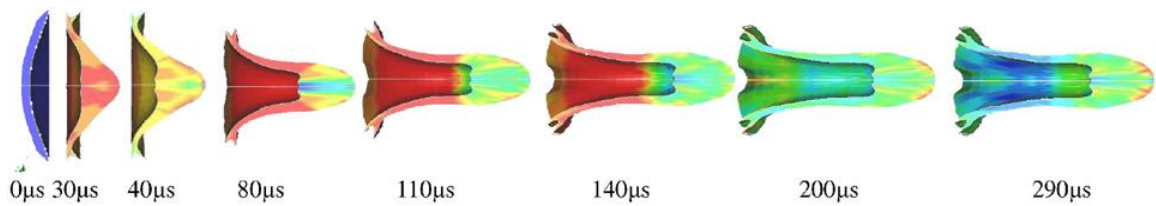


**Figure 2.3 Projectile Formation During Flight (Wu, 2007)**



**Figure 2.4 Penetration of a 2.54 cm Steel Plate (Wu, 2007)**

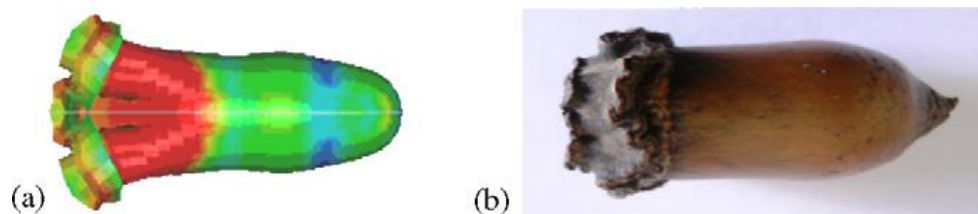


**Figure 2.5 Projectile Modeled (Left) and Projectile Collected (Right) (Wu, 2007)**

## **2.5 EXPLOSIVELY FORMED PROJECTILES, (DR. JAMES N. WILLSON; DR. DAVID E. LAMBERT, AND MR. JOEL B. STEWART, 2006)**

In this research, the authors designed an EFP by using computer modeling and empirical data to identify head height, liner thickness, profile of the top of liner surface, and profile of the bottom of the liner surface. A 500g projectile weight traveling at 1.45 km/sec achieved one mega-joule of kinetic energy. The authors constructed a soft catch device consisting of four sections: a 3.66 meter tube with polystyrene, a 2.43 meter tube with vermiculite, 2.43 meter tube of water, and 3.35 meter tube with sand. Using this method, projectiles were successfully collected with minimal deformation as illustrated in Figure 2.6.



**Figure 2.6 Figure collected during Explosively Formed Projectiles (Dr. James N. Willson; Dr. David E. Lambert, and Mr. Joel B. Stewart, 2006)**

## **2.6 STUDY OF THE PENETRATION OF WATER BY AN EXPLOSIVELY FORMED PROJECTILE, (C. LAM; D. MCQUEEN, 1998)**

In this research, the authors studied an EFP's ability to penetrate water for sea-mine neutralization operations. The authors designed two EFPs. The first had a charge diameter of 6 cm, steel confinement, a copper liner of uniform thickness, and a head height of half the charge diameter. The second design was the same except the head height was one-third the charge diameter, and the flyer thickness was not uniform. The center of the flyer plate was thicker than the edges. C-4 is the explosive used for both designs. The first EFP produces an elongated projectile shape with a velocity of 2 km/sec. The second design produces a "dumpling-like" projectile that had a velocity of 1.5 km/sec. Both designs do not maintain their velocity for more than 2-3 times the charge diameter. After the projectiles penetrated 2-3 times the charge diameter, the projectiles broke apart and lost velocity. The authors concluded that EFPs could not be used for sea-mine neutralization operations and no recommendations were given to improve the EFPs' performance.

## **2.7 EXPLOSIVES EFFECTS AND APPLICATIONS, SECTION 10.2, (CHRIS A. WEICKERT, 1998)**

The uses of an EFP's physical parameters in creating a projectile formation are discussed in Section 10.2 of this book. Computer generated models of forward, backward, and "W" folding projectiles with various outer diameter to inner diameter ratios (confinement thickness), confinement geometry, flyer thicknesses, and flyer material are compared to empirical data. The flyer shape and material was altered during the course of the experiments generating various projectiles with elongated shapes and

velocities ranging from 0.848 km/sec to 1.618 km/sec. An emphasis is made on the importance of computer modeling to generate an initial design based on performance, followed by empirical data gathering, and subsequent modification of the computer model to fit the empirical data prior to testing.

## **2.8 EXPLOSIVELY FORMED PENETRATOR RESEARCH, (HENRY S. MCDEVITT, 1997)**

In this research, an EFP was constructed and tested to weaken and destroy structures. The researcher designed two EFPs – one with a 45.72 cm (18 inch) diameter and one with a 55.88 cm (22 inch) diameter to be fired at bridge pillars in an attempt to weaken and destroy the bridge. The 45.72 cm diameter design proves to be the top performing EFP. This EFP had a 0.64 cm (0.25 inch) thick flyer plate, is packed with 10.2 kg (22.5 lbs) of C-4 (hand packed), and had an 45.72 cm diameter PVC pipe as its confining geometry. The cap depth is unknown. Projectiles from this EFP design reach a velocity of 1.98 km/sec and are accurate within 30.48 cm at 91.4 meters. The initial kinetic energy of the flyer was 18.98 Mega-Joules, and 91.4 meters from the charge position, it had dropped to 5.42 Mega-Joules.

## **2.9 AN INVESTIGATION INTO AN ALTERNATIVE FRAGMENT PROJECTOR FOR INSENSITIVE MUNITIONS QUALIFICATION, (C. LAM, T. LIERSCH AND D. MCQUEEN, 1997)**

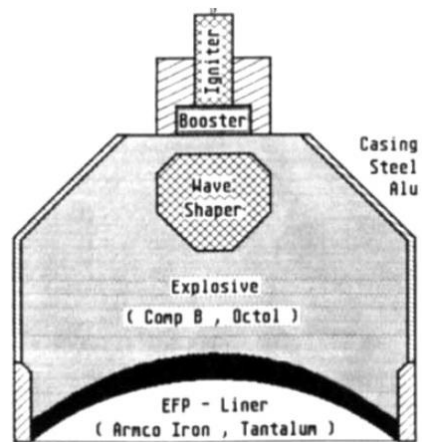
This research investigated the use of EFPs to produce cube projectiles traveling at 2.5 km/sec as a suitable replacement to the conventional steel cubes used in the Fragment Insensitive Munitions test. This research defined the physical parameters of an EFP as

liner material, radius of curvature, segmented liners, contoured liner thickness, confinement material, confining thickness, charge length, and charge diameter. The parameters for the EFP designs in this research were charge length of 10.16 cm, diameter of 5.08 cm, flyer diameter of 5.08 cm, and packed with C-4. The charge weights ranged from 227g to 300g. The authors used computer modeling to identify four designs that have cube-like projectiles traveling at 2.5 km/sec. The computer models were then supported with empirical testing, using flash radiography to identify the projectiles shape and velocity. Of the four designs tested empirically, one succeeded in producing a cube-like projectile useful for the Fragment Insensitive Munitions test.

#### **2.10 RESEARCH AND DEVELOPMENT IN THE AREA OF EXPLOSIVELY FORMED PROJECTILES CHARGE TECHNOLOGY, (WEIMANN, 1993)**

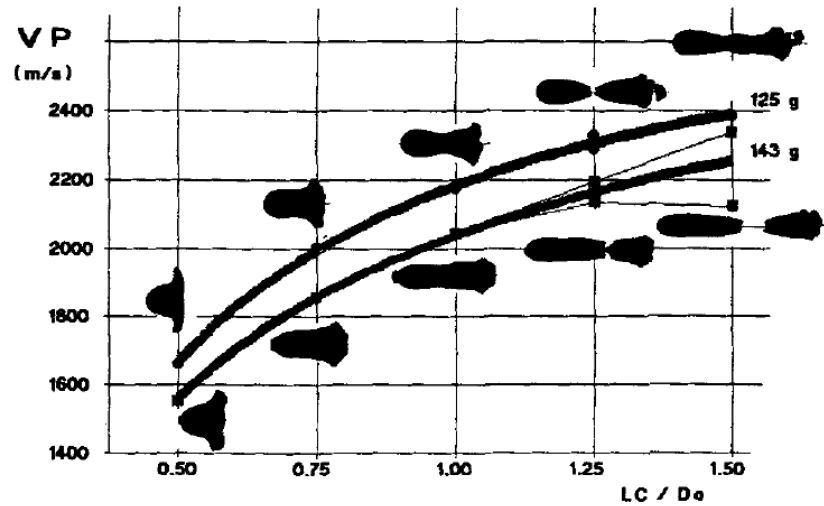
This paper discusses in depth the effects that charge length, confinement thickness, and cap depth have on the formation of a projectile in an EFP that uses a wave shaper. Figure 2.7 displays one of the EFP designs used in this research. The author does not provide information regarding the changes in the EFPs' physical parameters.





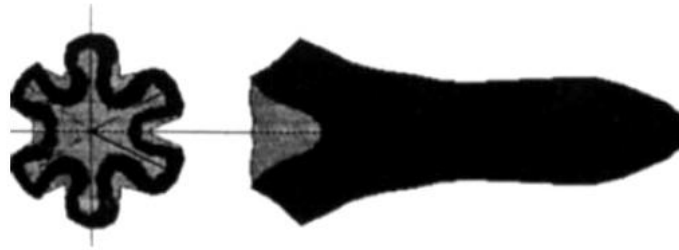
**Figure 2.7 EFP Design with Wave Shaper (Weimann, 1993)**

Figure 2.8 shows the velocity and charge length to charge diameter ratio (CL:CD ratio) for two EFP designs with different flyer weights. The top line is an EFP with a 125-gram flyer weight. The bottom line is an EFP with a 143-gram flyer weight. The flyer weight for these two designs was altered by changing the flyer thickness. However, the flyer diameter and flyer materials remain constant. As the charge length increases, the projectile length grows proportionally to the charge length and the velocity increases. Eventually the projectile grows to a length where it does not remain intact. The maximum charge length to charge diameter (CL:CD) ratio tested is 1.5. The velocities for the charge length experiment range from 1.5 km/sec to 2.4 km/sec.



**Figure 2.8 Projectile Velocity (VP) and Projectile Formation at Different Charge Lengths (Weimann, 1993)**

The EFP designs with thicker confinement produce projectiles that have a higher density than the EFP designs with thinner confinement. Velocities for the confinement thickness test range from 1.8 km/sec to 1.9 km/sec. Results of the cap depth test determine that inserting the blasting cap 7.5 cm into an EFP creates a more elongated projectile shape with a higher velocity than the projectiles produced from the EFP with a cap depth of 2 cm. The velocities range from 1.6 km/sec to 2.1 km/sec. Figure 2.9 shows the projectile produced with a star shaped base.



**Figure 2.9 Projectile Produced with Star Shaped Base (Weimann, 1993).**

### **2.11 A COMPARISON OF THE CTH HYDRODYNAMICS CODE WITH EXPERIMENTAL DATA, (EUGENE S HERTEL, 1992)**

This research tested the modeled velocity versus the empirical data and obtained a model that accurately predicts the velocity of the EFP designed. The researcher uses the EFP model to test modeled EFP armor. The velocity obtained through empirical data was 2.28 km/sec.

### **2.12 FUNDAMENTALS OF SHAPED CHARGES, (W. P. WALTERS, J. A. ZUKAS, 1989)**

This text describes the effects different liner shapes have on a computer-simulated formation of the projectile produced from an EFP. Physical parameters are not specified other than computer models similar to Figure 2.10. This figure identifies the “elongated” projectile shape discussed previously.

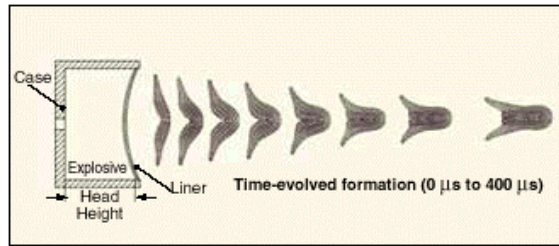


**Figure 2.10 Projectile Formation during Flight (W. P. Walters, J. A. Zukas, 1989).**

### 3. EFP DESIGN

The literature cited in Section 2 provides insight to the controllable physical parameters of an EFP as well as performance expectations for various designs. This section discusses the EFP designs that test the five physical parameters tested in this research. The purpose of the following experiments was to test the hypothesis that an EFP's performance varies with changes in its physical parameters. The author defines performance, for this research, as target penetration depth. Section 4.1 discusses penetration further.

The Original EFP design was the basis for the EFP designs in this research. The physical parameters of the Original EFP design include: type of explosive used, confinement thickness, confinement strength, confining geometry, thickness of the flyer, diameter of the flyer, charge diameter (CD), charge length (CL), the flyer's radius of curvature, flyer material, cap depth, and charge weight (CW). The distance for the cap depth is from the tip of the detonator, opposite of the wires and Duct tape placed 1.4 cm away from the tip of the detonator in order to show detonator depth and position. The blasting cap was inserted into the EFP until the tape on the detonator met the end cap. Head height (HH), which is the distance from the bottom of the blasting cap to the top of the flyer, is also a physical parameter of an EFP design. This distance is a function of the charge length, cap depth, flyer curvature, and flyer thickness, so it is not an independent parameter. The following figure (Figure 3.1) shows these EFP physical parameters.

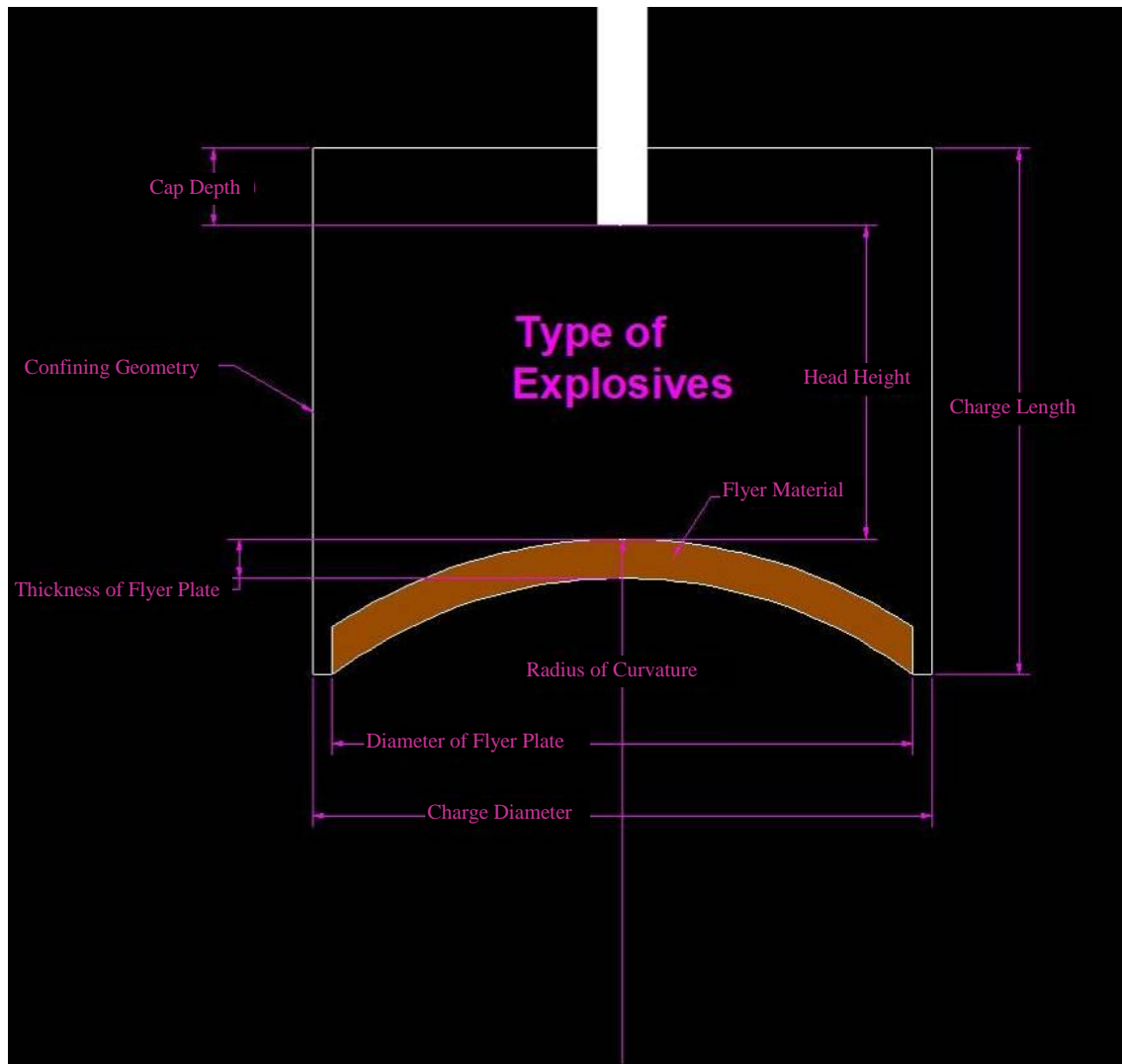


**Figure 3.1 Original EFP Design**

Of the twelve parameters mentioned, above, the five physical parameters chosen for this research were not dependent upon one another. These physical parameters were charge weight, type of explosive, flyer thickness, flyer's radius of curvature, and confining geometry. The remaining physical parameters were kept consistent throughout the testing process. The EFP design constants were: confinement type (a cylindrical PVC

sewer pipe with a 10.64 cm inner diameter and an 11.27 cm outer diameter), flyer diameter ( $2R = 9.525$  cm), flyer material (copper alloy 101), confinement thickness (0.318 cm), and the blasting cap was inserted 1.4 cm into the explosives (cap depth). For these tests, the CD (10.16 cm) remained constant, with the exception of the confining geometry design as explained in Section 3.2.

The CL is a function of charge weight, packing density of the explosive, charge diameter, and the total volume of the flyer. Charge weight was one of the physical parameters tested in this research. CD is a constant. The flyer volume is dependent upon flyer diameter, flyer's radius of curvature, and flyer thickness. The flyer diameter was constant. Flyer's radius of curvature and the flyer thickness were physical parameters tested in this research and therefore will not remain constant. Each EFP was hand packed with explosives, resulting in a slight change in density from one EFP to the next. Voort (2009) states in his research that an EFP using cast explosives, of constant density, did not out perform an EFP using a hand packed explosive with a packing density that varied slightly from charge to charge. Due to the changing charge weight, flyer thickness, packing density, and the flyer's radius of curvature, it was not possible to control CL to be the same for each EFP, but CL could be measured in each case.

The definition of performance varies, depending on the needs of the research. Lam, et al. (1997) define performance as the creation of a small "cube-like" projectile traveling 2.5 km/sec. This definition of performance is significantly different from McDevitt (1997) who defines performance as the ability to create a large projectile with high kinetic energy that can penetrate and destroy a concrete target at a significant standoff. Wu (2007) defines performance as the ability to create a projectile that is

capable of penetrating through, a 2.54 cm thick steel target. The EFPs in Wu's research were considerably smaller than the EFPs used by McDevitt. Both authors define performance as the ability to create a penetrating projectile. In order to determine how changing physical parameters of an EFP affect the EFP's performance, this author defines performance as the depth of penetration of the projectile produced by an EFP into a steel target.

The projectile's shape, density, velocity, kinetic energy, the target's thickness, and target density affect the penetration of a projectile (Plunkett, 2009). Therefore, the depth of penetration, production of a dominant projectile, velocity, and kinetic energy data assists this author in determining the top performing charge weight design. Section 4 further explains the test methods and how it is determined if the EFP design produced a dominant projectile. The top performing charge weight design was the design that penetrates the deepest into the steel target, produces a dominant projectile, the highest dominant projectile velocity, and the highest dominant projectile kinetic energy or the best combination of these four.

To understand how changing an EFP's physical parameters affects an EFP's performance, this author first created testing that established a design with the best performance. This design provided baseline information required to design EFPs and test how confining geometry, flyer thickness, radius of curvature, and explosive type affect and EFPs performance. Information such as head height, charge weight, charge weight to flyer weight (CW:FW) ratios, and the detonation wave's shape.

Section 4 explains the methods used to obtain each EFP's performance data. The following sub-sections discuss the five physical parameters of interest and how, each EFP



design was determined. In total, there were eighteen different EFP designs that were used to test the effects of the five selected variables.

### 3.1 CHARGE WEIGHT DESIGNS

This author used seven EFP designs to test the charge weight's effect on EFP performance. These designs were Original (CW-1,389g), Bravo (CW-1,301g), Foxtrot (CW-1,083g), Delta (CW-907g), Alpha (CW-867g), Echo (CW-811g), and Charlie (CW-454g). The names for the EFPs were assigned post testing, EFP Alpha was identified as the top performing design, EFP Original was the EFP created by Dr. Baird for EFP armor testing at Missouri S&T 2008, and the remaining designs were named alphabetically by charge weight. For these seven EFP designs, the charge weight was the only physical parameter, of the five physical parameters tested, that varied. The remaining four physical parameters held constant: explosive type (C-4), flyer thickness (0.635 cm), radius of curvature (6.223 cm), and confining geometry (a cylindrical PVC sewer pipe with a 10.64 cm inner diameter and an 11.27 cm outer diameter). Figure 3.2 shows four of the seven charge weight designs.

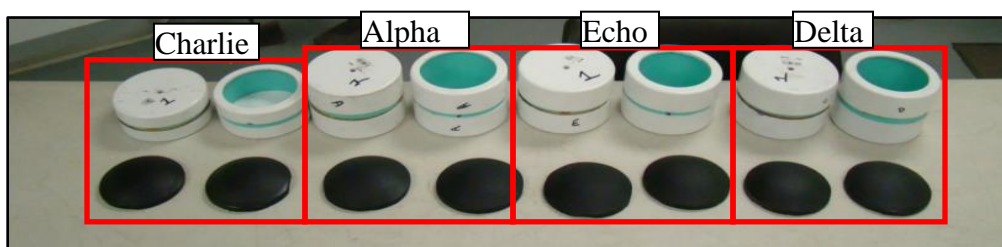


**Figure 3.2 Various Charge Weight Designs**

With the charge weight changing for the various EFPs designs detailed in this section, the charge length changed proportionally with the charge weight, due to the charge diameter and total volume of the flyer remaining constant. The change in charge length results in a changing HH, which is the distance the detonation wave travels prior to interacting with the projectile. See Figure 3.1 (page 19).

The distance the detonation wave travels directly affects the detonation wave's shape, as well as how the detonation wave interacts with the flyer plate. The interaction between the flyer plate and detonation wave influences the projectile's shape and formation. For each EFP, an AutoCAD drawing was made of the explosive's detonation wave, in microsecond steps, traveling at the explosive's detonation velocity for the explosive's theoretical maximum density (TMD) and is given in the Appendix. These drawings assume that the reflected and release waves have not interacted with the detonation wave. Therefore, their effects were not included in these drawings. By assuming that the reflected and release waves have not interacted with the detonation wave, it allows for a simplistic visual analysis of the detonation wave shape for each design. The release waves and reflected waves do interact with the detonation wave in some of the EFP designs. However, reflected wave interaction with the detonation wave varies, depending upon the length of the EFP. Section 3.4 explains this interaction further. These drawings provide insight to the general detonation wave's shape upon interaction with the flyer plate. This information, in combination with the projectile shape produced from each design, help identify how the changing charge weight designs affected an EFP's performance. Table 3.1 displays the design information from each EFP used to test the charge weight's effect on performance.

Table 3.1 Averaged Charge Weight Design Information

<b>EFP</b>	<b>Number of EFPs Tested</b>	<b>Weight of explosives (grams)</b>	<b>Flyer Weight (grams)</b>	<b>Ratio (CW:FW)</b>	<b>Ratio (FW:CW)</b>	<b>Height of EFP (cm)</b>	<b>Head Height (cm)</b>	<b>Ratio (CL:CD)</b>	<b>Ratio (HH/CD)</b>	<b>Packing Density (grams/cm<sup>3</sup>)</b>
Original	1	1,389.13	442.25	3.14	0.32	13.17	9.06	1.24	0.89	1.41
Alpha	4	867.50	442.96	1.96	0.51	9.24	5.13	0.85	0.50	1.31
Bravo	2	1,301.24	432.33	3.01	0.33	12.03	7.91	1.12	0.78	1.46
Charlie	4	453.59	439.42	1.03	0.97	5.91	1.79	0.52	0.18	1.15
Delta	4	907.18	440.84	2.06	0.49	9.43	5.31	0.87	0.52	1.34
Echo	4	810.80	445.80	1.82	0.55	8.79	4.67	0.80	0.46	1.29
Foxtrot	4	1,082.95	442.25	2.45	0.41	10.98	6.86	1.02	0.68	1.34

Table 3.1 outlines the averaged information for each EFP design intended to test the effects the charge weight had on an EFP's performance. The author fired twenty-three EFP tests using the seven EFP designs to identify charge weight's effect on performance as well as to identify a top performing charge weight. The EFP design order is as follows: Original, Bravo, Delta, Charlie, Foxtrot, Echo, and Alpha.

EFP Original is the previous design, designed by Dr. Baird, used at Missouri S&T for armor testing. The remaining EFPs in this section were based on recommended charge weight and CW:FW ratios as recommended by explosive experts Dr. Jason Baird, Dr. Paul Worsey, and SFC Jason T. Gerber, a U. S. Army Explosives Ordnance Disposal

technician. The testing order for the EFP designs was set up to identify a top performing charge weight design. Identifying a charge weight, with C-4, that performs the best while holding the remaining physical parameters constant, provides design information used to test the remaining four physical parameters.

For the designs based on the recommended CW:FW ratios, the charge weight was calculated by taking the flyer weight times the CW:FW ratio. The calculated charge weight divided by the TMD of C-4 ( $1.58 \text{ g/cm}^3$ ) provides the total volume of the explosives. The flyer volume was then added to the volume of explosives and divided by the area calculated ( $81.073 \text{ cm}^2$ ) using the charge diameter to calculate the charge length.

EFP design “Bravo” had a calculated charge weight of three times the flyer weight. The calculated charge weight of 1,301g (2 lbs 13.9 oz) was determined using an average flyer weight of 434g (15.3 oz). This suggestion came from Dr. Worsey, who states that this charge weight to flyer weight ratio produces the desired performance with respect to producing a dominant projectile and velocity (Worsey, 2009). Dr. Worsey used this ratio in a research project. However, he was unable to provide information, as to the performance data obtained in that project since the U.S. Department of Defense restricts access to the document.

SFC Gerber suggested the charge weights for EFP designs Charlie and Delta, in a conversation with the author of this research in June 2009 (Gerber, 2009). He stated that given the flyer thickness, flyer weight, and the performance of EFP Original, he believed that the optimal CW:FW ratio would lay between 2:1(Delta) and 1:1 (Charlie). The EFPs that he saw during his deployment to a combat zone typically had CW:FW ratios in this

range. EFP Delta had a charge weight of 907g (2 lbs) and EFP Charlie had a charge weight of 454g (1 lb).

To this point, EFP Delta performs the best in penetration, but this author was not able to identify a single dominant projectile in the high-speed video taken during the testing of EFP Delta.

EFP Foxtrot had a charge weight in-between EFP Bravo and EFP Delta. This enabled this author to identify whether the top performing charge weight design had a charge weight higher or lower than Delta. Accordingly, a charge weight of 1,083g (2 lbs 6.2 oz) was selected and a CW:FW ratio of 2.45 calculated.

The performance of EFP Foxtrot enabled this author to determine that the top performing charge weight design was in-between the CW:FW ratios 2:1 and 1:1, as recommended by SFC Gerber (Gerber, 2009). Given the poor performance of EFP Charlie, this author concluded that the top performing charge weight design lies closer to EFP Delta's charge weight. This conclusion was supported by Dr. Worsey (Worsey, 2009), and in collaboration with Dr. Baird and Dr. Worsey, a charge weight of 811g was decided upon. This was the charge weight for EFP design Echo, giving Echo a calculated CW:FW ratio of 1.82.

EFP Echo and EFP Delta were the top performing charge weight designs with respect to penetration, velocity, and production of a dominant projectile. Echo had a higher penetration than Delta and an easily identifiable dominant projectile. Delta does not penetrate as well as Echo, nor does it have a dominant projectile easily identifiable in the high-speed video. However, Delta had a higher velocity. The performance data from the charge weight designs identify a decline in velocity with a decrease in charge weight.

The performance data also identifies an increase in the production of a dominant projectile with a decrease in charge weight. Therefore, this author selected a charge weight in-between Echo and Delta for the charge weight of EFP Alpha. The charge weight EFP Alpha was the top performing charge weight design. Figure 3.3 shows the penetration data and whether or not the EFP design produced a dominant projectile in the order the EFPs were tested. Section 5.1 provides further evidence that Alpha was the top performing charge weight design.

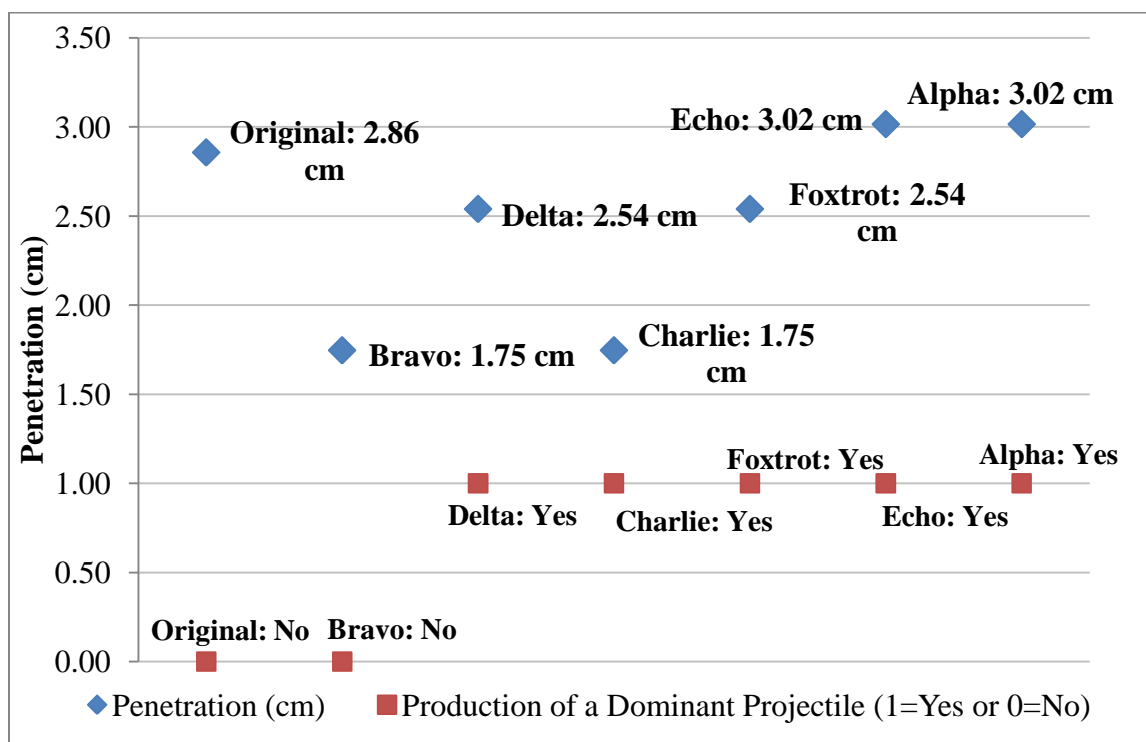


**Figure 3.3 Penetration and Production of a Dominant Projectile**

This design provided the information required to design EFPs used to test the remaining four physical parameters. The following information from EFP Alpha was used to design the subsequent EFPs: head height (5.13 cm), charge weight (867g), CW:FW ratio (1.96), and detonation wave shape (see Appendix). Using this information to design EFPs and test the remaining four physical parameters allowed for a comparison of the five physical parameters and assisted in the identification of how changing charge weight, type of explosive, flyer thickness, flyer's radius of curvature, and confining geometry affect an EFPs performance. The performance data collected for the charge weight experiment is in Section 5.1.

### **3.2 CONFINING GEOMETRY DESIGNS**

Explosive expert Dr. Melvin A. Cook explains how altering the confining geometry of a shaped charge can produce a performance similar to a shape charge with cylindrical confinement, with a charge length 3-4 times the charge diameter (Cook, 1958). The changes Dr. Cook made to the confining geometry of shaped charges lead to an investigation of how the confining geometry affects an EFPs performance.

Head height is critical to the development of the detonation wave. As the detonation wave travels through the explosive, it expands equally in all directions, forming a spherical shape. Eventually the detonation wave will interact with the confinement causing reflected waves. The reflected wave travels at a velocity nearly twice the detonation velocity (Cooper, 1996). If the charge length is 3.5 times the charge diameter, the spherical detonation wave appears to become a relatively flat wave (a

nearly planar wave, of very long radius of curvature) by the time it reaches the end of the charge (Cook, 1958).

There is a small portion of the EFP, opposite the flyer plate, that is not required for the detonation wave's development. In Figure 3.4, this small portion of the EFP is shaded blue. In this area, the detonation wave is not interacting with the side confinement. A change in the confining geometry can remove this portion of the EFP (explosive charge and confinement) in order to reduce the amount of explosive needed to obtain results similar to the top performing charge weight design.

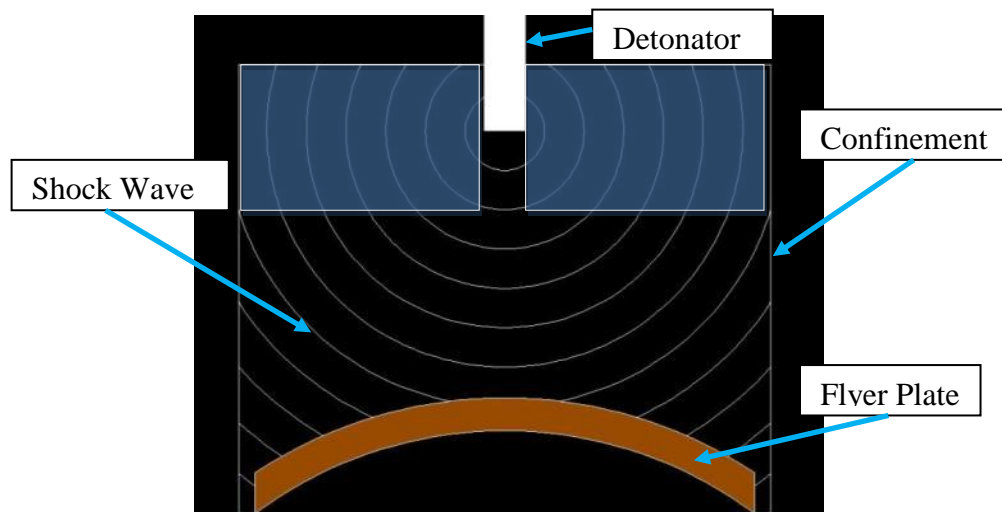


**Figure 3.4 Basic EFP Detonation Wave Expansion**

The detonation wave travels through the explosive expanding toward the flyer plate, approximately 5.08 cm (2 inch), before the detonation wave interacts with the side



confinement. The optimal length and width of the confining geometry that is removable, while maintaining performance is undetermined. Removing this small portion of the EFP creates a change in the confining geometry.

To change the confining geometry of an EFP, this author selected a 5.08 cm to 10.16 cm PVC pipe reducer. The manufacturer of the pipe reducer labels it as “5.08 cm inner diameter to 10.16 cm inner diameter reducer.” However, the actual measurements were 6.03 cm inner diameter to 11.44 cm inner diameter. The other PVC pipe reducers considered do not have dimensions that allow for the charge diameter around the flyer to be 10.64 cm. An inner diameter of 10.64 cm allows the flyer diameter to remain constant. A 10.64 cm inner diameter, by 12.52 cm tall insert allows the charge diameter around the flyer plate and the flyer diameter to remain constant. This insert also allows for three stages of packing of the confining geometry EFPs: the bottom insert, the cone portion of the reducer, and a top insert. The top insert was a 5.08 cm inner diameter cylindrical PVC pipe of various lengths. Figure 3.5 shows the three sections of the confining geometry designs.

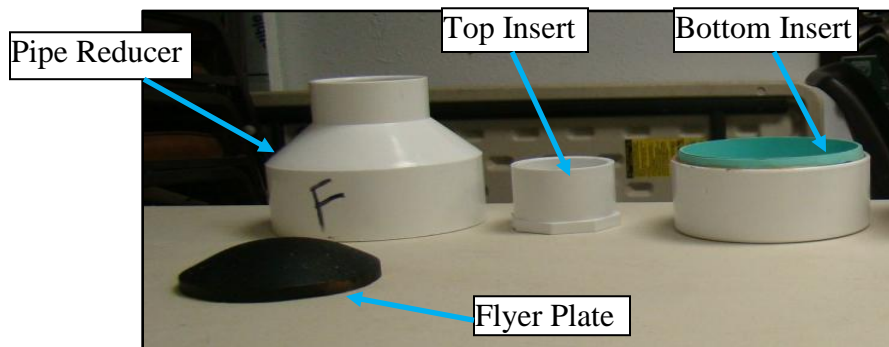


**Figure 3.5 Components of the Confining Geometry Designs**

As the detonation wave enters the cone portion of the EFP, the charge diameter changes from 5.08 cm (2 inch) to 10.64 cm (4.19 inches) at an angle of 142.9 degrees. There is a diffraction point that occurs at the corner where the reducer starts to expand (Baird, 2009). At the diffraction point, the wave expands spherically from that point. In theory, the new wave combines with the initial detonation wave, thereby producing a third detonation wave with a similar shape to that of the top performing charge weight design (Baird, 2009). See Figure 3.6.

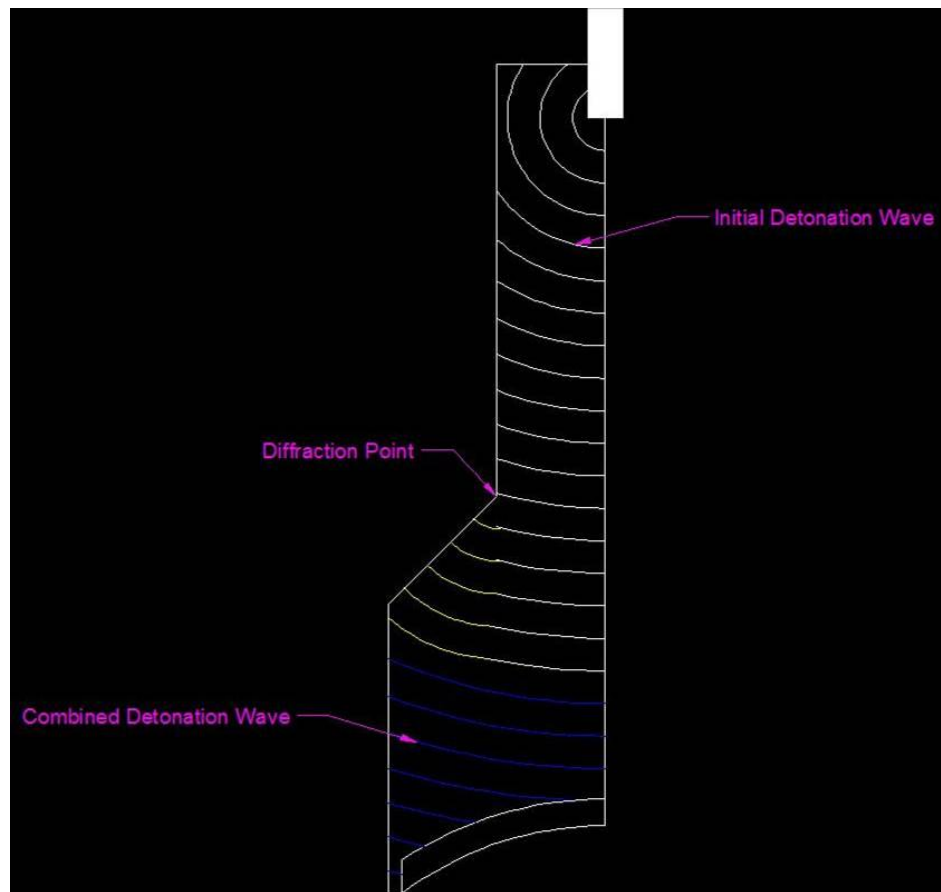


**Figure 3.6 Hypothetical Detonation Wave Expansion**

Three different EFP designs test the effects confining geometry had on performance. These designs were Golf, Hotel, and India. Each EFP had the same general shape as shown in Figure 3.5. However, the length of the top insert for the three different designs was different. The changing length of the top insert determines the volume of explosive used, the confinement, and the detonation wave's shape. Table 3.2 displays the design information.

**Table 3.2 Averaged Confining Geometry Design Information**

<b>EFP</b>	<b>Tested Within Each Design</b>	<b>explosives (grams)</b>	<b>Flyer Weight (grams)</b>	<b>Ratio (CW:FW)</b>	<b>Ratio (FW:CW)</b>	<b>Height of EFP (cm)</b>	<b>Head Height (cm)</b>	<b>Ratio (CL:CD)</b>	<b>Ratio (HH/CD)</b>	<b>Packing Density (grams/cm<sup>3</sup>)</b>
Golf	2	1,107.616	433.748	2.235	0.392	20.127	16.010	1.576	1.171	1.450
Hotel	2	978.626	438.000	2.554	0.448	16.015	11.897	1.981	1.576	1.477
India	6	785.282	442.253	1.776	0.563	12.167	8.049	1.198	0.792	1.471

The confining geometry design had three sections packed in stages and was difficult to construct. If there was a void between the sections, or the sections had different densities, the performance could vary significantly. Testing of EFP India resulted in this conclusion. In one of India's four penetration tests, the projectile broke apart to due to errors in packing.

Ten EFP designs tested the confining geometry's affects on performance. Each design had the same flyer thickness (0.635 cm), radius of curvature (6.22 cm), and explosive type (C-4). The explosive weights depended on the volume of the EFP.

The top insert for EFP Golf had a length of 10.16 cm. This length was twice the inner diameter of the top insert (5.08 cm). A length of two times the charge diameter in the top insert allows the detonation wave to develop spherically and then to diffract in order to develop a third detonation wave similar to the top performing charge weight design (See Appendix). Golf had a charge weight of 1,107g (2 lbs 7.07 oz).

After testing EFP Golf this author concluded, given Golf's performance, that the third detonation wave produced was too planar and EFP Hotel needed a top insert of a shorter length. Therefore, EFP Hotel had a length of 5.08 cm. The top insert for this design had a length to inner diameter ratio of 1:1. Hotel had a charge weight of 978g (2 lbs 2.52 oz).

EFP Hotel's test results also indicated that the top insert length was too long, allowing the third detonation wave to become too planar. Therefore, EFP India used the minimum top insert length available, for a 10.64 cm to 5.08 cm reducer of 3.27 cm. Thus, India had a charge weight of 785g (1 lb 11.7 oz). Obtaining a shorter top insert length than 3.27cm would require the top of the pipe reducer to be shortened, and given the equipment and materials available, shortening the reducer was deemed to be potentially dangerous and was not done.

Each EFP design in the confining geometry test tested the confining geometry's affect on performance. The performance data obtained is in outlined Section 5.2.

### 3.3 FLYER THICKNESS DESIGNS

The flyer thickness experiment's objective was to identify how changing the flyer thickness from 0.635 cm to 0.318 cm will affect the EFP's performance, while keeping CW:FW ratios consistent with the charge weight experiments. The theory is that an EFP with a flyer thinner than 0.635 cm will form a projectile with less explosives and explosives energy, resulting in performance similar to the top performing charge weight design. Figure 3.7 shows the two flyer thickness. The flyer thickness used for the flyer thickness designs is on the left and on the right is the flyer thickness of the top performing charge weight design.

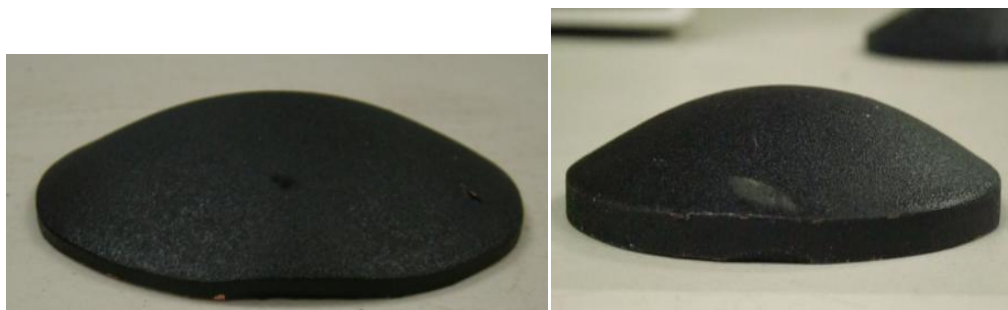


**Figure 3.7 0.318 cm Thick Flyer (Left) and 0.635 Thick Flyer (Right)**

To test this theory three CW:FW ratio were used from the charge weight test: the ratio of the top performing charge weight design 1.96:1 and the recommended ratios, in Section 3.1, 2:1 and 3:1. A CW:FW ratio of 1:1 was also considered; however, the calculated charge weight of a 1:1 ratio was 218.29 grams (7.7 oz). This charge weight

does not provide enough explosive for the needed 1.27 cm cap depth, and was therefore eliminated from testing. The design parameters for the flyer thickness EFP designs are in

Table 3.3

**Table 3.3 Averaged Flyer Thickness Design Information**

EFP	Tested Within	Each Design explosives (grams)	Flyer Weight (grams)	Ratio (CW:FW)	Ratio (FW:CW)	Height of EFP (cm)	Head Height (cm)	Ratio (CL:CD)	Ratio (HH/CD)	Fracking Density (grams/cm <sup>3</sup> )
Juliet	2	733.686	218.291	3.361	0.298	7.697	3.739	0.696	0.352	1.361
Kilo	2	489.029	218.291	2.240	0.446	5.809	1.692	0.510	0.167	1.267
Lima	4	405.398	218.291	1.870	0.538	5.813	1.695	0.511	0.167	1.092

Eight EFPs tested the three designs to identify how flyer thickness affected performance. The explosive type (C-4), radius of curvature (6.22 cm), and confining geometry (10.16 cm diameter cylinder, length dependent upon volume of explosives) remained constant for each design. The average flyer weight for the flyer thickness designs was 218g.

Dr. Paul Worsey recommended a charge weight to flyer weight ratio of 3:1 for EFP Bravo, one of the charge weight designs. Dr. Worsey stated that this ratio produced the desired performance with respect to production of a dominant projectile and velocity

(Worsey, 2009). Therefore, EFP Juliet had a CW:FW ratio of 3:1. This charge weight to flyer weight ratio provides Juliet with a charge weight of 734g (1 lb 9.88 oz).

SFC Jason T. Gerber recommended a charge weight of 907g for EFP Delta, one of the charge weight designs. The recommended charge weight provides EFP Delta with a CW:FW ratio of 2:1. Therefore, EFP Kilo had a CW:FW ratio of 2:1. This charge weight to flyer weight ratio provides Kilo with a charge weight of 489g (1 lb 1.25 oz).

The top performing charge weight design, EFP Alpha, had a CW:FW ratio of 1.96:1. Therefore, EFP Lima was designed to have a CW:FW ratio of 1.96:1. This CW:FW ratio provided Lima with a charge weight of 405g (14.3 lbs). Figure 3.8 Shows the correlating CW:FW designs.



**Figure 3.8 Charge Weight to Flyer Weight Ratios**

A comparison outlining the performance of the EFPs with similar ratios; Juliet to Bravo, Kilo to Delta, Alpha to Lima can be found in Section 5.3.5.

**3.4 FLYER RADIUS OF CURVATURE DESIGNS**

This author uses the Open-Faced-Sandwich Gurney equation to approximate the theoretical maximum velocity of the EFPs’ projectiles. The Open-Faced-Sandwich Gurney equation, referred to as the Gurney equation in this research, uses the FW: CW ratio of the EFPs and the specific explosive kinetic energy (E) of the explosive given in



*Fundamentals of Shaped Charges* (W. P. Walters, J. A. Zukas, 1989). The Gurney equation used does not include shock as a variable. Theoretically, there should not be a difference in the velocity of two EFPs with different radii of curvature, having identical charge weights and flyer weights, with all other physical parameters remaining constant.

The charge weight designs produce velocities 30 percent slower than the velocities calculated with the Gurney equation. *Fundamentals of Shaped Charges*, by W.P Walters and J.A Zukas, Chapter 4, helps to explain why some of the discrepancy exists between the actual velocity of the EFPs and the Gurney equation calculation. In chapter 4 of *Fundamentals of Shaped Charges*, Walters and Zukas states: “The range of applicability of the Gurney equation is restricted due to the simplifying assumptions in the derivation ...” [the restrictions are listed in Table 3 of the book but their details are not necessary for this explanation]. Walters and Zukas also state:

“These errors are caused by ignoring rarefaction waves passing through the detonation product gases, which causes the calculated to be too high, and assuming an initial constant-density distribution of the detonation product gases rather than a distribution with a peak at the surface of the charge caused by the detonation wave, which causes the calculated velocity to be too low...” “...The results represent excellent engineering approximations, within 10% of the experimental results or detailed numerical results...”

With the discrepancy being over 10%, it shows that there is a loss of energy and not all of the explosive energy in the EFP is working to push the projectile. This

difference is most likely due to the Gurney equation being used for an application it was not designed for and creating variables that the Gurney equation used does not consider such as side loss and the rarefaction wave interacting with the flyer plate. Side loss is a term used to describe the explosives energy that is lost due to explosive charge not being an infinite charge of uniform thickness, i.e. energy that is lost out the side of the charge.

If an EFP with a flyer that has an infinite radius of curvature (flat flyer) produces a velocity that is closer to the velocity calculated with the Gurney equation, it may provide insight as to how much of the difference between the calculated gurney equation and the actual velocity is a result of the flyer's radius of curvature. Figure 3.9 shows a flat flyer.



**Figure 3.9 Flat Flyer Plate**

In this experiment, two EFP designs using a flyer with an infinite radius of curvature test the affects the radius of curvature had on the velocity, penetration, and

projectile formation of an EFP. Table 3.4 displays the design parameters for these two EFP designs.

**Table 3.4 Averaged Flyer Curvature Design Information**

EFP	Tested Within Each Design	Weight of explosives (grams)	Flyer Weight (grams)	Ratio (CW:FW)	Ratio (FW:CW)	Height of EFP (cm)	Head Height (cm)	Ratio (CL:CD)	Ratio (HH/CD)	Packing Density (grams/cm <sup>3</sup> )
Mike	3	867.495	422.408	2.054	0.487	8.376	5.846	0.763	0.575	1.278
November	1	4,493.399	419.573	10.709	0.093	38.090	35.560	3.688	3.500	1.455

EFPs Mike and November have a constant flyer thickness (0.64 cm), explosive type (C-4), and confining geometry (a cylindrical PVC sewer pipe with a 10.64 cm inner diameter and an 11.27 cm outer diameter). Four EFPs tested and identified radius of curvatures affects on performance.

EFP Mike had the charge weight of the top performing charge weight design, 867g (1 lb 14.6 oz). If Mike, an EFP with a flat flyer plat, produced a projectile with a velocity closer to the velocity calculated from the Gurney equation, that would identify how much of the difference between the Gurney equation's predicted velocity and actual velocity is due to the flyer's radius of curvature. Since, Mike and Delta have identical FW:CW ratios their velocity is compared in Section 5.4.5.

During testing of EFP Mike, the projectile impacts the target leaving a doughnut-like impact point. A theory of why this doughnut-like impact point occurs is that the curvature of the blast wave in EFP Mike causes the flyer plate to spall. When a shock wave is traveling through a material and interacts with a free surface, it causes a release wave. The release wave puts the material in tension. When the tension caused by the release wave exceeds the maximum tensile strength of the material, sections of the material breaks away from the main body of the material. This is spallation (Baird, 2008). The curvature of the detonation wave and the flyer's radius of curvature determine the time it takes for the flyer to become fully shocked. If the shock wave travels through the center of a flat flyer, spallation could occur.

To test this theory, this author designed EFP November with a head height of three and a half times the charge diameter, providing November with a charge weight of 4.49 kg (9 lbs 14.5 oz). According to explosive experts Melvin A. Cook (Cook, 1958) and Paul W. Cooper (Cooper, 1996), the detonation wave in a cylindrical charge becomes a planar wave when the detonation wave travels a distance three and a half times the charge diameter. A planar detonation wave shocks a flyer with an infinite radius of curvature evenly. Shocking the flyer evenly could eliminate the center of the flyer spalling and eliminate the doughnut-like impact point. Spallation may still occur; however, it will most likely occur across the entire flyer, not just the center. Section 5.4 discusses the results of the radius of curvature test.

### 3.5 EXPLOSIVE TYPE DESIGNS

The explosive type experiment tests how an explosive with a lower detonation velocity and detonation pressure than that of C-4 would affect an EFP's performance.

Unigel, a nitroglycerin-based explosive (i.e. dynamite) produced by Dyno Nobel, was the explosive tested in the explosive type experiment. Unigel is an explosive with a significantly lower detonation velocity and low detonation pressure. It had a detonation velocity of 4.3 km/sec and a detonation pressure of 60 KBar (0.87 million psi) (Nobel). Compared to the C-4 used which has a detonation velocity of 7.565 km/sec and a detonation pressure of 257 KBar (3.7 million psi) (B. M. Dobratz, P. C. Crawford, 1985). The three EFP designs using Unigel were Oscar, Papa, and Quebec. Table 3.5 lists the Unigel designs and their parameters.

**Table 3.5 Averaged Unigel Design Information**

EFF	Number of EFPs Tested Within Each Design	Weight of explosives (grams)	Flyer Weight (grams)	Ratio (CW:FW)	Ratio (FW:CW)	Height of EFP (cm)	Head Height (cm)	Ratio (CL:CD)	Ratio (HH/CD)	Packing Density (grams/cm <sup>3</sup> )
Oscar	3	1,301.243	423.825	3.053	0.326	14.471	9.483	1.424	0.933	1.196
Papa	2	714.408	428.078	1.669	0.599	9.961	5.843	1.040	0.635	0.926
Quebec	4	867.50	436.58	2.02	0.50	10.59	6.32	1.00	0.58	1.17

Nine EFPs tested the effects a lower detonation velocity and pressure explosive had on performance. The Unigel EFP designs keep flyer thickness (0.64 cm), radius of curvature (6.22 cm), explosive type (Unigel), and confining geometry (10.16 cm diameter cylinder, length dependent upon volume of explosives) constant.

EFP Oscar had a charge weight of 1,301g (2 lbs 13.9 oz), which was three times the flyer weight. This was consistent with the 3:1 (Bravo) charge weight to flyer weight ratio recommended by Dr. Paul Worsley (Worsley, 2009), explained in Section 3.1. However, this charge weight also had the energy equivalent to 867g (1lb 14.6 oz) of C-4, the charge weight of the top performing charge weight design. According to Dyno Nobel specialist Scott Giltner (Giltner, 2009), 454g (1 lb) of Unigel produces energy equivalent to 408g (0.9 lbs) of TNT (Trinitrotoluene). According to *LLNL Explosives Handbook – Properties of Chemical Explosives and Explosive Simulants* (B. M. Dobratz, P. C. Crawford, 1985), 454g (1 lb) of C-4 produces energy equivalent to 680g (1.35 lbs) of TNT. Based on this information, this author determined that 454g (1 lb) of C-4 is equal to 680g (1.5 lbs) of Unigel.

EFP Papa had a head height equal to the head height of the top performing charge weight design, EFP Alpha (5.13 cm). This head height determined the volume of explosives used in this EFP design. The volume, calculated from the head height, was multiplied by the TMD of Unigel ( $1.3 \text{ g/cm}^3$ , (Nobel), providing a charge weight of 714g (1 lb 9.2 oz).

EFP Quebec had the identical charge weight of the top performing charge weight design, EFP Alpha. Therefore, the same charge weight of Unigel used in EFP Quebec was equal to 867g (1 lb 14.6 oz) of C-4. This allowed for comparison of charge weights and their effects on performance. The results are given in Section 5.5.

#### 4. TESTING METHODS

The projectile's shape, density, velocity, kinetic energy, the target's thickness, and target density affect the penetration of a projectile (Plunkett, 2009). Therefore, the depth of penetration, production of a dominant projectile, velocity, and kinetic energy data assisted this author in determining how changing the physical parameters of an EFP design affects an EFP's penetration. To ensure that the target thickness and target density were constant for each test, the same target was used to test each projectile's depth of penetration.

Three resulting values were measured for each test. These were depth of penetration, production of a dominant projectile, and velocity. The kinetic energy for the projectile was calculated using the simple kinetic energy Equation 4.1.

$$\textit{Kinetic Energy} = \frac{1}{2}MV^2 \quad \{4.1\}$$

Where M is the mass of a projectile collected during the dominant projectile test and V is the corresponding average velocity of the projectile.

The testing facilities at Missouri S&T were used for testing, which is located on the Experimental Mine off Bridge School Road. The facilities used included above ground and belowground tests. The above ground testing facility is a small quarry developed by the University. See Figure 4.1





**Figure 4.1 Above Ground Testing Facility**

The underground testing facility is a limited underground tunnel system that was originally excavated for military warhead demilitarization and has since been converted into the underground explosives research facility. It is capable of handling a detonation equivalent to 7.7 kg (17 lbs) of C-4. Figure 4.2 shows the layout of the underground testing facility. Its advantage is that lighter charge weights can be shot and shrapnel contained but its disadvantage is that special lighting has to be used for video and equipment requires more protection.

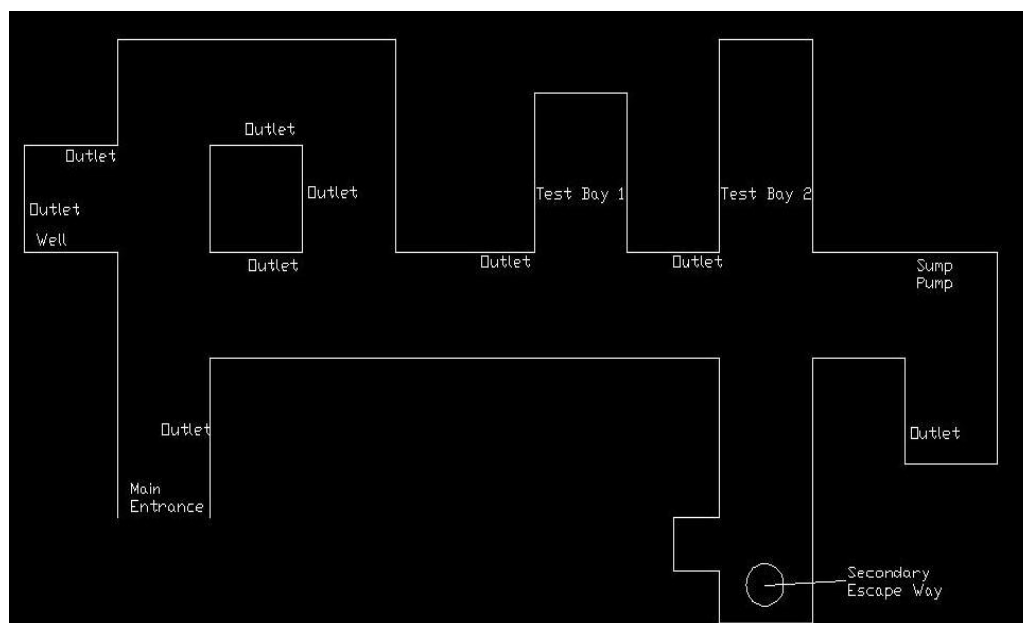


**Figure 4.2 Layout of the Underground Testing Facility**

During the course of this research, the University's' above ground unconfined explosives charge size limit were reduced from 1,360g (3 lbs) to 907g (2 lbs). The change in the above ground's unconfined explosives charge size limit, resulted in some EFP designs such as EFP Original (1.389 kg of C-4) to have a recorded velocity, while EFPs with a smaller charge weight, such as EFP Bravo (1.301 kg of C-4), do not have a recorded velocity. The EFP designs that have a charge weight exceeding the above ground 907g explosive testing limit required testing in the underground testing facility due to mine limits. These charge weight restrictions contributed to the design of the three testing methods. The following sections explain the three testing methods used as well as the setup for the above ground and underground testing facilities.

#### 4.1 PENETRATION TEST

The penetration test collects the depth of penetration data of a projectile, produced from an EFP, into a solid steel plate 7.62 cm thick, 1.2 meters wide by 1.2 meters tall.

Two steel beams attached to the bottom of the steel plate allow the steel plate to stand upright. Figure 4.3 shows the steel plate used as the target for the penetration test.

Available material determined the dimensions of the target. The plate size had a surface area large enough to conduct the entire penetration test series on one plate. This allowed for a comparison of the performances of each EFP's penetration in the same material.



**Figure 4.3 Target for Penetration Test**

Devices such as laser depth finders, tape measures, molds of the impact points, and calipers proved ineffective in measuring the depth of penetration. Therefore, to measure the depth of penetration, this author designed and constructed a “depth finder” device. See Figure 4.4.

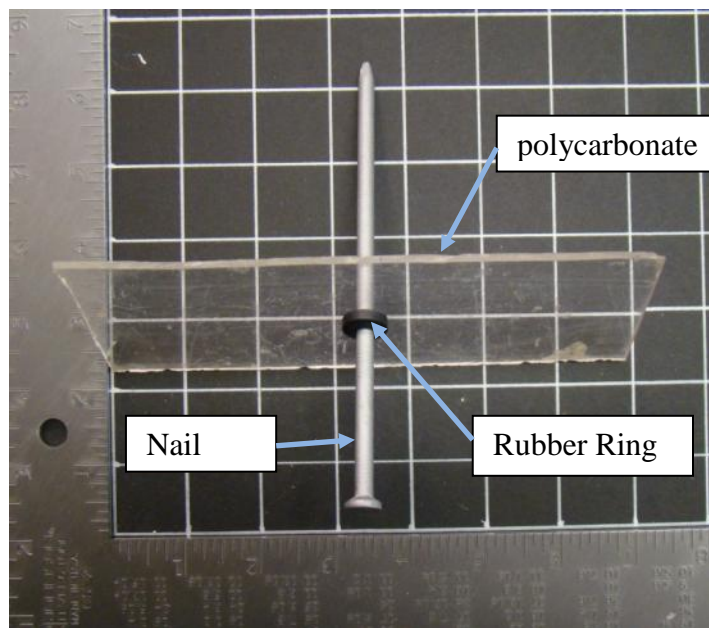


**Figure 4.4 Depth Finder Configuration**

The depth finder device consisted of a 0.48 cm (3/16 inch) nail 12.7 cm long (5 inch), placed through a piece of polycarbonate with dimensions of 0.32 cm (1/8<sup>th</sup> inch) thick by 6.35 cm (2.5 inches) wide by 17.78 cm long (7 inches). The nail had a rubber ring placed on one side of the polycarbonate, which marks the total depth of penetration.

To measure the total depth of penetration, the depth finder was placed to cover the point of impact and five depths for each impact point were measured. See Figure 4.5.

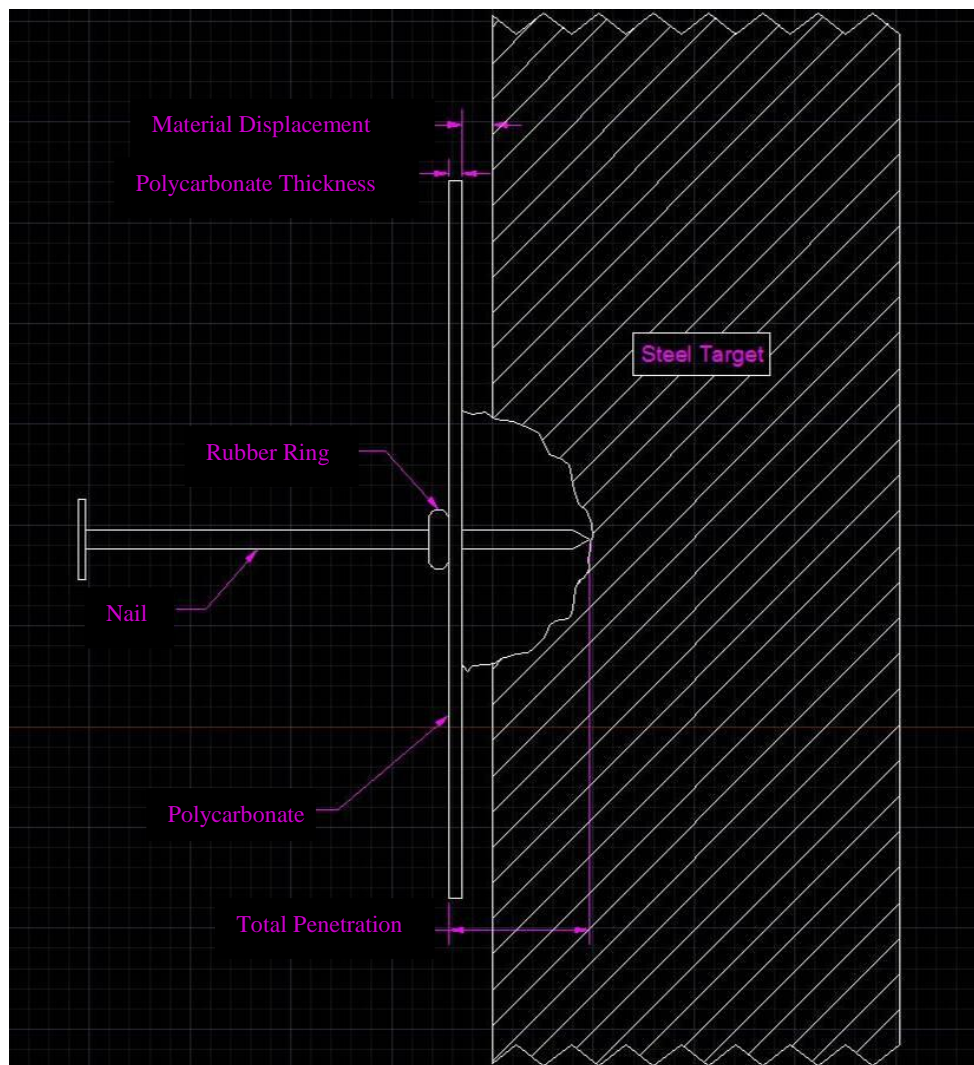


**Figure 4.5 Depth of Penetration**

Inserting the nail farther into the impact point moved the rubber ring up the depth finder. Measuring the distance from the tip of the depth finder to the bottom of the rubber ring provided the total depth of penetration. However, this was not actual depth of penetration. When the projectile impacted the target, material was displaced around the edge of the impact point. The displacement of material prevented the depth finder from being in contact with the target. Therefore, the calculation for actual depth of penetration was: Total penetration minus the polycarbonate thickness minus the material displacement. This calculation for the depth of penetration determined the EFP's performance. In the event that a projectile impacted a previously impacted point on the target, that data was not used. These points did not provide a true representation of the EFP's ability to penetrate the target.

In the event that a projectile broke into fragments during flight or the flyer plate fragmented prior to forming the projectile, multiple impact points occurred on the target from the fragments. When these multiple impact points occurred in a small area, they were an "impact cluster". See Figure 4.6.

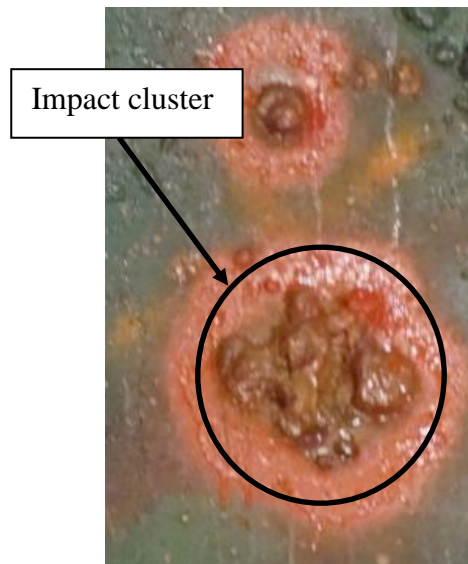


**Figure 4.6 Impact Cluster**

The deepest impact point of the cluster was determined to be the depth of penetration for that EFP. Each EFP design had multiple EFPs that contributed a depth of penetration, allowing for a calculated average depth of penetration for that EFP design. The Appendix displays a photo of the actual depth of penetration for each design.

Section 4.4 explains how the penetration test was set up for the above ground facility and underground facility. Both facilities use the method explained this section, to obtain the depth of penetration. Section 5 examines the average penetration for each design. The penetration depths recorded are for comparison purposes, the penetration will vary depending on the target.

## 4.2 VELOCITY TEST

The velocity test obtained the horizontal velocity of the projectiles produced from each EFP design. The velocity data obtained assisted this author in determining how changing select physical parameters of an EFP affected an EFP's performance, by identifying changes in velocity correlating to the changes in the EFP's physical parameters and providing a velocity value for the kinetic energy equation, shown in Equation 4.1. Due to the squared velocity value in the kinetic energy equation, the velocity of a projectile greatly affected the projectile's kinetic energy, and therefore significantly affected the projectiles ability to penetrate a target (Baird, 2009).

The velocity test used a Phantom high-speed video camera to collect a video recording of the projectile's path. The Phantom high-speed camera was set to 10,000 frames per second (fps). At 10,000 fps, the amount of light produced from the detonation of the EFP can cause the video to white out, commonly known as blooming. Blooming tends to happen when recording explosives at high frame rates, if the researcher does not take preventative measures. This author placed the V-screen 2.74 meters away from the EFPs' firing position, parallel to the projectiles path. This allowed the light, produced from the detonation of the EFP, to dilute and the light did not bloom out the high-speed video. See Section 4.4 Test Set-up.

The camera records video in black and white and has a memory of approximately 2 gigabytes. The recording speed and video quality determine the length of video that the camera is capable of recording. With the video quality and recording speed set for this research, the camera had approximately 2 seconds of record time. The projectile traveled across the cameras field of view in just a few milliseconds. These few milliseconds of the



video recording were all that was relevant to the velocity test. The remaining video was unused.

The Phantom 630 computer software that accompanies the Phantom high-speed camera enabled this author to edit the video recordings to contain the few microseconds relevant to the velocity test. The Phantom software can also analyze the velocity of a projectile within the videos recorded by the high-speed camera. To do this, the user of the Phantom software must first scale the high-speed video so the software knows the distance the projectile travels. This author used a red and white striped V-screen to scale the high-speed video. The red and white stripes on the V-screen were 10.16 cm (4 inches) wide. Figure 4.7 shows the V-screen.

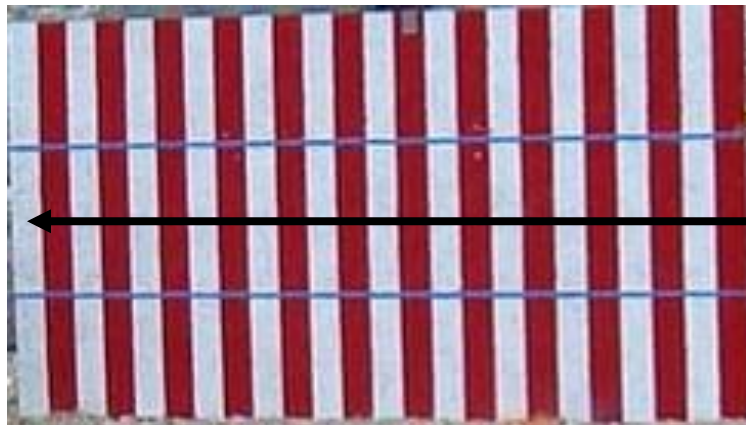


**Figure 4.7 Scale/Reference Board (V-Screen)**

Once the high-speed video was scaled using the software, the user clicked on a fixed point on the projectile (selected for each projectile) in successive frames as it

traveled across the V-screen. This provided the Phantom software with the distance the projectile traveled and the time it took the projectile to travel that distance. To calculate the velocity of the projectile, the accuracy of the point selection was dependent upon the user's ability to select the same point on the projectile's leading edge, as the projectile traveled across the V-screen. This introduced human error to the computer software's ability to calculate the velocity of the projectile, as it was difficult to ensure that the user indicated the exact same point on the projectile. In order to reduce the possibility for error this author used the Phantom software to calculate the velocity five times for each EFP, selecting new points for each calculation. The average of the five velocities was determined to be the actual velocity of the EFP.

The Gurney equation was used to calculate a predicted velocity for each EFP design. These calculated velocities were used to help determine the recording speed for the high-speed camera. Ronald W. Gurney developed the original Gurney equation by using conservation of momentum and energy (W. P. Walters, J. A. Zukas, 1989). Kennedy later derived Equation 4.2, the Gurney equation, from Gurney's original equation where  $V$  is the projectile velocity,  $M$  is the initial mass of the flyer,  $C$  is the charge weight, and  $E$  is the specific explosive kinetic energy of the explosive used (W. P. Walters, J. A. Zukas, 1989).

$$V = \sqrt{2E} \left[ \frac{\left( \left( 1 + \frac{2M}{C} \right)^3 + 1 \right)}{6 \left( 1 + \frac{M}{C} \right)} + \left( \frac{M}{C} \right) \right]^{-\frac{1}{2}} \quad \{4.2\}$$

The Gurney equation is defined under the circumstance that a semi-infinite slab of explosive is in intimate contact with a semi-infinite metal flyer plate. See Figure 4.8.



**Figure 4.8 Open-Faced-Sandwich Gurney Equation Configuration**

Dyno Nobel does not have a specific kinetic energy value for Unigel. Therefore, this author used Cooper's equation for approximating the value of  $\sqrt{2E}$  for Unigel, Equation 4.3 (Cooper, 1996).

$$\sqrt{2E} = \frac{D}{2.97} \quad \{4.3\}$$

In Equation 4.3, D is the detonation velocity of Unigel, 4.3km/sec (Nobel), and 2.97 is a constant (Cooper, 1996). This approximation of  $\sqrt{2E}$ , will most likely increase the difference between the Gurney equation's predicted velocity and the actual velocity;

the exact value of E is unknown. Using Equation 4.3 the value for the square root of 2E was calculated at 1.448.

The actual velocity of each design was compared to the corresponding velocity predicted by the Gurney equation. This comparison allowed the identification of the Gurney equation's accuracy in predicting the velocity of a projectile produced from an EFP. As the test progressed, this author observed that the actual velocity was considerably slower than the velocity predicted by the Gurney equation.

Section 5 discusses and analyzes the velocities collected. Section 5.6 also analyzes the Gurney equation's ability to predict the velocity of a projectile from an EFP. The velocities obtained allowed the kinetic energy calculation of each projectile collected in the dominant projectile test. The high-speed video assisted in the dominant projectile test as explained in Section 4.3.

### **4.3 DOMINANT PROJECTILE TEST**

The data obtained through the test methods described in Sections 4.1 and 4.2 assisted in determining if a dominant projectile exist. The dominant projectile test determined, which EFP designs, produce a dominant projectile. It also provided information about the general shape of the projectiles and the mass of the projectiles collected. For this research, a dominant projectile is a projectile easily identifiable in the high-speed video and in which a dominant impact point can be correlated to the projectile identified. Figure 4.9 shows a dominant projectile that was collected during testing.



**Figure 4.9 Dominant Projectile Collected During Testing**

The Phantom software that accompanies the Phantom high-speed camera is capable of generating still images from the high-speed video. The images of the projectile in flight, along with the examination of the impact point determined whether or not the EFP design produced a dominant projectile. If one was identifiable in the images taken from the high-speed video and there was a dominant impact point, the EFP design was determined to produce a dominant projectile. If a dominant projectile was not identifiable in the images and there was a dominant impact point, it was inconclusive as to whether or not the EFP design produces a dominant projectile. In this case, the projectile may have broken apart and the fragments impacted the same point. If a dominant projectile was not identifiable in the images, and a dominant impact point does not exist, the EFP design did not produce a dominant projectile. Figure 4.10 shows an image, taken from the high-speed video, where the EFP design produces a dominant

projectile. Figure 4.11 shows a series of images, taken from the high-speed video, where the EFP design did not produce a dominant projectile.

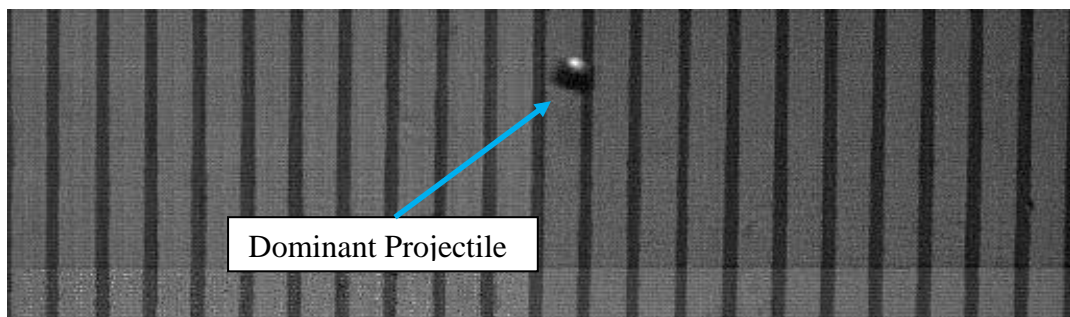


**Figure 4.10 Picture from High Speed Video of a Dominant Projectile**

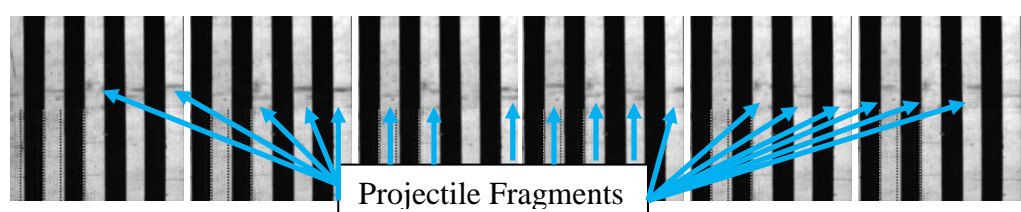


**Figure 4.11 Image from High Speed Video of a Non-Dominant Projectile**

The penetration test and velocity test provide information that allows this author to determine which EFP designs to test in the dominant projectile test. How the projectile impacted the target during the penetration test was the first identifier that the EFP design produces a dominant projectile. When a dominant impact point was identifiable, a

dominant projectile was probable. When an impact cluster was identifiable instead of a dominant impact point, a dominant projectile was not probable. See Figure 4.12.

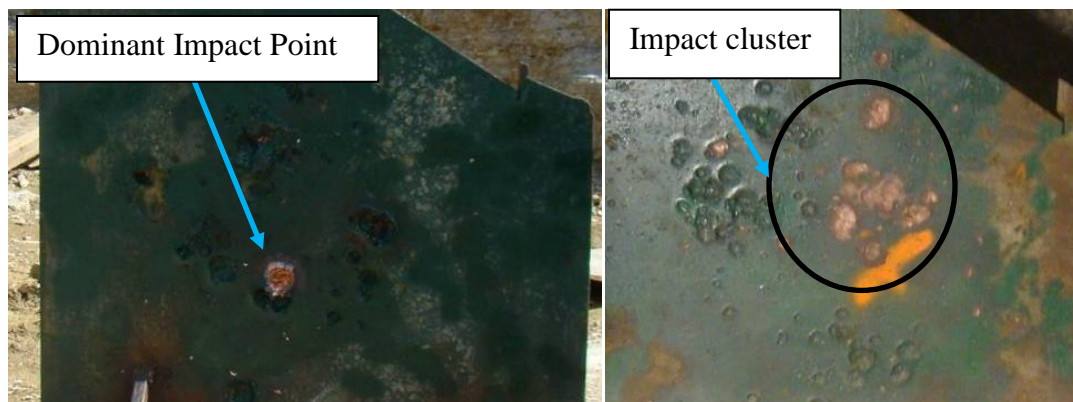


**Figure 4.12 Dominant Impact Point (Left) and Impact Cluster (Right)**

To collect the projectile from the EFP designs that produced a dominant projectile, this author fired the EFPs into a series of horizontal water barrels. The projectile collected provides a projectile weight, and in some cases, a projectile shape.

The barrels filled with water worked well but caused some deformation of the projectiles, due to the violent initial impact of the projectile hitting the first barrel. The extent of the deformation is unknown. The deformation of a projectile depends on its density, velocity, and how it impacts the first barrel. In some cases, the projectiles shattered upon impact. In other cases, the projectile lost mass but stayed intact. “*IED Effects Research at TNO Defense Security and Safety*”, cited in Section 2.2, describes a similar method of catching the projectiles. In this method, a PVC pipe filled with

sawdust, positioned in front of a pipe filled with water, slowed down the projectile enough to where it was not deformed upon impacting the water. This set-up was not applicable in the underground testing facility due to space limitations. The following section, Section 4.4, discusses the test set-up for the three tests.

#### **4.4 TEST SET-UP**

This section discusses the setups for the penetration, velocity, and dominant projectile tests in the above ground testing facility and the underground testing facility. Hanging the EFPs with a three-wire-system connected to six points on the EFP, made it easier to aim the EFPs and increase the aiming accuracy. The EFP height from the ground varied for each design depending on the intended impact point. Figure 4.13 shows four of the six connections points (yellow circles) and the three wires (blue arrows) used to suspend the EFPs. This method of suspension prevents reflected waves, from the ground or a stand, from interacting with the formation of the projectile.



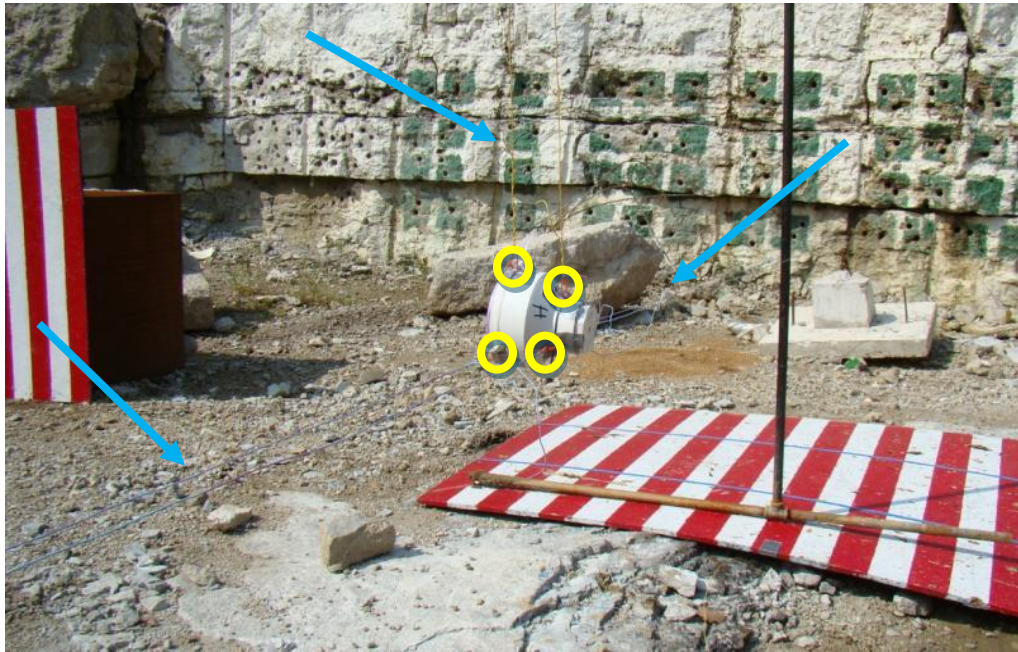


**Figure 4.13 Suspended EFP. Noted are Suspension Wires (blue arrows) and Connection Points (yellow circles).**

A laser pointer proved to be the best method for aiming the EFPs. The laser pointer was placed on top of the EFP allowing this author to determine where the EFP would impact the target, resulting in increased accuracy. However, inaccuracies still occurred during testing due to wind and human error.

The penetration test and velocity test were tested simultaneously in the above ground testing facility. The distance between the firing position of the EFPs and the target for the penetration test (6 meters) fit the 1.22 meter by 2.44 meter V-screen. The high-speed video camera was in a steel box 21.34 meters (70 ft) from the V-screen and perpendicular to the projectile's flight path. Figure 4.14 shows the set-up for the above ground testing facility. The picture was taken from the high-speed camera's position.

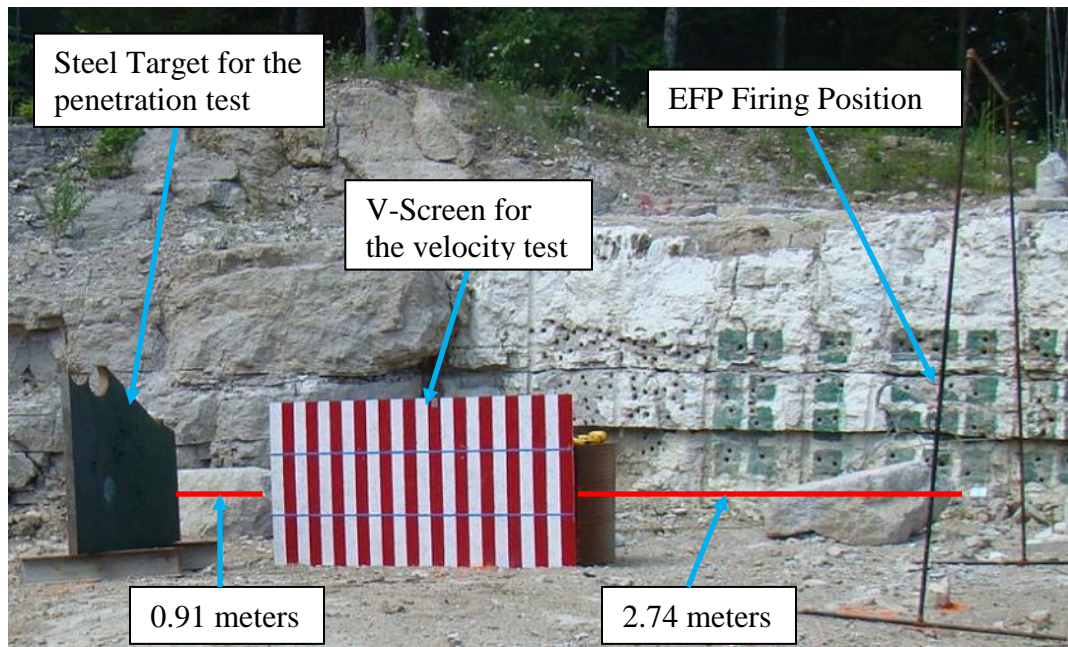


**Figure 4.14 Above Ground Facility, Penetration and Velocity Tests Set-up**

One end of the V-screen was 0.91 meters (3 ft) from the target, and the opposite end of the V-screen was 2.74 meters (9 ft) from the EFPs' firing position. Positioning the V-screen 2.74 meters from the EFP firing position allowed the light produced from the detonation of the explosive to dissipate, and no blooming affects occurred in the high-speed video recording at this distance. There was a total standoff EFP to target distance of 6.10 meters (20 ft).

The penetration tests conducted in the underground testing facility did not have velocity data because the underground testing facility has an environment that is too dark for high-speed video and is hazardous to the camera. Adding additional lighting to the underground testing facility in order to enable high-speed video would increase the cost of the testing. The blast pressures from the explosives and stray fragments from the

projectile would destroy the lights during each test. The penetration tests were conducted in Test Bay 2, which allowed the EFP firing position to be at the same standoff as outside and the penetration tests conducted in both facilities to be consistent. The tests also used the same target.

The original dominant projectile tests in the above ground testing facility had four 55-gallon barrels positioned horizontally on a stand, and each barrel was in contact with the barrel in front of it. See Figure 4.15.

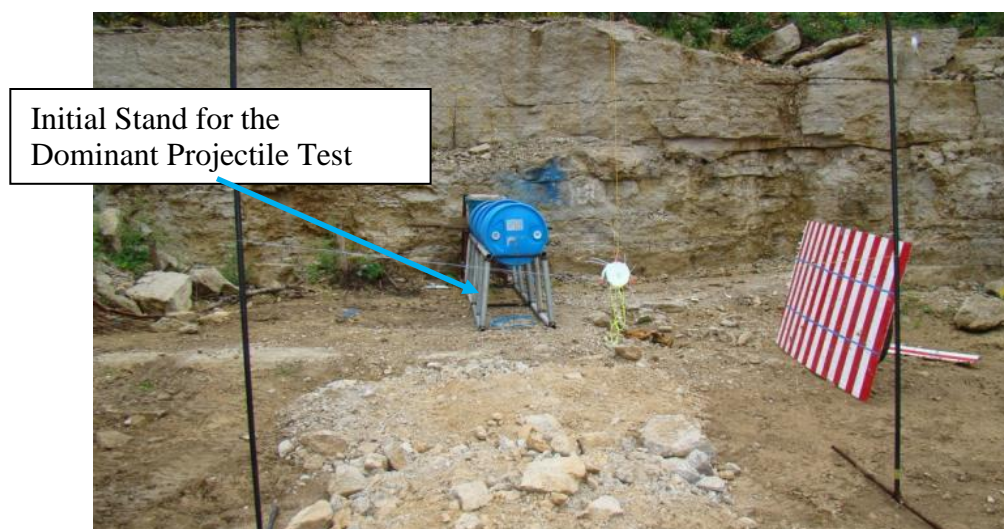


**Figure 4.15 Initial Dominant Projectile Test Set-up**

This resulted in approximately 3.66 meters (12 ft) of water to catch the projectile. Initial attempts to use welded steel pipes as a stand for the four barrels as in Figure 4.15, proved to be inadequate, as the stand did not remain intact after the first test. The outward

pressure of the water produced when the projectile impacted the barrels bent the steel pipes beyond repair. The first test showed that three barrels would be adequate to catch the projectiles. A new three-barrel design replaced the damaged stand. This second stand design used a series of railroad ties used in a cribbing pattern; see Figure 4.16.



**Figure 4.16 Second Stand Design for Dominant Projectile Test**

When the projectile impacted the water barrels, the new stand allowed the pressure produced to escape without being destroyed. The railroad ties were set in place with no connections binding the railroad ties together. This allowed the railroad ties to move as the water pressure impacted them, thus preventing them from being destroyed with each test. The railroad ties were repositioned as needed after each test.

Some of the projectiles fragmented when impacting the barrels. These fragments were difficult to find in the above ground testing facility if they were not in the barrels.

To ensure the collection of the projectile fragments, the test was relocated to Test Bay 1, in the underground testing facility. To ensure the EFP did not damage the surrounding structure and to increase the chances of hitting the barrels, the EFP's firing position was 2.44 meters from the front of the first barrel.

Each 55-gallon barrel weighed 199.6 kg (440 lbs) when full, giving a total weight of the three barrels of 598.8 kg (1,320 lbs). The barrels were placed end-to-end horizontally, with each barrel in contact with the barrel in front of it. The orientation of the barrels plus the combined weight provided resistance and reduced the barrels movement during impact. Section 5 discusses the data collected from each testing method described in Section 4 and analyses the data from the physical parameters with the top performing charge weight design.

## 5. DATA ANALYSIS

The data acquired using the test methods described in Section 4, for the EFP designs, assisted in determining how changing the five physical parameters examined in this research affect an EFP's performance. Physical parameter testing consisted of the following tests in the following order: charge weight, confining geometry, flyer thickness, flyer radius of curvature, and explosive type. The EFP designs tested were Original, Bravo, Delta, Charlie, Foxtrot, Echo, Alpha, Golf, Hotel, India, Juliet, Kilo, Lima, Mike, November, Oscar, Papa, and Quebec. This testing order enabled the identification of a top performing charge weight design and a comparison between physical parameters. The test series allowed for comparison of the top performing charge weight EFP's ability to penetrate the target, velocity, production of a dominant projectile, and kinetic energy to the remaining EFP designs.

The following Sub-Sections are by physical parameter and the appropriate test. They discuss the results of the four testing methods of the five physical parameters tested, which are now analyzed, averaged, and discussed.

### 5.1 CHARGE WEIGHT

The charge weight experiment is the first of the physical parameters tested in this research. It identifies how changing the charge weight of an EFP affects the projectile's velocity, the projectile formation, and the projectile's penetration. The charge weight experiment alters the charge weight for seven EFP designs to identify a top performing

charge weight design and to identify how changing the charge weight affects an EFP's performance.

The EFPs testing order was as follows: Original, Bravo, Delta, Charlie, Foxtrot, Echo, and Alpha. The testing order identifies a top performing charge weight design by enabling this author to use the performance data from each EFP to design EFP Alpha. The following sub-sections show the velocity, dominant projectile, kinetic energy, and penetration data for the charge weight designs.

**5.1.1. Charge Weight Velocity.** This test, helped to identify a correlation between charge weight and velocity. As expected, the EFPs with a higher charge weight produces a higher velocity than the EFPs with a lower charge weight. EFP Charlie has the lowest charge weight in all of the charge weight designs (454g), and produces a velocity of 0.84 km/sec; whereas EFP Original has the highest charge weight (1,389g), and produces a velocity of 1.39 km/sec.

As the charge weight increased the difference of the actual projectile velocity and the velocity calculated with the Gurney equation increases. EFP Bravo was tested in the underground facility and therefore has no velocity data. The actual velocities of the projectiles in the charge weight test are, on average, 32% slower than their calculated velocities. This indicates that not all of the explosive energy was working to push the projectile, which supports the ECW calculations previously discussed. The designs that produced a dominant projectile in the high-speed video were tested in the dominant projectile test. See Figure 5.1.

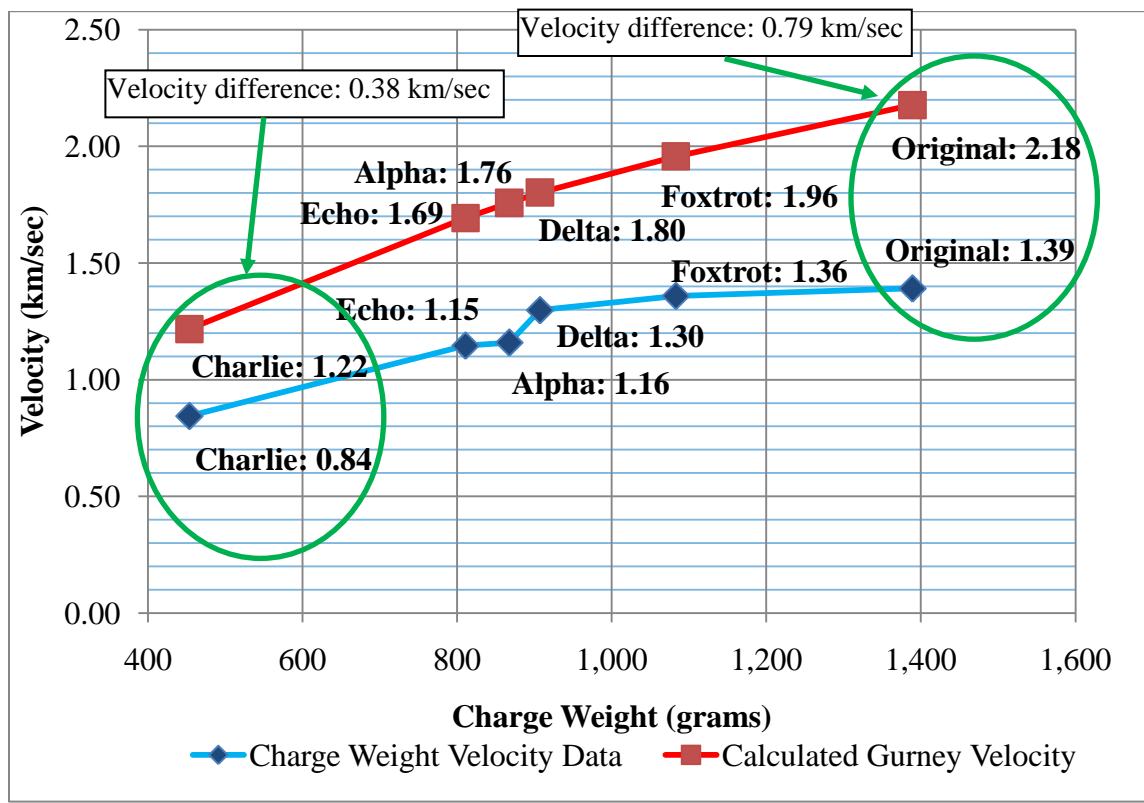


Figure 5.1 Charge Weight Velocity Data

Original's difference between its actual velocity and calculated velocity is 0.79 km/sec twice that of Charlie's difference.

**5.1.2. Charge Weight Dominant Projectile.** The charge weight dominant projectile test provides insight as to how changing the charge weight of an EFP, and resulting head height, affects the flyer formation and production of a dominant projectile. As the charge weight increases, the projectiles broke apart. Table 5.1 shows the data collected on the production of a dominant projectile.



**Table 5.1 Dominant Projectile Data**

	EFP	Dominant Impact Point	Dominant Projectile on High Speed Video
<b>CHARGE WEIGHT</b> ↓	Charlie	X	X
	Echo	X	X
	Alpha	X	X
	Delta	X	X
	Foxtrot	X	X
	Bravo	-	-
	Original	-	-

An “X” in the Dominant Impact Point column indicates that a dominant impact point existed, where a “-” indicates that a dominant impact point was not present. An “X” in the Dominant Projectile on High Speed Video column indicates that dominant projectile was present in the high-speed video recording, where a “-” indicates that there was no evidence of a dominant projectile in the high-speed video recording. For the EFP designs that have an “X” in both columns, the projectile’s weight is displayed in Figure 5.22.

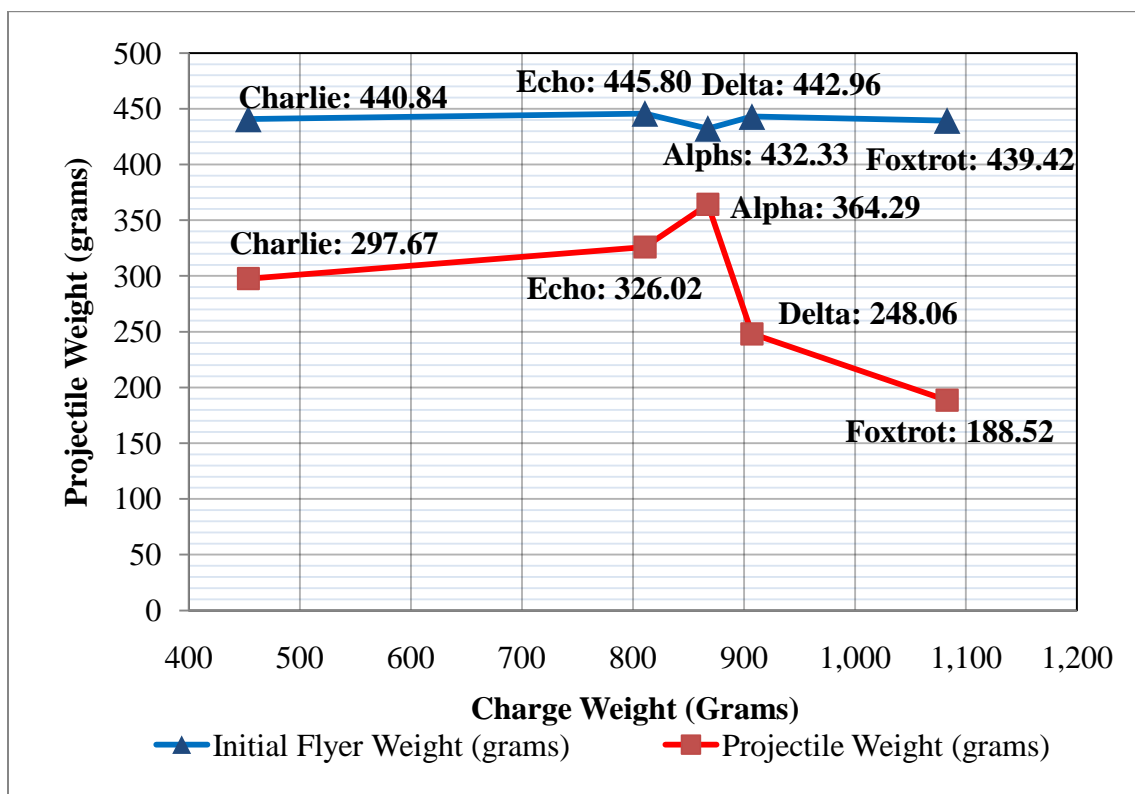


**Figure 5.2 Projectile Weight for the Charge Weight Designs**

EFP Alpha has the highest projectile weight (364.29 grams) and retained 82% of the initial flyer weight. As the charge weight decreases, the EFP designs retain more of the initial flyer weight and dominant projectiles are easily identifiable in the high-speed video. EFP Foxtrot broke into three projectiles, the largest projectiles weight is shown in Figure 5.22. EFP Delta produces a dominant projectile; however, the projectile appears to have broken apart during flight and spun, impacting the barrels backwards. See Figure 5.3.

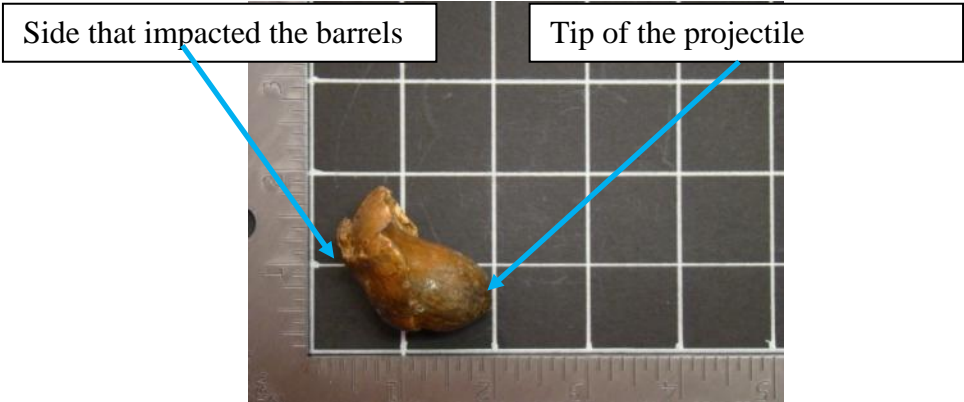


**Figure 5.3 Projectile Produced from EFP Delta**

EFP Alpha produces a dominant projectile with a “cigar-like” shape. When the projectile impacts the barrels there was some deformation. Both pictures in Figure 5.4 show the projectile produced from Alpha. The left picture is one of the projectiles produced from an Alpha design, after it has been cut in half.

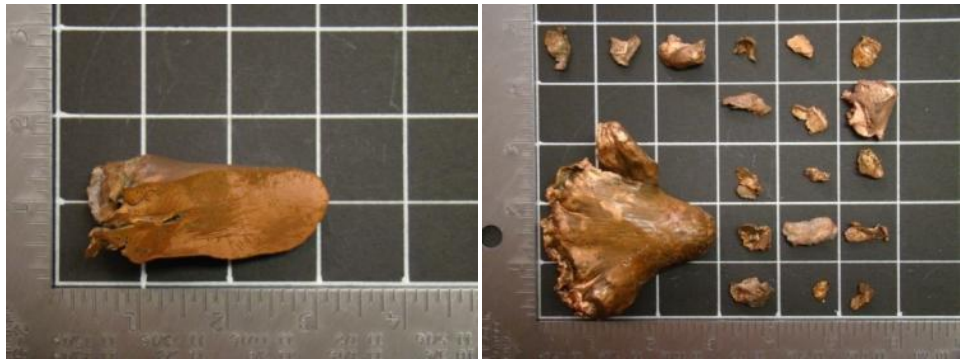


**Figure 5.4 Projectiles Produced From the Alpha EFP Design**

EFP Echo produced a projectile similar to Alpha, however when it impacted the barrels deformed and lost mass. Both Echo and Charlie appear to have deformed and lost mass upon impacting the barrels. The projectile weights collected during this test are used to calculate the designs kinetic energy

**5.1.3. Charge Weight Kinetic Energy.** The projectile mass collected in the dominant projectile test as well as the velocity collected in the velocity test, provide the needed information to calculate the kinetic energy of each EFP design. The kinetic energy allows this author to identify a charge weight design that balances projectile velocity and projectile mass. As charge weight increases, the velocity increases. However, the larger the charge weight, the more likely the projectile broke apart.

Of the charge weight designs, EFP Alpha produces the highest kinetic energy with a velocity of 1.16 km/sec and a projectile with a mass of 364.3g. This author concluded that when the projectile fragments, during the formation process or during flight, the velocity of the projectile decreases and even though the larger charge weights produces higher velocities, the increase in velocity was not enough to compensate for the loss in mass. Figure 5.5 shows the kinetic energy data for the charge weight designs that produced a dominant projectile.

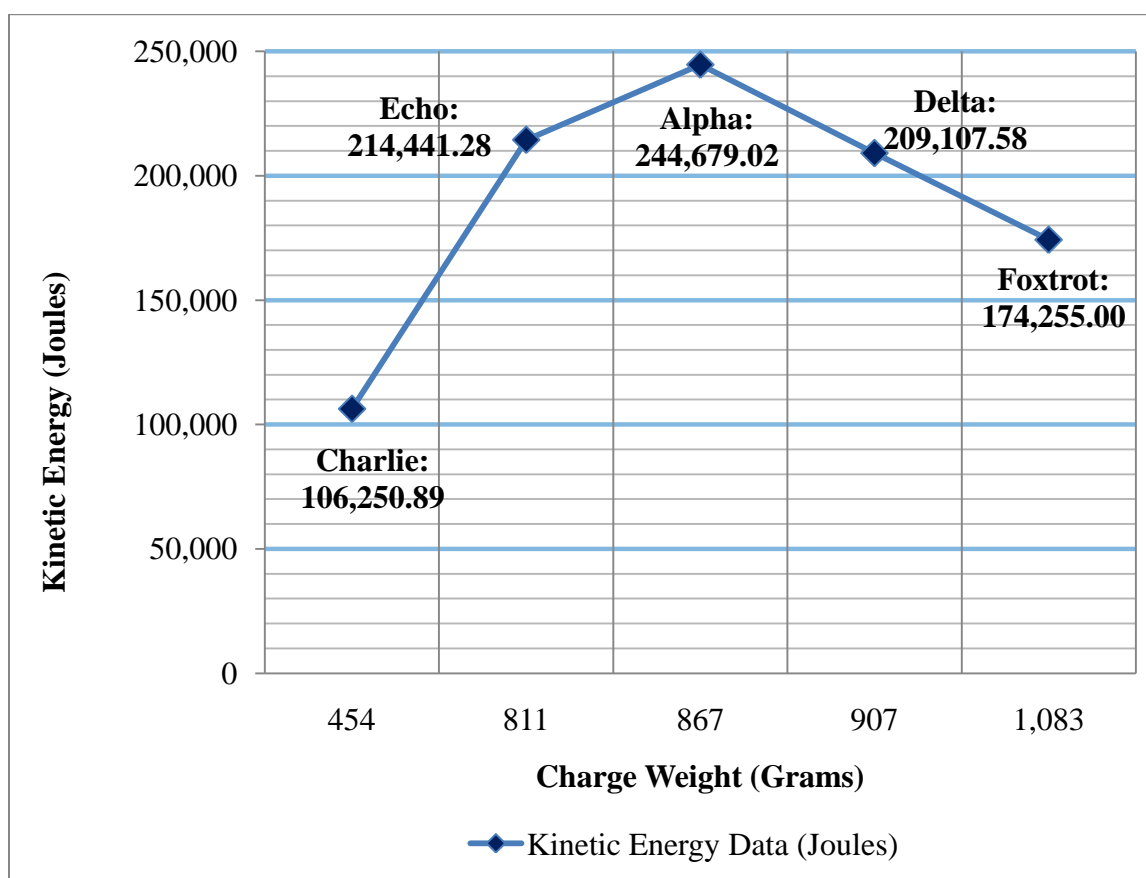


**Figure 5.5 Kinetic Energy Data for Charge Weight Designs**

Often fragments of the projectiles could be located after firing the EFPs at the barrels. However, the fragment velocities are not identifiable in the high-speed video. Therefore, no kinetic energy was calculated. In addition, it was not determined where each fragment impacts the target, therefore a penetration depth cannot be connected to the mass of the fragments. Kinetic energy is an indicator of the projectiles ability to penetrate the target Plunkett (2009).

**5.1.4. Charge Weight Penetration.** Penetration is the main indicator of performance. Therefore, the design that penetrates the deepest is the top performing design. Projectile velocity, projectile weight and kinetic energy assist in determining the top performing design in the event that two designs have the same penetration. Throughout the penetration test, the larger charge weight designs produce multiple impact points. These larger designs are Original, Bravo, Foxtrot, and Delta. Figure 5.6 shows the averaged penetration data for the charge weight designs.

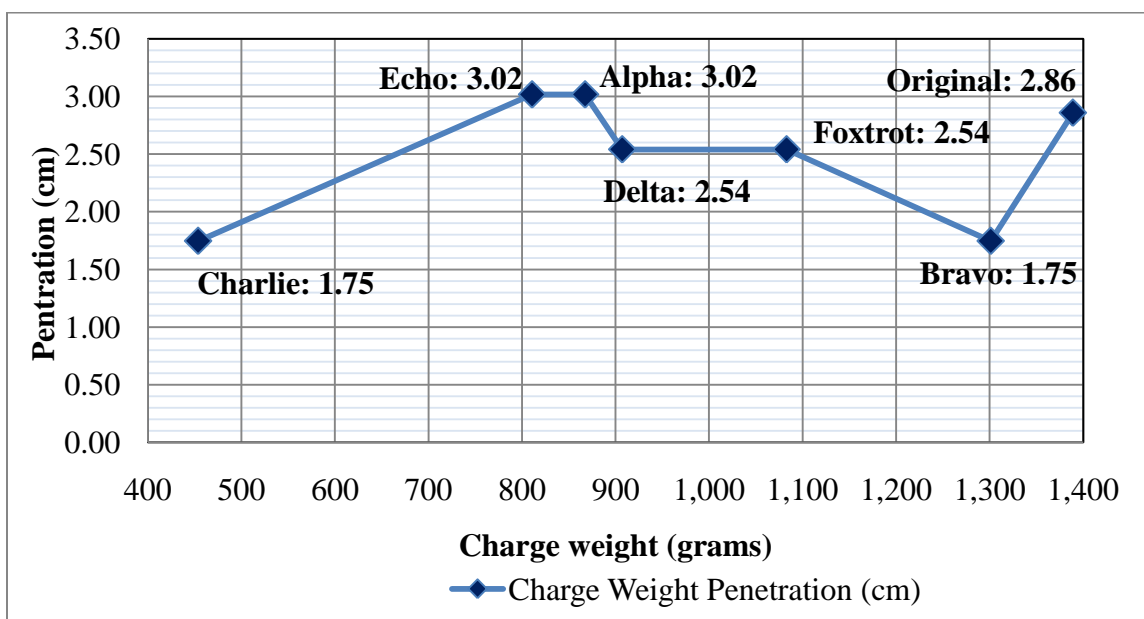


**Figure 5.6 Penetration Data for the Charge Weight Designs**

EFP Original has the second deepest penetration (2.86 cm). This was a result of the smaller fragments having a high velocity. However, this penetration was only for the deepest impact point, most of the impact points, for this design, are less than 2.54 cm.

EFPs Echo and Alpha produce the deepest penetration for the charge weight test with a penetration of 3.02 cm. Performance is defined, in Section 3, as the EFPs' ability to penetrate the target; therefore, Echo and Alpha perform the best out of the charge weight designs. Alpha has a higher velocity, produces a projectile that retains more of the initial flyer weight, and has a higher kinetic energy than Echo, and therefore Alpha was the top performing charge weight design. Echo has a higher efficiency than Alpha, because of its ability to penetrate the target with less explosive.

This author compares the penetration of Alpha to the penetration for the remaining designs in order to identify how changing each physical parameter affects an EFP's performance, in charge weight analysis.

**5.1.5 Charge Weight Analysis.** Echo (810.8 grams) and Alpha (867.5) had the deepest penetration of the charge weight experiment. Alpha and Echo had the highest projectile weights collected, but their velocities were close to the average velocity of the charge weight designs. See Figure 5.7

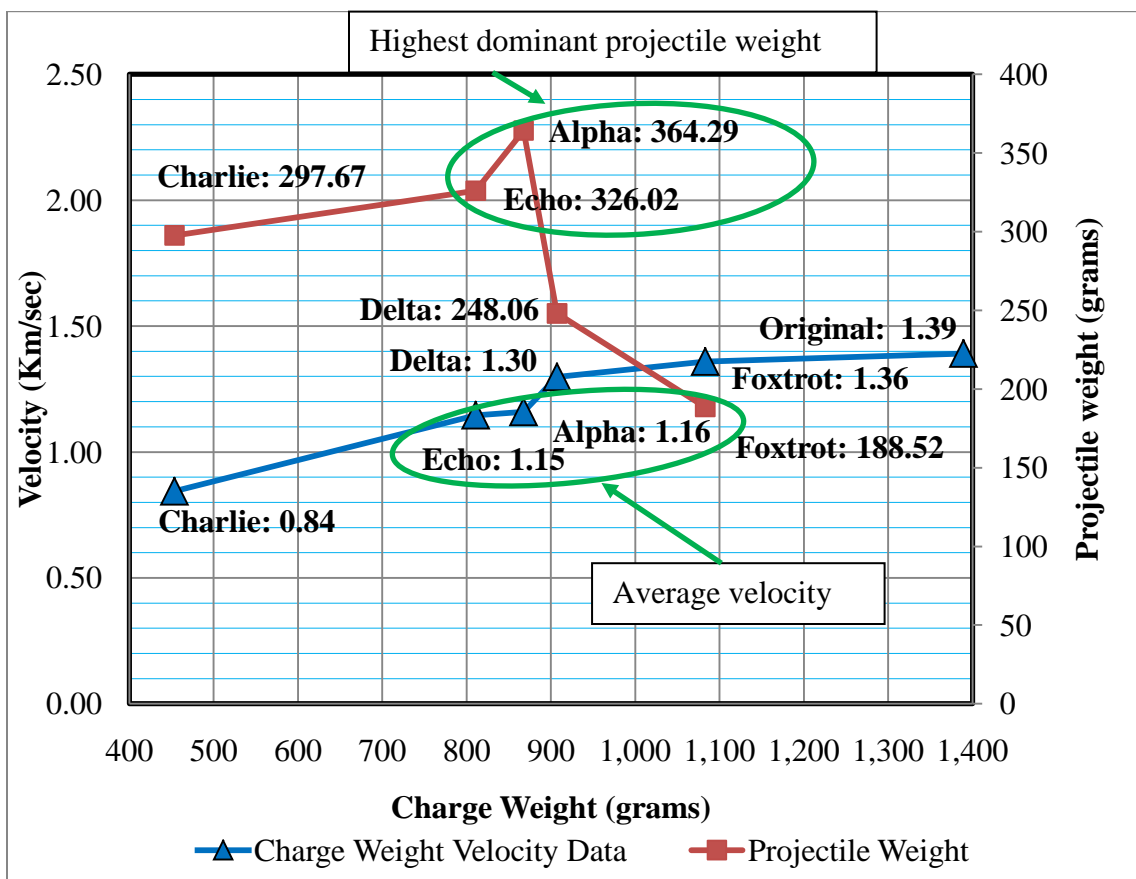


**Figure 5.7 Charge Weight Experiment Comparison of Velocity Data and Projectile Weight.**

Once the charge weight exceeded Alpha's, the projectile weight collected dropped significantly. As the charge weight increased the projectiles velocity continued to increase. This indicates that there is an optimal charge weight for penetration, for an EFP with the physical parameters explained in Section 3, of 868 grams. This also indicates that larger charge weights do not improve EFP performance.



## 5.2 CONFINING GEOMETRY

The confining geometry is compared to the top performing charge weight design discussed in Section 5.1.5. The confining geometry EFP designs test the theory that if a small portion of the explosive opposite the flyer plate is removed, the EFP is still capable of performing as well as or better than the top performing charge weight design while using less explosives. The EFP designs tested are Golf, Hotel, and India. The following sub-sections show the velocity, dominant projectile, kinetic energy, and penetration data for the confining geometry designs. Section 5.2.5 compares the top performing confining geometry design to Alpha's performance.

**5.2.1. Confining Geometry Velocity.** The velocities for confining geometry designs Golf and Hotel were hard to obtain. Golf produced 10 projectiles, identifiable in the high-speed video, in a long thin trail spanning 3.96 meters horizontally and 15.24 cm vertically. Hotel produced eighteen projectiles, identifiable in the high-speed video, in a short thick trail spanning 2.44 meters horizontally and 35.56 cm vertically. These distances were obtained using the Phantom software. The time difference and velocity between the first and last projectile for each design was recorded. Given the time difference and velocity of the first projectile, the distance the projectiles spread horizontally could be calculated. By identifying where the upper most and lower most vertical projectiles cross the V-screen, the Phantom software calculated the distance between the two points providing the vertical spread.

EFP design India only produces one dominant projectile. This author measured each velocity in accordance with the method described in Section 4.2. Each projectile velocity recorded is in Figure 5.8. Each number on the X-axis correlates to the order the

projectiles traveled across the V-screen in the high-speed video. The later the projectile was seen, the slower the velocity of the projectile. Even though velocities are measured for the individual projectiles of Golf and Hotel, a dominant projectile was not identifiable for either design. Golf has a peak velocity of 1.53 km/sec and an average velocity of 1.25km/sec. Hotel has a peak velocity of 1.54 km/sec and an average velocity of 1.09 km/sec.

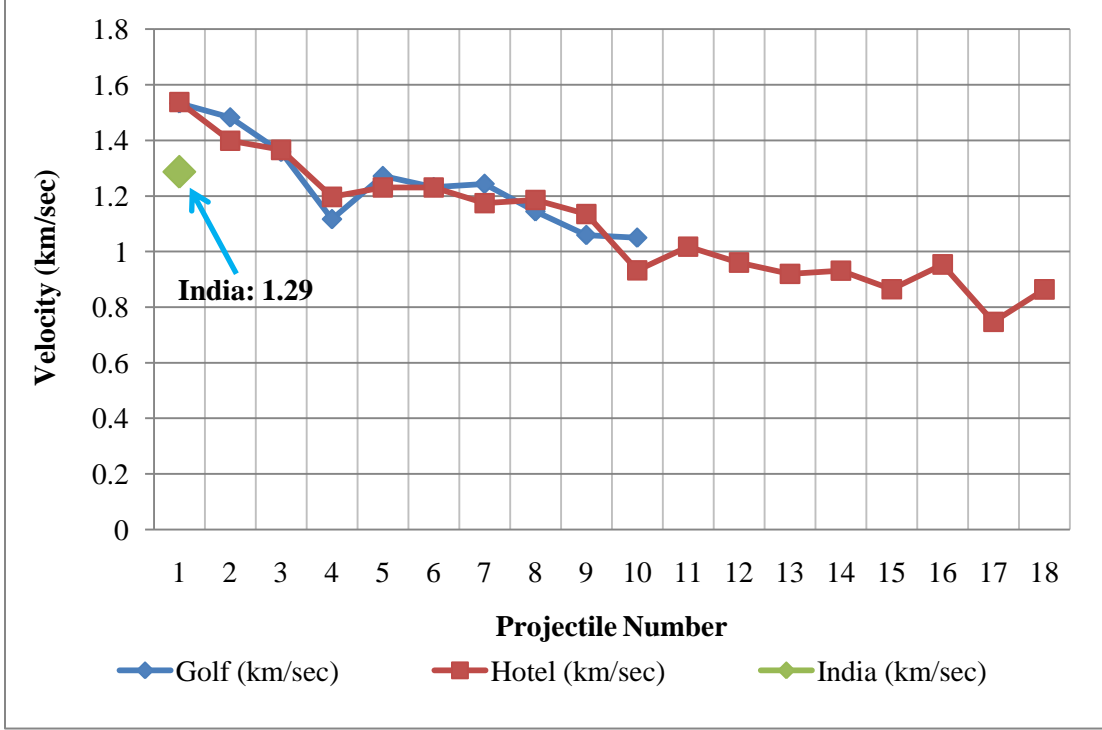
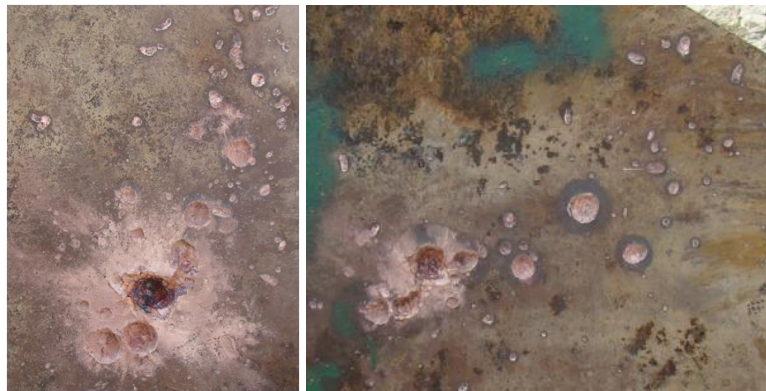


Figure 5.8 Confining Geometry Velocity Data

EFP India produced one projectile that has a velocity of 1.29 km/sec. EFP India had a difference between the actual velocity and the calculated Gurney velocity of 23% and an ECW that is 64% of its initial charge weight. Indicating that more of the explosive is working to push the projectile and thus reducing the amount of explosives wasted.

**5.2.2. Confining Geometry Dominant Projectile.** Of the three confining geometry designs, only India produces a dominant projectile that was identifiable for the three confining geometry designs. Neither EFP Golf nor EFP Hotel produce a dominant impact point. The new wave created by the diffraction of the detonation at the location where the confining cross-section increases (see Section 3.2) for EFPs Golf and Hotel, causes the projectile to break into several fragments. Figure 5.9 shows the impact clusters for Golf and Hotel.



**Figure 5.9 Impact cluster of EFP Golf (Left) and Hotel (Right)**

EFPs Golf and Hotel do not produce a dominant projectile. Even though projectiles are identifiable in the high-speed video, a dominant impact point was not present for either EFP design. EFP India produces a dominant impact point that was clearly identifiable, see Figure 5.10, and a dominant projectile was identifiable in the high-speed video, see Figure 5.11.

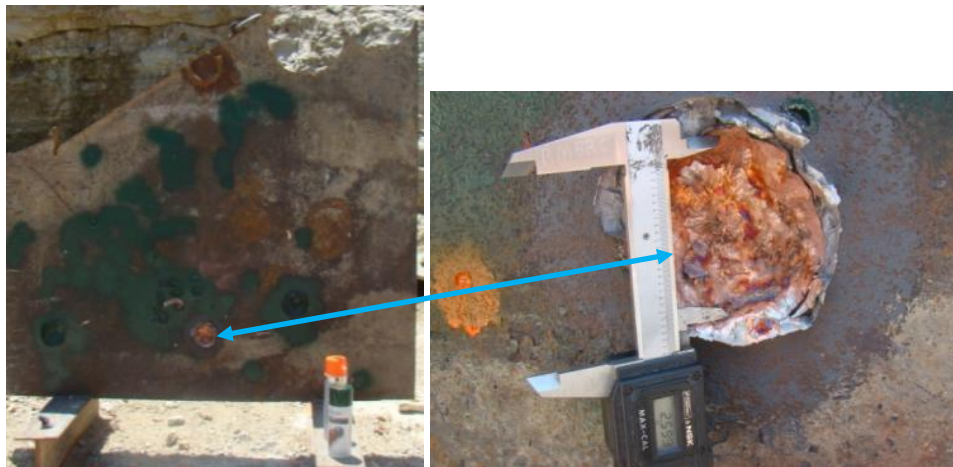


**Figure 5.10 Impact point from India**

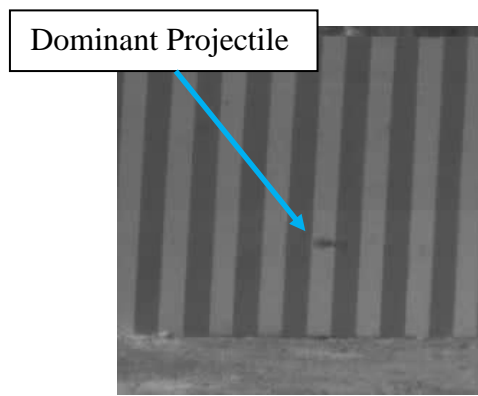


**Figure 5.11 High-speed Image of India's Projectile**

The projectile produced from EFP India has an irregular shape that was not the “cigar-like” shape recommended in Voort (2009). See Figure 5.12.



**Figure 5.12 Projectile Produced from India**

This projectile was 198.45 grams, 44% of the initial flyer plate mass (442.25 grams). This author concluded that the projectile’s shape minimizes the drag created by the water and thus allows the projectile to penetrate 2.74 meters of water.

**5.2.3. Confining Geometry Kinetic Energy.** A kinetic energy cannot be calculated for EFPs Golf and Hotel, as they do not produce a dominant projectile. India’s projectile has a velocity of 1.29 km/sec and projectile weight of 198.45 grams, producing a kinetic energy of 237,464.78 Joules.

**5.2.4. Confining Geometry Penetration.** The confining geometry test shows significant information as to how changing confining geometry affects an EFPs' performance. EFP Golf had a top insert length of 10.16 cm. At this length, the flyer plate breaks into 10 pieces that form a long thin line as they travel towards the target. Golf has a maximum penetration of 2.54 cm.

EFP Hotel has a top insert with a length of 5.08 cm. At this length, the flyer plate breaks into 18 pieces that form shorter thicker lines as they travel towards the target. Hotel has a maximum penetration of 2.54 cm. Figure 5.13 compares the confining geometry penetration data (blue).

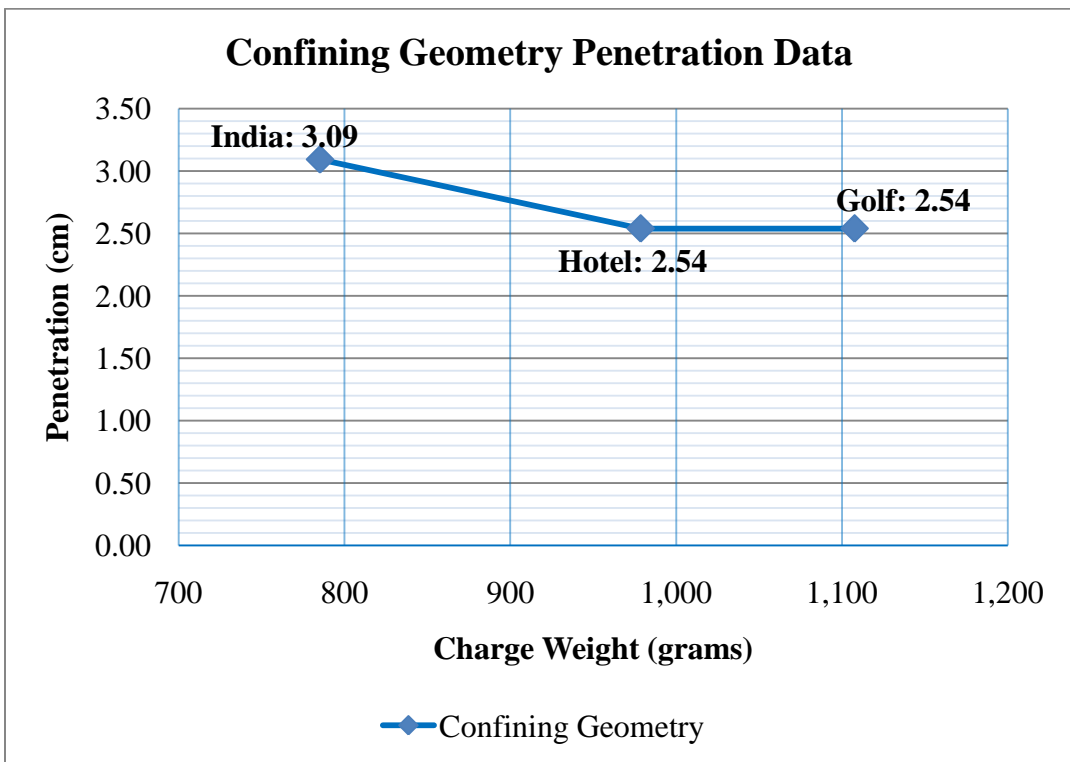


**Figure 5.13 Confining Geometry's Penetration Data**

India's projectile does not have an elongated "cigar-like" shape, but had a penetration of 3.09 cm. However, the pointed, triangular shape of the projectile resulted in one of the deepest penetration depths of this research and assisted the projectile in penetrating 2.74 meters of water.

**5.2.5 Confining Geometry Analysis.** India was the only confining geometry design that produced a dominant projectile. India's velocity was 1.29 km/sec, 0.13 km/sec faster than Alpha's. India had a deeper penetration than Alpha, 3.09 cm and 3.02 cm respectively. However, India had a slightly smaller kinetic energy than Alpha, with a kinetic energy of 237,465 joules compared to Alpha's 244,679 joules. The higher penetration with a lower kinetic energy is most likely due to the projectile's shape. See Figure 5.14.

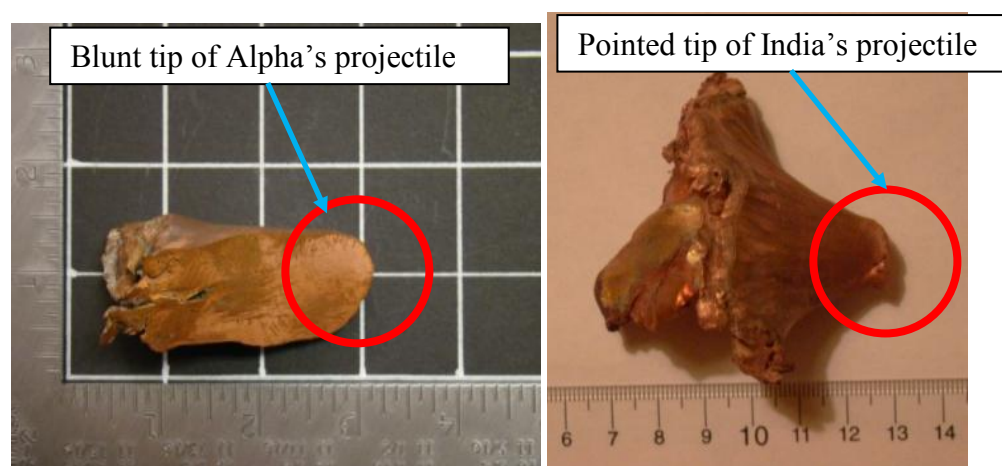


**Figure 5.14 Blunt Tipped Projectile Produced from EFP Alpha (Left) and Pointed Tipped Projectile Produced from India (Right)**

India shows improvement over EFP Alpha in percent error, charge weight used, and velocity indicating that it is possible to remove a small portion of the EFP opposite the flyer plate and still achieve a performance better than the cylindrical confinement of Alpha.

### 5.3 FLYER THICKNESS

The flyer thickness experiments test the affects the flyer thickness has on the EFPs' performance. The flyer thickness designs use a flyer with a thickness of 0.318 cm. In order to determine how the flyer thickness affects an EFPs' performance the designs tested are Juliet, Kilo, and Lima. Each flyer thickness design has a charge weight design that it was based on: Juliet uses the CW:FW ratio of Bravo, Kilo uses the CW:FW ratio of Delta, and Lima uses the CW:FW ratio of Alpha. The following sub-sections show the velocity, dominant projectile, kinetic energy, and penetration data for the flyer thickness designs. Section 5.3.5 compares the flyer thickness designs to the charge weight designs with the similar CW:FW ratio.

**5.3.1. Flyer Thickness Velocity.** The flyer thickness designs had the highest velocities of this research. EFP Juliet had a velocity of 1.71 km/sec, which was the highest velocity of any of the designs tested in this research. The difference between the calculated Gurney velocities and the actual velocities was 23%; a significant improvement over the charge weight designs. The flyer thickness designs also increase the amount of the initial charge weight used to 60%. Figure 5.15 shows the velocity data for the flyer thickness designs.



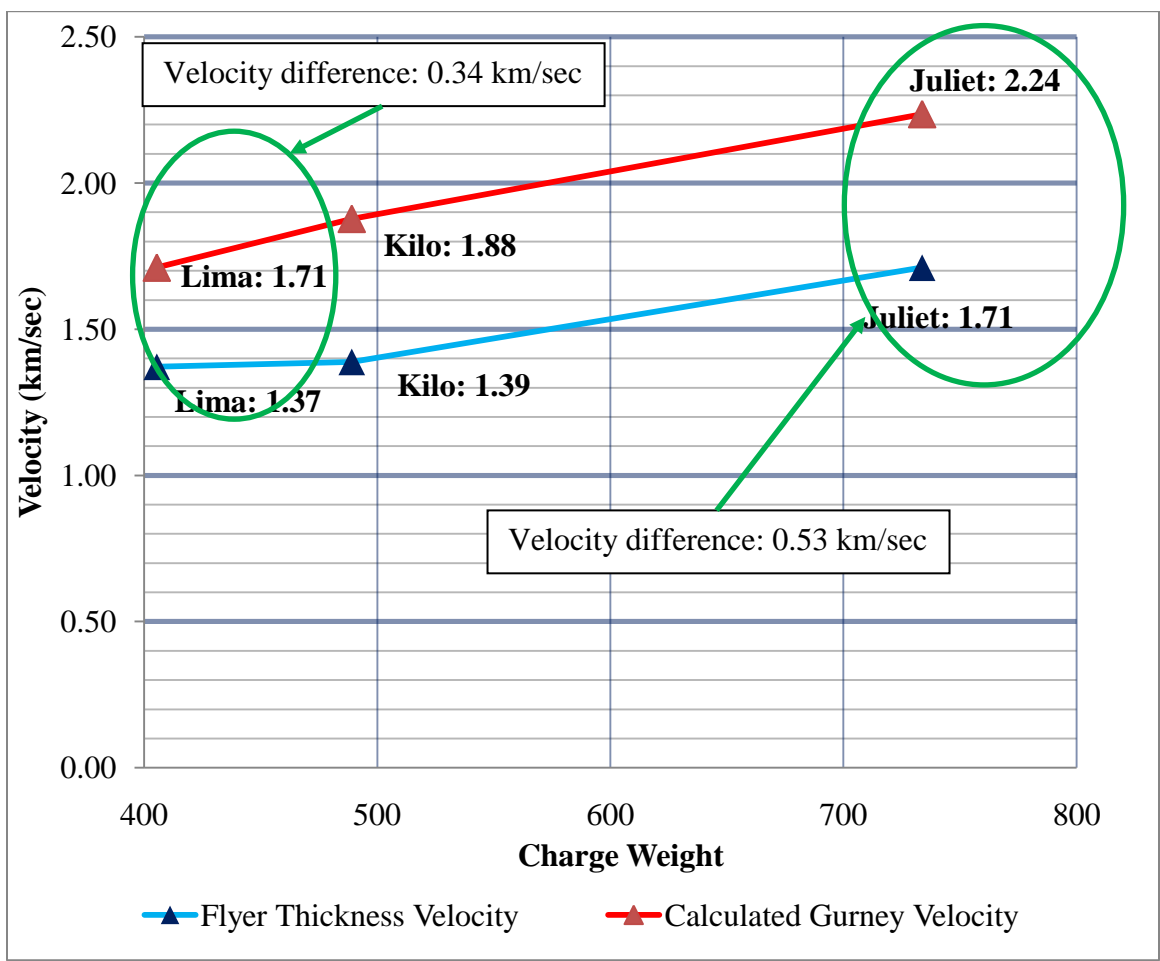
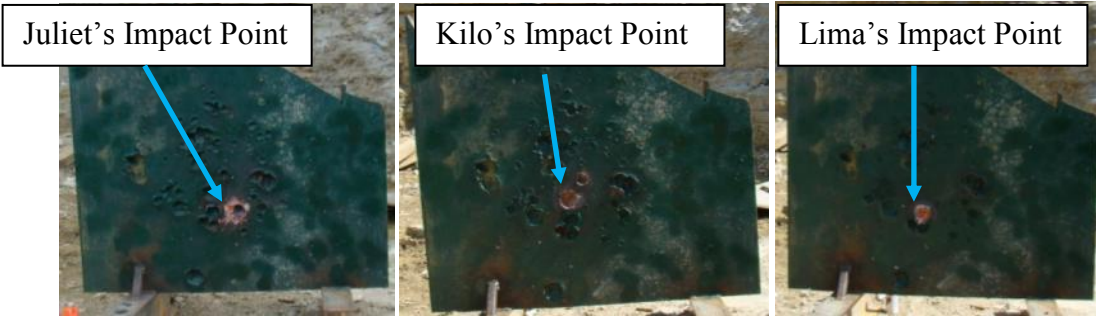


Figure 5.15 Flyer Thickness Velocity Data

Lima has a velocity difference between the actual velocity and the calculated velocity of 0.34 km/sec, 0.19 km/sec less than Juliet’s difference of 0.53 km/sec.

**5.3.2. Flyer Thickness Dominant Projectile.** The projectiles produced during the flyer thickness test are identifiable in the high-speed video and a dominant impact point exists, on the target. Figure 5.16 shows the impact point for the three flyer thickness designs.



**Figure 5.16 Flyer Thickness Impact Points: Juliet, Kilo, Lima**

When fired at the barrels filled with water, EFPs Juliet and Kilo projectiles fragmented from the impact. EFP Lima produces a projectile that was 116.23 grams, 53% of the initial flyer mass (218.29 grams). The projectile shape was an elongated “cigar-like” shape. See Figure 5.17.



**Figure 5.17 Lima's Projectile**

The flyer thickness designs are capable of forming projectiles over a large CW:FW ratio range. For this experiment, the CW:FW ratio ranged from 1.86:1 to 3.36:1.

**5.3.3. Flyer Thickness Kinetic Energy.** The projectiles produced from EFPs Juliet and Kilo broke apart during testing. Therefore, projectile weights were not available for kinetic energy calculations. Lima's projectile has a velocity of 1.37 km/sec and projectile weight of 116.23 grams, producing a kinetic energy of 109,372.18 Joules.

**5.3.4. Flyer Thickness Penetration.** The projectiles produced during this test were among the top penetrating projectiles of this research. At 3.37 cm, EFP Juliet has the deepest penetration of this research. See Figure 5.18.

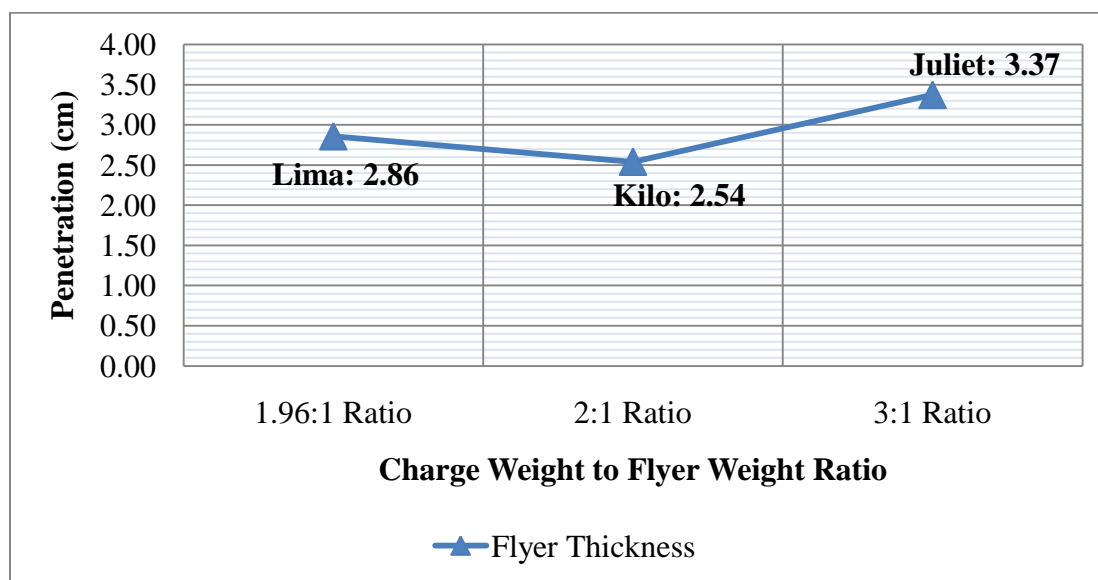


**Figure 5.18 Flyer Thickness Penetration Data**

It is unknown if charge weights larger than Juliet's will produce better performance or if there is an optimal charge weight for penetration.

**5.3.5 Flyer Thickness Analysis.** When compared to the corresponding CW:FW ratios used in the charge weight test, the reduced flyer thickness designs produce higher velocities. The calculated velocities are similar for the flyer thickness designs and their corresponding charge weight designs since the Gurney equation uses FW:CW ratios and the explosive-type is the same.

The difference between the calculated Gurney velocities and the actual velocities, for the flyer thickness designs, was 23%; a significant improvement over the charge weight designs. The flyer thickness designs also increase the amount of the initial charge weight used to 60%. Figure 5.19 shows the penetration of Alpha and Lima and their kinetic energy.

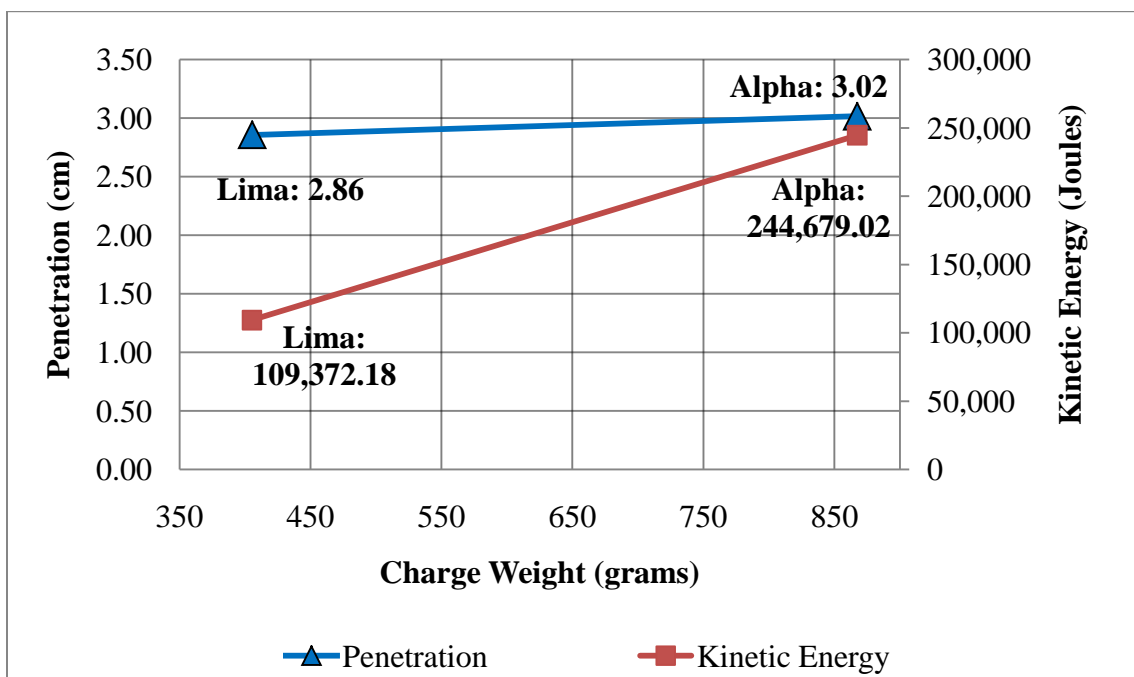


**Figure 5.19 Kinetic Energy and Penetration Comparison of Alpha and Lima**

Lima's kinetic energy was less than half of Alpha's kinetic energy but was still able to achieve a penetration of 2.86 cm, 0.16 cm less than Alpha. This indicates that kinetic energy was not a direct indicator of the projectiles ability to penetrate a target, but more so a variable of the projectiles energy density. Energy density refers to the amount of energy stored in a given system or region of space per unit volume (Dictionary.com, 2009). This means that two EFPs can produce projectiles with identical kinetic energies, but if one has a smaller cross-sectional area and a higher density than the other, it was capable of deeper penetration. The energy density could not be calculated due to the deformation of the projectiles during the soft catch.

EFP Juliet had a velocity of 1.71 km/sec, which was the highest velocity of any of the EFP designs in this research. Bravo does not have a recorded velocity and therefore there was no corresponding velocity to compare Juliet too. Kilo and Lima both produced projectiles with faster velocities than their charge weight counter parts. Figure 5.20 shows a penetration and velocity comparison of the flyer thickness designs and their charge weight counter parts.

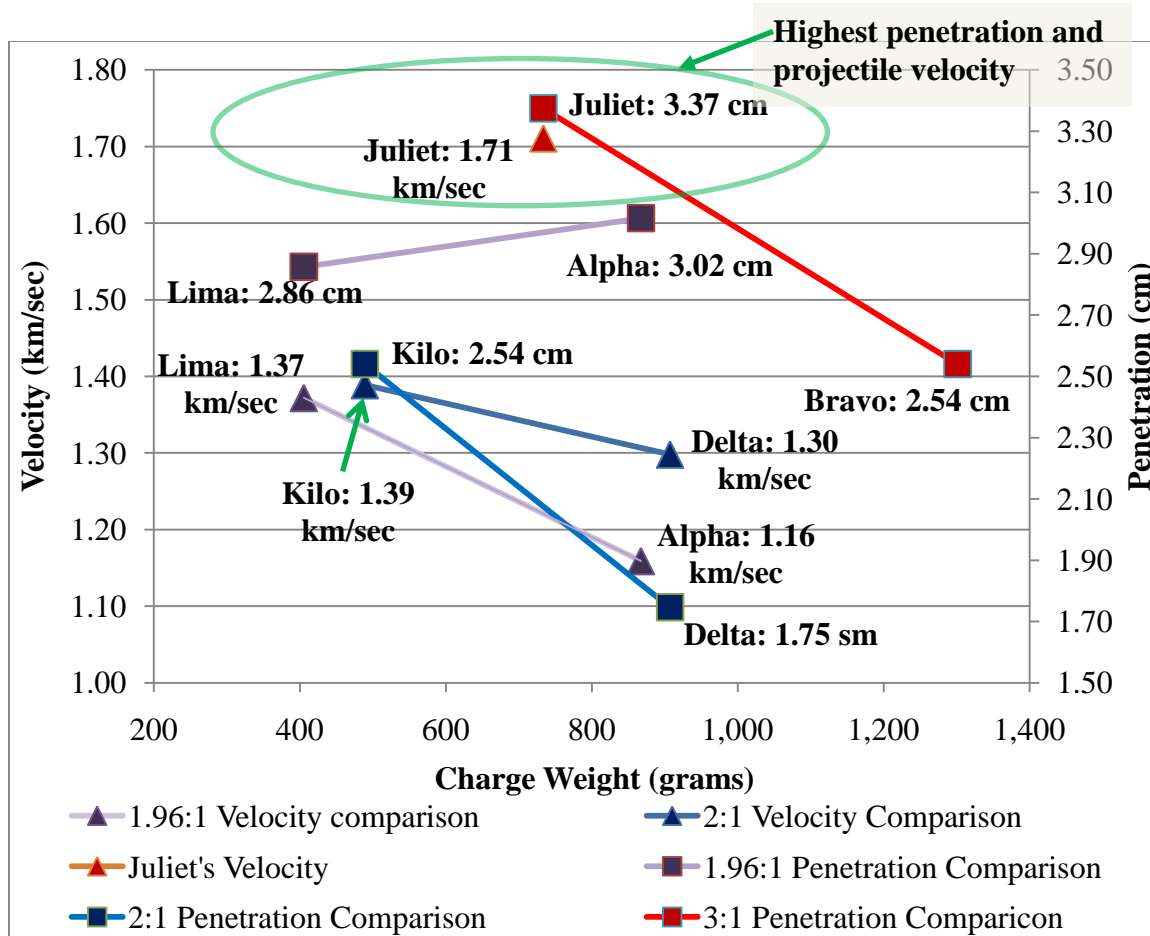


**Figure 5.20 Penetration and Velocity Comparison of Similar CW:FW Designs; Solid Color Connecting Lines Show Similar CW:FW Ratios**

Juliet had the best performance of all the EFP designs tested. This indicates that with a charge diameter of 10.16 cm, the 0.318 cm thick flyer plates significantly improved the EFPs' performance.

#### **5.4 FLYER RADIUS OF CURVATURE**

The radius of curvature designs allow for an analysis of how the flyer's radius of curvature affects an EFP's performance. The two EFP designs for this experiment are Mike and November. These designs allow this author to conclude how the flyer's radius of curvature affects the velocity of the projectiles, how the projectiles form, and how it affects penetration. Only one EFP November was tested for this research, and the impact of a planar detonation shock on a flat flyer was determined to be beyond the scope of this project; nevertheless, the important aspect is that a flat flyer plate (i.e., a so-called "platter charge") did not penetrate steel plate well enough to be of interest in this research.

The EFP designs tested are Mike and November. The following sub-sections show the velocity, dominant projectile, kinetic energy, and penetration data for the flyer radius of curvature designs. Section 5.4.5 compares the performance of EFP Mike to EFP Alpha.

**5.4.1. Flyer Radius of Curvature Velocity.** The flyer curvature test identifies how the flyer curvature affects performance. The velocity of EFP Mike's projectile was 1.27 km/sec. Mike uses 53% of its initial charge weight and has an ECW angle of 83.4 degrees. EFP November was fired in the underground testing facility and therefore, there is no recorded velocity data for EFP November.

**5.4.2. Flyer Radius of Curvature Dominant Projectile.** The projectile identified on the high-speed video, for EFP Mike, appears to be a flat flyer. Upon inspection of the impact point, this author noticed that the center of the impact has no penetration. See Figure 5.21.

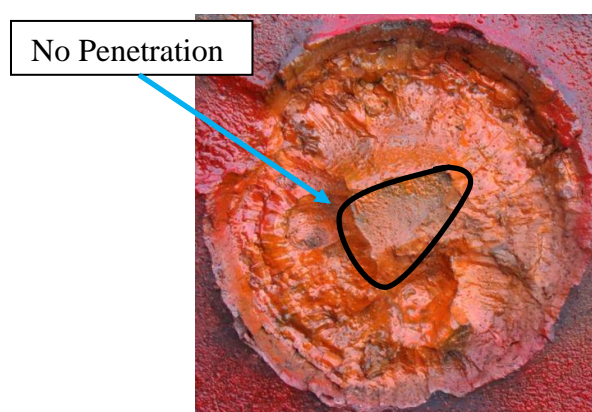


**Figure 5.21 Impact Point of EFP Mike**

The lack of penetration was assumed to be a result of the shock wave traveling through the center of the flat flyer prior to the flyer being fully shocked. This would result in the center of the flyer plate spalling, leaving a hole similar to the area outlined in black in Figure 5.21. Based on the impact point, this author concluded that the projectile produced, from Mike, has a similar shape to Mike's initial flyer plate, with the center of the flyer spalled out generating the impact point shown in Figure 5.21.

The flyer plate from EFP November fragmented prior to impacting the target, creating 10 impact points. See Figure 5.22.



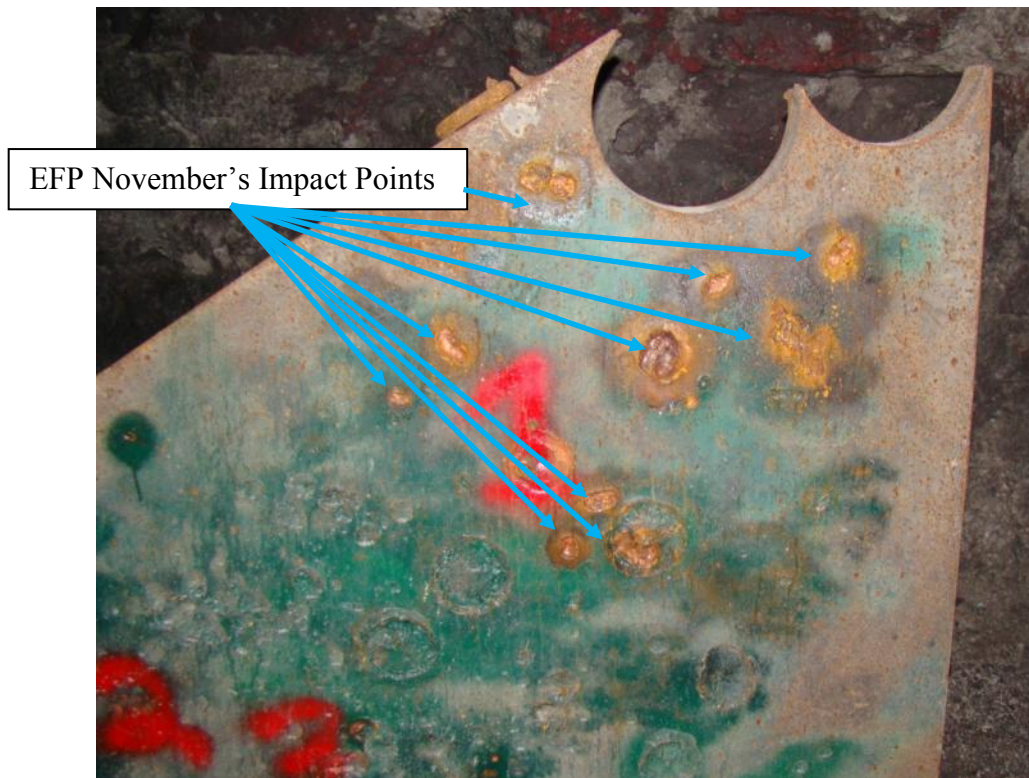


**Figure 5.22 EFP November's Impact Points**

When EFP Mike was fired into the barrels to collect the projectile, the projectile fragments and no dominant projectile weight can be collected.

**5.4.3. Flyer Radius of Curvature Kinetic Energy.** Kinetic energy calculations cannot be calculated for the flyer curvature test. The projectiles produced from EFP Mike breaks apart upon impacting the barrels; typically less than 60 grams of copper was found after the test. Penetration was the only test conducted for EFP November, and no dominant impact point was noted.

**5.4.4. Flyer Radius of Curvature Penetration.** When testing EFP November, the flyer plate breaks apart. The resulting fragments have a penetration of 2.72 cm. When testing EFP November, the flyer plate broke apart. The resulting fragments had a penetration of 2.72 cm.

When this author measured the penetration for Mike, the deepest penetration was around the center of the impact point, which was 1.2 cm. Figure 5.23 shows the penetration data for the flyer radius of curvature designs.

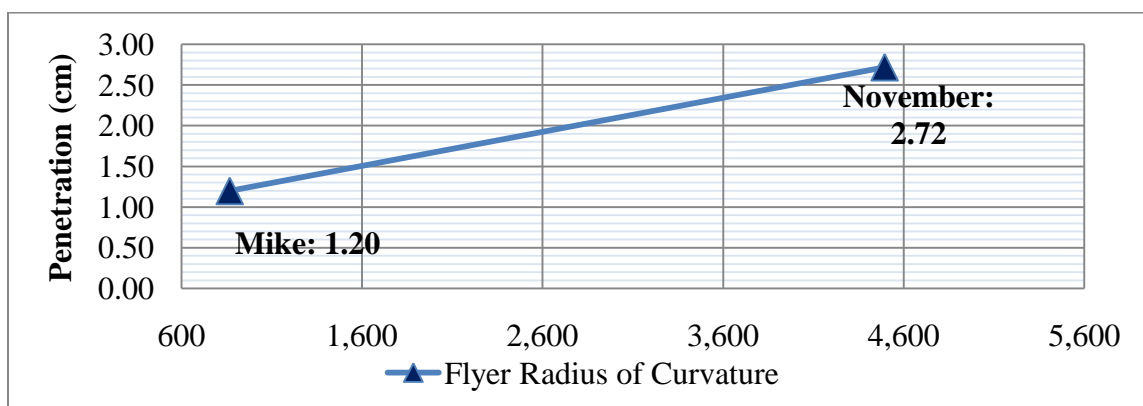


**Figure 5.23 Flyer Radius of Curvature Penetration Data**

November had a charge weight approximately five times greater than Mike's charge weight, but November's penetration is just over two times Mike's penetration indicating a significant drop in efficiency.

**5.4.5 Flyer Radius of Curvature Analysis.** Mike has an initial flyer plate that was 20.55 grams lighter than EFP Alpha, making its CW:FW ratio 2.05:1 which was closer to Delta's CW:FW ratio of 2.06:1. Therefore, to identify how the flyer's radius of curvature affects an EFP's velocity, Mike's actual and calculated velocities are compared to both Alpha and Delta's velocities in Figure 5.24.

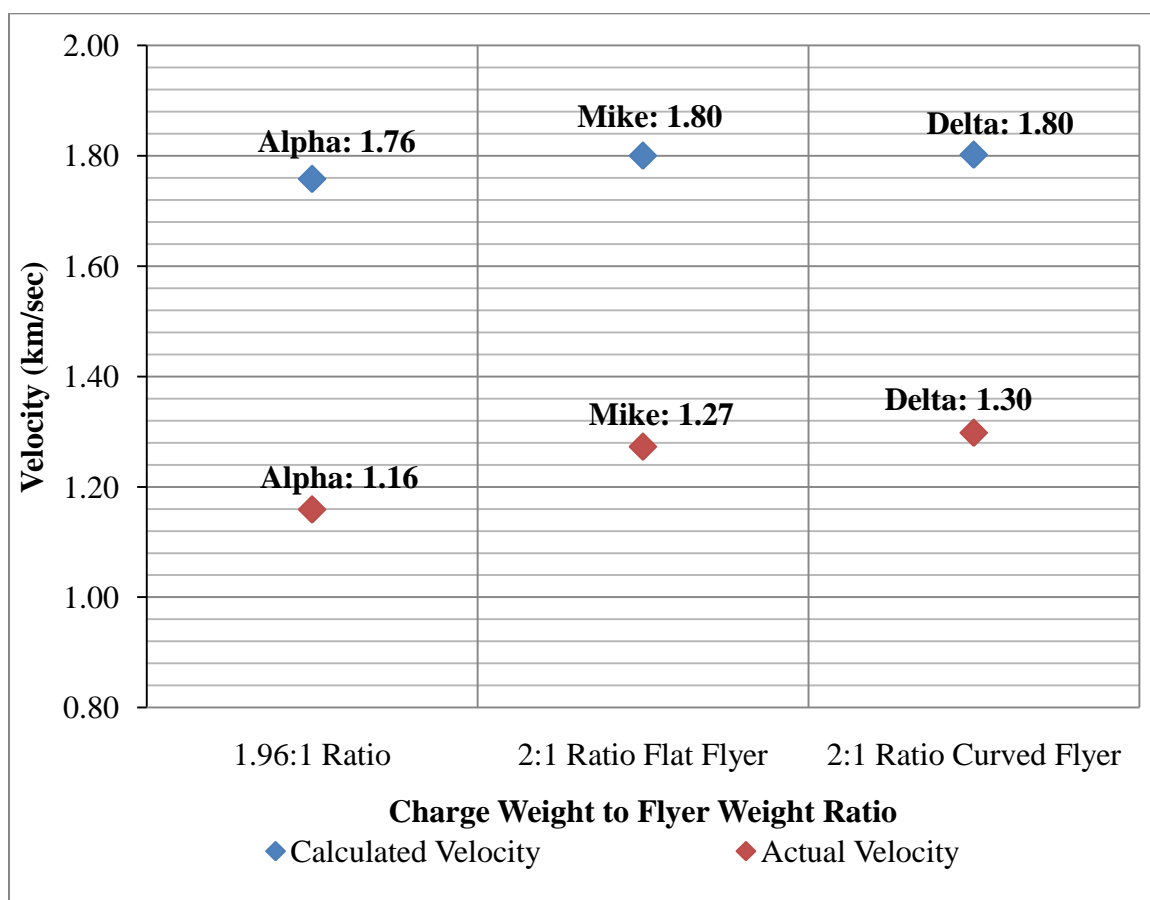


**Figure 5.24 Flyer Radius of Curvature's Velocity Data**

The velocity difference between Alpha and Mike was 0.11 km/sec. However, the difference between Delta and Mike's velocity was 0.03 km/sec. Mike and Delta have similar ECW angles, velocities, and use the same amount of explosives but EFP Delta has a penetration of 2.54 cm and Mike penetrates 1.2 cm and significantly different impact points. See Figure 5.25.



**Figure 5.25 Mike's Impact Point (Left) and Delta's Impact Point (Right)**

With Mike and Delta having the same CW:FW ratio the flyer radius of curvature test indicates that the flyer plate's radius of curvature does not affect the projectile velocity, but it does effect the projectiles formation and penetration.

## 5.5 EXPLOSIVE-TYPE

The explosive-type test used Unigel as the explosive. Unigel has a lower detonation velocity and detonation pressure than C-4. The data obtained assisted in determining how changing the explosive-type affects an EFPs' performance. The three Unigel EFP designs, for the explosive-type experiment are Papa, Oscar, and Quebec. The following sub-sections show the velocity, dominant projectile, kinetic energy, and penetration data for the explosive-type designs. Section 5.5.5 compares the explosive-type data to Alpha's performance.

**5.5.1. Explosive-Type Velocity.** The percent difference of the calculated velocity was 49%, the highest of all the EFP designs. Using the Gurney equation to calculate the velocity utilizes an approximation of  $\sqrt{2E}$ . This approximation may contribute to the increased difference. Also, using the algebraic manipulation of the Gurney equation to find the ECW with the approximation of  $\sqrt{2E}$  value may be contributing to the low percentage of initial charge weight used. The percentage of the ECW used was 33%. However, the ECW angle for the Unigel design ( $70.6^\circ$ ) was similar to the ECW angle of the charge weight test. The three EFP designs used to test explosive-type have CW:FW ratios of 3:1, 2:1, and 1.67:1. This range of ratios produces similar velocities of 0.65, 0.64, and 0.58 km/sec. Figure 5.26 shows the velocity data for the explosive-type designs.

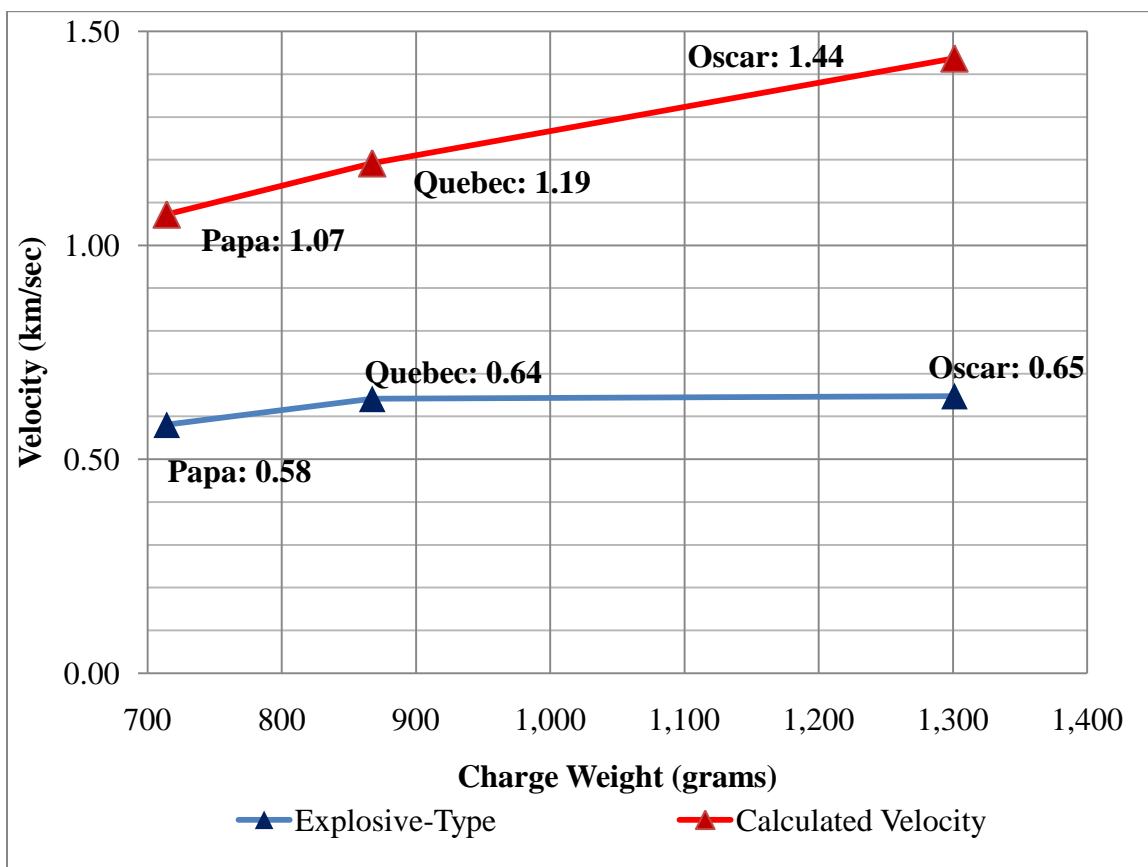


**Figure 5.26 Explosive-Type Velocity Data**

**5.5.2 Explosive-Type Dominant Projectile.** The projectiles produced from the explosives-type test had the highest percentage of the initial flyer mass, EFPs Papa and Quebec had a percentage of 99%. The projectiles retained a large percentage of the projectile weight, due to Unigel having less shock than C-4 (Worsey, 2011). A dominant projectile was identifiable in the high-speed video and a dominant impact point was present. See Figure 5.27.

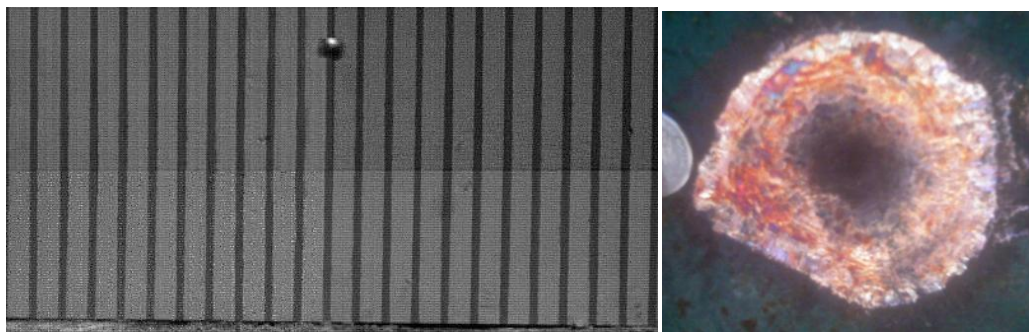


**Figure 5.27 Explosive-Type High-Speed Video (Left) and Impact Point (Right)**

The projectiles produced had a shape similar to the inverse of the initial flyer plate, where the front of the flyer plate becomes the front of the projectile. See Figure 5.28.

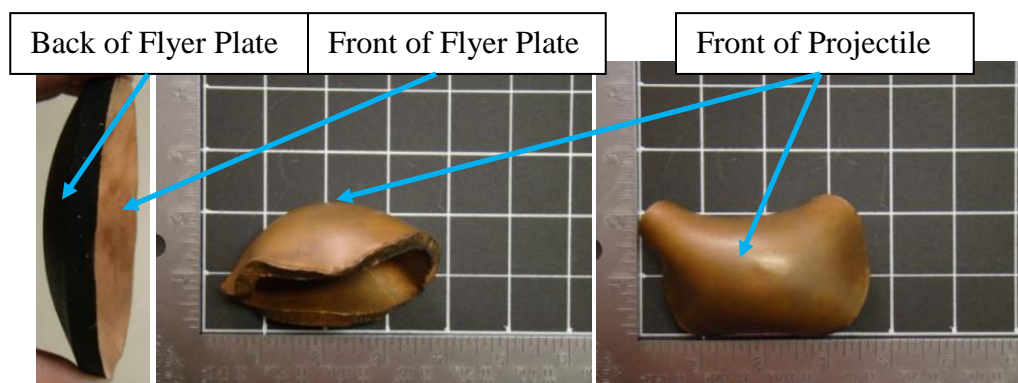


**Figure 5.28 Flyer Plate (Left), Projectile Produced from EFP Quebec (Middle and Right)**

EFP Oscar produces a projectile, which broke apart. The fragment collected indicates that the larger charge weight stretches the projectile instead of forming it. See Figure 5.29.

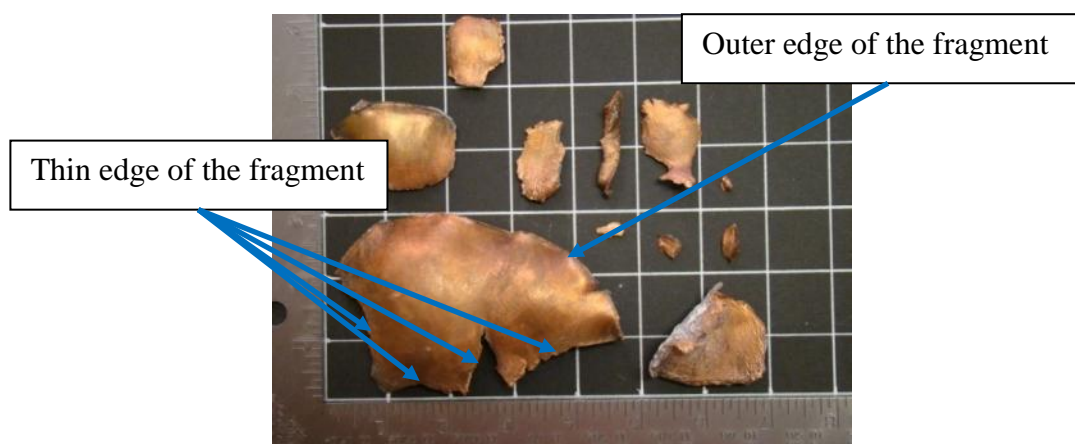


**Figure 5.29 Fragment of EFP Oscar's Projectile**

The projectile from Oscar appeared to be a dominant projectile in the high-speed video, indicating the projectile broke apart upon impact. There was one impact point on the target, indicating the projectile did not fragment upon impact the steel target. With the appearance of a dominant projectile in the high-speed video and a single impact point, indicates that the effect seen in Figure 5.29 occurred due to the soft catch method used in this research. The outer edge of the fragment is thicker than the middle, implying that the projectile stretched and tore apart from the detonation wave.



**5.5.3. Explosive-Type Kinetic Energy.** The explosive-type EFP designs produce the lowest kinetic energy of this research. EFPs Papa and Quebec have the highest projectile weights of this research, with weights of 425g and 434g. Figure 5.30 shows the kinetic energy data for the explosive-type experiment.

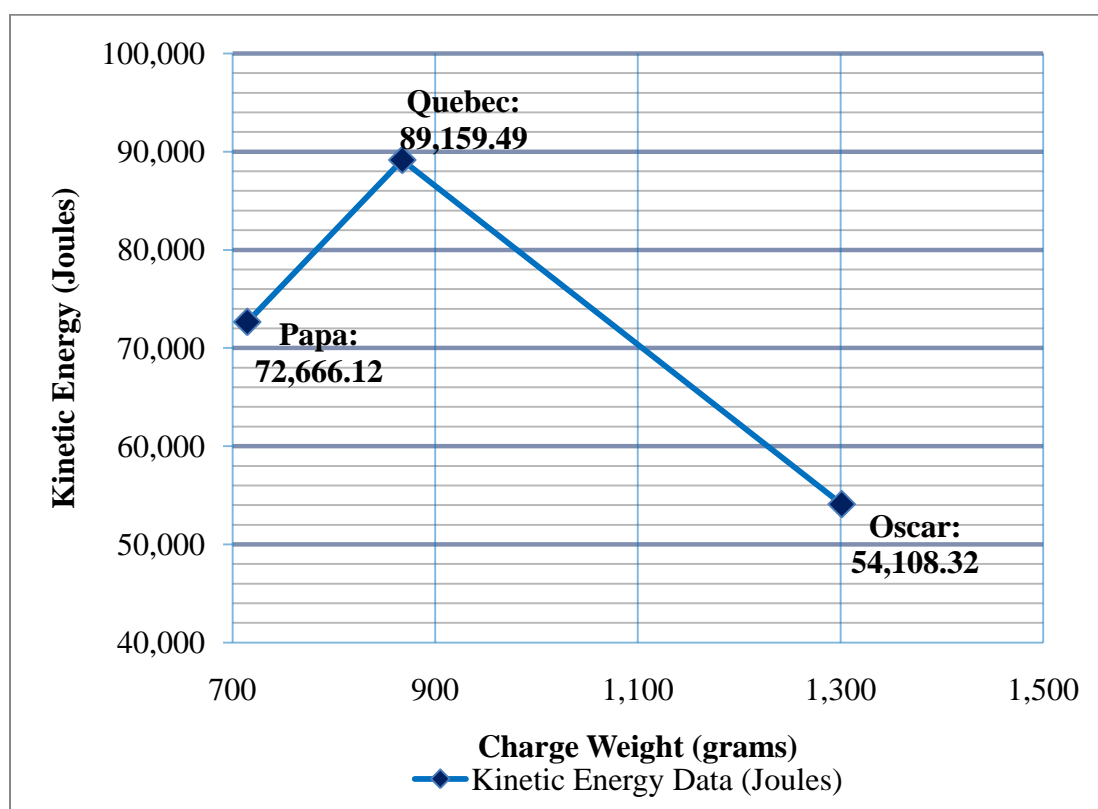


**Figure 5.30 Explosive-Type Kinetic Energy Data**

The low velocities and high projectile weights produce a low kinetic energy of 72,666.12 Joules and 89,159.49 Joules, respectively. EFP Oscar's projectile broke apart

upon impacting the barrel. However, it did produce a large fragment, shown in Figure 5.29, with a weight of 258g that was used to calculate a kinetic energy of 54,108.32 Joules.

**5.5.4. Explosive-Type Penetration.** The Unigel used in the explosives test produces dominant projectiles. However, the total depth of penetration for each impact point was 0.15 cm. Unigel does not have a high enough detonation pressure or detonation velocity to form and propel a projectile that was capable of penetrating the target more than 0.15 cm.

**5.5.5 Explosive-Type Analysis.** The Unigel designs produced projectiles with significantly slower velocities and penetration than Alpha. This indicates that Unigel does not have a high enough detonation pressure and detonation velocity to form and push a projectile that can perform as well as Alpha.

The Unigel designs had the highest projectile weight out of all the designs tested. The projectiles retained 99% of the initial flyer weight. This is because the flyer plates are not being shocked as hard as they are with C-4.

## **5.6 EFFECTIVE CHARGE WEIGHT ANALYSIS**

During the research, this author noticed a discrepancy between the actual velocity of projectiles and the velocities calculated using the Gurney equation. The calculated velocity is 20-55 % faster than the actual velocity. This is explained as follows.

According to *Explosives Engineering*,

*“The gases expanding to the sides will not exert any pressure on the plate; so their energy is lost. This can be thought of as effectively reducing the mass of the explosive charge. It has been found through numerous experimental observations that the effective charge weight,  $C_e$ , is that which would be contained within a cone with a 60 degree base angle and a base diameter equal to the charge diameter.” (Cooper, 1996).*

Therefore,  $C_e$  is the amount of explosive that pushes a projectile, essentially the ECW. In order to better approximate the projectile’s velocity with the Gurney equation, for this research one must first identify the ECW and the ECW angle. Cooper provides a method for calculating the ECW volume, as shown in Equation 5.1.

$$\text{Effective Charge Weight Volume} = \frac{\pi R_1^3}{3} \text{Tan}(\theta) \quad \{5.1\}$$

**(Cooper, 1996)**

Where,  $R_1$  equals half the flyer diameter and  $\theta$  is the angle of the ECW cone. Cooper states that the angle  $\theta$  for the ECW of an unconfined explosive cylinder is 60 degrees.

Lim (2010) states in his research *Deformation of an Explosively Driven Flat Metallic Flyer during Projection* that the ECW angles he tested were 40 and 60 degrees.

Given that both Lim and Cooper use 60 degrees as an ECW angle, this author used 60 degrees for  $\theta$  in Equation 5.1. For this equation,  $R_1$  is 4.76 cm (1.875 inches). This equation was used to calculate the ECW volume for every EFP.

When calculating the ECW volume of a cylindrical charge with a height less than  $R_1 \tan(\theta)$ , the maximum height of the cone is where the explosive column ends. The explosives column is the charge length. See Figure 5.31.

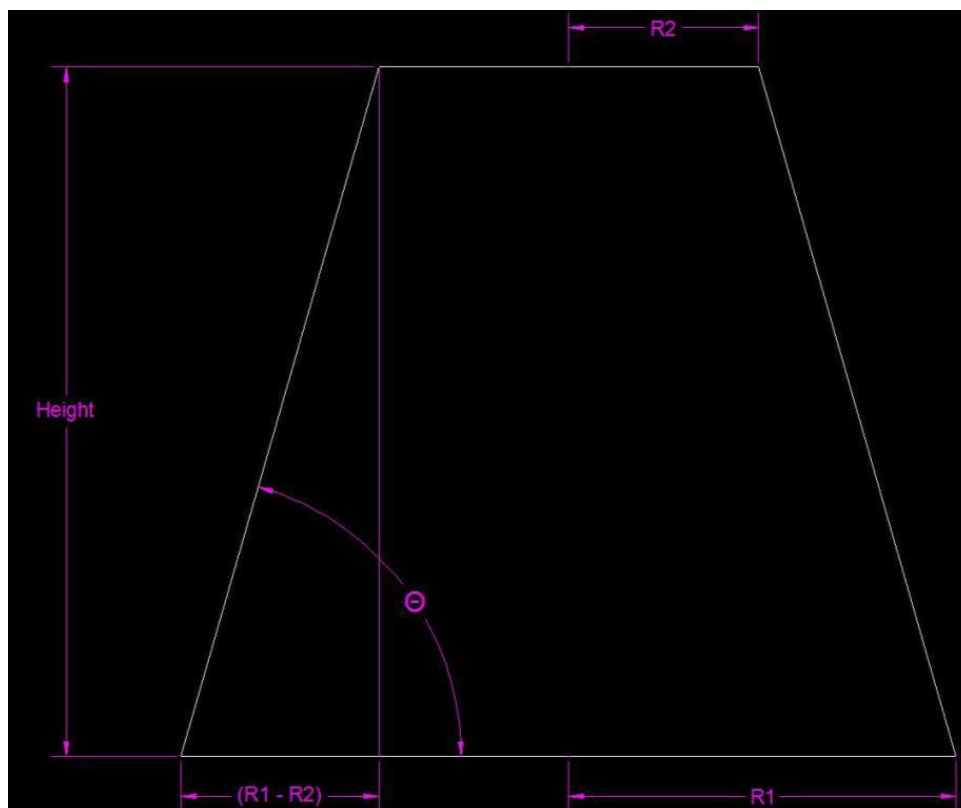


**Figure 5.31 Effective Charge Weight**

In *Explosives Engineering*, Cooper does not identify how deep the blasting cap is inserted into the charge. He also does not identify if a blasting cap is inserted into the charge, or if the end of the cylindrical charge is the point from the bottom of the blasting cap to the flyer, or if a donor charge is used to set off the explosive (planar wave initiation). A donor charge is an exploding charge producing an impulse that impinges upon an explosive “Acceptor” charge (Rudolf Meyer, Josef Kohler, Axel Homburg, 2007).

Therefore, this author assumed a point initiation and the ECW has a maximum height explained in Equation 5.2.

$$\textit{Maximum Height for ECW Cone} = CL - CD - \textit{Flyer Thickness} \quad \{5.2\}$$

This makes the ECW the frustum of a right circular cone. Therefore, to calculate the ECW volume, Equation 5.3 is used.

$$\textit{Volume} = \left(\frac{h\pi}{3}\right) (R_1^2 + R_1r + r^2) \quad \{5.3\}$$

(2010)

Where  $R_1$  is the radius of the flyer and  $r$  is the radius of the top of the cone, and  $h$  is the height calculated in Equation 5.2.

Once the ECW volume was calculated, this author calculated the ECW two ways. The first method for calculating the ECW, was multiplying the ECW volume times the TMD of C-4,  $1.58 \text{ g/cm}^3$  (W. P. Walters, J. A. Zukas, 1989). The second method of calculating the ECW volume was multiplying the ECW by the packed density of each individual EFP. Due to author's decision to hand pack each EFP, each design did not have the same packing density. Voort's research *IED Effects Research at TNO Defense Security and Safety* identified that varying packing density does not significantly affect the EFPs performance. The packed density is the EFPs' charge weight divided by the volume of each EFP.

To identify if the calculated ECWs are indeed the ECWs that produced the actual velocity, the ECWs are placed into the Gurney equation and the velocities are recalculated. When using both methods of calculating the ECW, a discrepancy still existed between the actual velocity and the velocities calculated with the ECWs calculated using the method described in *Explosive Engineering*. This implies that the ECW volume has an ECW angle,  $\theta$ , equal to something other than 60 degrees and led to an algebraic manipulation of Equation 5.4.

$$2E = \frac{MV^2}{c} + \frac{1}{3}(V_0^2 - VV_0 + V^2) \quad \{5.4\}$$

$$V_0 = V\left(1 + \frac{2M}{C}\right) \quad \{5.5\}$$

Where V is velocity, M is the initial mass of the flyer, C is the charge weight, E is the specific explosive kinetic energy, and Equation 5.5 replaced  $V_0$ . Manipulation of Equation 5.4, using the Quadratic equation, to solve for  $C_e$  results in Equation 5.6.

$$C_e = \frac{-(-5M) \pm \sqrt{(-5M)^2 - 4\left(\frac{6E}{V^2}\right)}}{(6E/V^2)} \quad \{5.6\}$$

By solving Equation 5.4 for  $C_e$ , based on the actual velocity, the value calculated for  $C_e$  is the ECW. After calculating the ECW,  $C_e$  is inserted into the Gurney equation to verify that the calculated ECW will give the actual velocity of the projectile. This author calculated  $C_e$  for each EFP design.

To calculate the ECW angle  $\theta$ , the ECW is divided by the packing density for each EFP tested; not the TMD of the explosive used. This provides the ECW volume. The ECW volume is added to the volume of the flyer. See Figure 5.32.

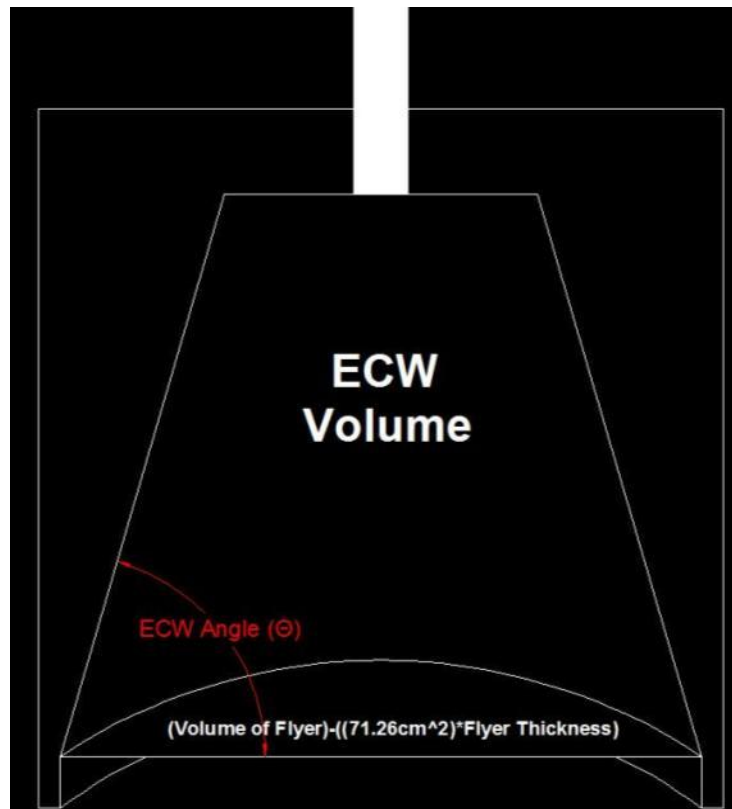


**Figure 5.32 Volume of ECW Volume used in Calculating ECW Angle**

To solve for  $\theta$ , insert the calculated ECW volume into Equation 5.3, to solve for  $r$ , and then place the data for  $r$  into Equation 5.7.

$$\theta = \tan^{-1}\left(\frac{h}{R-r}\right) \quad \{5.7\}$$



The Theta calculations for each EFP design, are in Table 5.2. An unknown (unk) is in the cells for EFP designs Bravo and November, because EFPs Bravo and November have no velocity data to calculate the ECW angle.

**Table 5.2 Effective Charge Weight Angle for Each EFP Design**

Experiment	EFP Design	$\theta$ (°)	Physical Parameter $\theta$ (°)
CHARGE WEIGHT	Original	76.42	78.63
	Bravo	unk	
	Foxtrot	76.45	
	Delta	85.78	
	Alpha	82.30	
	Echo	83.85	
	Charlie	66.98	
Confining Geometry	Golf	71.04	72.99
	Hotel	73.78	
	India	74.15	
Flyer Thickness	Juliet	85.05	75.12
	Kilo	81.71	
	Lima	58.60	

**Table 5.2 Effective Charge Weight Angle for Each EFP Design, Continued**

Flyer Radius of Curvature	Mike	83.43	83.43
	November	unk	
Explosive Type	Oscar	70.95	70.62
	Papa	69.07	
	Quebec	71.83	

The average ECW angle for all the EFP designs is 76.2 degrees. The ECW angles shown in Table 5.2 indicate that the PVC confinement increases the ECW angle from the 60 degrees described for an unconfined cylindrical charge in *Explosives Engineering*. As PVC does not have a high confining strength, and it increases the ECW angle to 76.2 degrees, a material with a higher confining strength may increase the ECW angle to utilize more of the initial charge weight of the Original EFP design, reducing the difference between the actual velocity and the predicted velocity using the Gurney equation.

## 6. CONCLUSIONS AND RECOMMENDATIONS

This author selected and tested five physical parameters of an EFP, to identify how changing each physical parameter affects an EFP's performance. The intent of this research is to assist in producing a matrix, which enables a researcher to choose a desired projectile performance need, and identify what physical parameters will produce the desired results. In addition, this will provide an understanding of how changes in the physical parameters of an EFP allow for a design that utilizes each of its physical parameters to achieve a higher performance. This understanding will allow Missouri S&T to produce future EFP designs suitable for a wide range of performance needs.

Eighteen EFP designs were constructed and tested for projectile velocity, production of a dominant projectile, and penetration. The kinetic energy was also calculated for designs that produced a dominant projectile and had a recorded velocity. This author concluded that modeling of the EFP designs prior to testing would reduce the overall time and cost by identifying designs that perform poorly. *Explosives Effects and Applications*, Section 10.2 Explosively Formed Projectiles (Chris A. Weickert, 1998), supports this conclusion. Weickert also states that modeling requires support from empirical data. Therefore, modeling the designs should be the first step in identifying how changing the physical parameters of an EFP affects its performance.

Table 6.1 shows a summary of the data for each EFP, discussed in Section 5. An "unk" is placed in the cells that no data was obtained. The EFPs are in the appropriate testing order. For each column, the highest data is highlighted in green.

**Table 6.1 Data Summary**

<b>Experiment</b>	<b>FFP</b>	<b>Penetration (cm)</b>	<b>Actual Velocity (km/sec)</b>	<b>Projectile Weight (grams)</b>	<b>K.E. Test (Joules)</b>
<b>Charge weight</b>	Original (1,389.123 grams)	2.86	1.39	Unk	Unk
	Bravo (1,301.243 grams)	1.75	unk	Unk	Unk
	Foxtrot (1,082.952 grams)	2.54	1.36	188.52	174,255.00
	Delta (907.185 grams)	2.54	1.30	248.06	209,107.58
	Alpha (867.495 grams)	3.02	1.16	364.29	244,679.02
	Echo (810.796 grams)	3.02	1.15	326.02	214,441.28
	Charlie (453.592 grams)	1.75	0.84	297.67	106,250.89
<b>Confining Geometry</b>	Golf (1107.616 grams)	2.54	1.25	Unk	Unk
	Hotel (978.626 grams)	2.54	1.09	Unk	Unk
	India (785.282 grams)	3.09	1.29	198.45	237,464.78
<b>Flyer Thickness</b>	Juliet (733.686 grams)	3.37	1.71	Unk	Unk
	Kilo (489.029 grams)	2.54	1.39	Unk	Unk
	Lima (405.398 grams)	2.86	1.37	116.23	109,372.18
<b>Flyer Radius of Curvature</b>	Mike (867.495 grams)	1.20	1.27	Unk	Unk
	November (4,493.399 grams)	2.72	unk	Unk	Unk
<b>Explosive-Type</b>	Oscar (1,301.243 grams)	0.15	0.65	257.98	54,108.32
	Papa (714.408 grams)	0.15	0.58	425.24	72,666.12
	Quebec (867.495 grams)	0.15	0.64	433.75	89,159.49

The following sub-sections discuss the data Shown in Table 6.1.

## 6.1 CHARGE WEIGHT

The charge weight experiment identifies a connection of the head height to projectile performance. An explosive does not produce more energy per unit volume of explosives with a larger explosive charge weight than it will per unit volume of explosives with a smaller explosive charge weight. What does increase with a larger charge weight is the volume of gas produced (W. P. Walters, J. A. Zukas, 1989). It is for this reason that the Gurney equation value for  $E$  does not change with the charge weight. Therefore, the detonation wave's shape, and how the detonation wave interacts with the flyer plate, forms the projectile's shape. A change to the charge weight creates changes in the charge length and head height, thus changing the head height and detonation wave's shape.

With the larger charge weights, the FW: CW is reduced, indicating the potential for an increased projectile velocity. The velocity data acquired indicates that the decrease in charge weight results in a decrease in velocity. However, the designs with a larger charge weight than Alpha (867.495 grams), had projectiles that broke apart, resulting in the absence of a dominant projectile. This indicates that there is an optimal charge weight for penetration, of an EFP with the physical parameters explained in Section 3, of 868 grams.

EFP designs Alpha and Echo had similar performances. However, Alpha's projectile had a higher projectile weight and kinetic energy than Echo. The difference in the projectile weight could be due to Echo's projectile losing mass when it impacted the barrels for the dominant projectile test. A different soft catching method might better determine if the projectiles produced from Alpha and Echo have the same projectile

weight. In addition, a different soft catching method may allow for more accurate projectile shape determinations and weights for all of the EFP designs.

## **6.2 CONFINING GEOMETRY**

This experiment supported the theory that it is possible to remove a portion of the cylindrical charge and still obtain equal or higher performance to the top performing charge weight design.

India had a higher velocity, penetration, and a higher percentage of EFW to initial charge weight than that of EFP Alpha. When comparing the percentage of the initial charge weight used to propel the flyer, India used more of the initial charge weight than Alpha. This indicated that a small portion of the EFP charge near the initiation end of the Original design did not push the projectile, although it was required for the detonation wave development.

The projectile formed from India has a pointed tip instead of a blunt tip similar to the projectiles observed in the charge weight test. The pointed tip and the increased velocity of India generated a higher energy density resulting in higher penetration. Figure 5.14 (page 84) shows the projectile produced from Alpha and the projectile produced from India. The pointed, triangular shape of the projectile penetrated 2.74 meters of water, one of the highest penetration depths of this research. India penetrated the target 3.09 cm.

Using a shorter top insert length, for example 2.54 cm, could improve the performance while using less explosives. In addition, the angle in which the pipe reducer expands from the top insert inner diameter to the diameter of the top insert could be

examined. Several different confining geometries could be constructed and tested to further identify how changing the confining geometry affects the wave dynamics inside the EFP and ultimately affect the EFP's performance.

### **6.3 FLYER THICKNESS**

The flyer thickness experiment provided valuable insight into the affects flyer thickness has on penetration, and demonstrated how energy density is important to the projectile's ability to penetrate a target. The flyer thickness experiment shows that the 0.32 cm thick flyer plates form dominant projectiles for CW:FW ratios ranging from 3:1 to 1.92:1. The resulting projectiles have higher velocities and penetrations than the charge weight designs that have similar CW:FW ratios.

EFP Juliet has the highest penetration and velocity of the flyer thickness designs. Juliet had a flyer thickness of 0.32 cm and a charge weight of 733.69 grams. Juliet has the highest penetration and velocity of all the EFP designs in this research and it was the top performing EFP of this research.

The improved velocity of the projectile, given the same FW:CW ratio and a lighter flyer plate, implies that the confining strength of the PVC cylinder has an effect on the velocity, which is supported by the ECW calculations performed in Section 5.6.

Since the flyer plate is half as thick as the 0.68 cm flyer plate, it took half the time for the shock wave to travel through the apex of the flyer plate with C-4 as the explosive. Further research is needed to identify how flyer plates of the same diameter, but of different masses, are pushed by identical FW:CW ratios. In addition, further research is

needed to identify if a flyer plate thickness to flyer diameter ratio and/or a flyer plate thickness to charge diameter ratio exists.

#### **6.4 FLYER RADIUS OF CURVATURE**

The flyer curvature experiment identifies that there is an interaction between the flyer's radius of curvature and the detonation wave, and this interaction determines the projectile's shape. When EFP Mike's projectile is compared to Delta's projectile, the velocities are similar, differing by 0.03 km/sec. Mike and Delta have the same FW:CW ratio. This indicates that the two flyer plate radii, tested in this research, do not affect the projectile's velocity.

Mike's projectile penetration is 1.2 cm, about half of Delta's projectile penetration. This indicates that the flat flyer plate effects the projectile's formation, resulting in a projectile with low energy density and a poor penetration.

Further research is needed to identify the full effects the flyer plate's radius of curvature has on an EFP's performance. Such research should include a plate with a radius of curvature of 4.75 cm (hemispherical flyer plate) and other flyer plate radii in between the flat flyer plate and a hemispherical flyer plate.

#### **6.5 EXPLOSIVE-TYPE**

The data obtained in the explosives-type experiment indicates that Unigel does not perform as well as C-4 when used as the explosive for an EFP. The Unigel EFPs have poor penetration. This is most likely due to their projectile shape and slow projectile velocities.



Papa, Oscar, and Quebec have dominant projectiles that are 99 % of the initial flyer weight. The explosive-type designs have projectile velocities of 0.65 km/sec (Papa), 0.58 km/sec (Oscar), 0.64 km/sec (Quebec). These velocities are approximately half of Alpha's projectile velocity, 1.16 km/sec. Each design penetrated the target 0.15 cm, which is considerably lower than EFP Alpha's 3.02 cm. However, the explosive-type designs retained the highest percentage of the initial flyer weight.

This performance data indicates that there is a correlation of the explosive detonation pressure and detonation velocity to the projectiles' performance. The detonation pressure and detonation velocity of Unigel is incapable of producing performance data similar to Alpha.

In addition, an examination of Unigel with a thinner flyer plate will assist in identifying the explosive -type's effect on an EFPs performance.

## **6.6 OVERALL CONCLUSION**

Of the physical parameters tested, the charge weight and flyer thickness affected the projectile's performance the most. In the charge weight experiment the penetration increased with charge weight until the charge weight exceeded Alpha's. Once the charge weight exceeded Alpha's there was a decrease in projectile weight, penetration, kinetic energy and energy density. As the charge weights increase the recorded velocity for each projectile continued to increase. It appears as though the velocity starts to flatten out with the higher charge weights. With EFP Original the penetration begins to increase again. This is due to Original's high velocity overcoming the loss of energy generated from the projectile's breaking apart.

The flyer thickness designs had the best performance of all the EFPs tested and indicate that the 0.635 cm flyer thickness is too thick for an EFP of this charge diameter. The data obtained throughout the course of this research indicates that a design with a curved flyer plate 0.318 cm thick flyer, a confining geometry similar to the geometry used in the confining geometry experiment, and with C-4 as the explosive could be the optimal design, with the physical parameters that were held constant for this research. Further testing is needed to identify the ideal top insert length and charge weight.

## 7. FUTURE WORK

Future work should address the several recommendations made in the subsections of Section 6, Conclusions and Recommendations. Also, from the conclusions drawn in Section 6, future research should investigate how changing multiple physical parameters affect an EFP's performance. This research only covers five of several physical parameters of an Original EFP. Of the physical parameters discussed in Section 3, the remaining physical parameters to be analyzed are confinement thickness, confinement strength, diameter of the flyer, diameter of the EFP, charge length, flyer material, and cap depth. A further study on the affects an EFP's physical parameters have on its performance, in combination with the analysis performed in this research, will allow researchers and Missouri S&T to generate an EFP design optimal for future testing needs.

One of the problems encountered during this research is that the projectiles tended to break apart upon impacting the capture barrels. A soft catching method using a series of materials with different densities, positioned so the projectile impacts a material less dense than water and then progresses into water would assist in preserving the projectile's shape and weight. Similar to the soft catching methods described in *IED Effects Research at TNO Defense Security and Safety* (Voort, 2009) or *Explosively Formed Projectiles* (Dr. James N. Willson; Dr. David E. Lambert, and Mr. Joel B. Stewart, 2006), these methods could also reduce the number of projectiles that shatter when impacting the barrels.

A collection method for the velocity data utilizing an oscilloscope, in addition to a high-speed camera, could increase the accuracy of the velocity data. This would enable

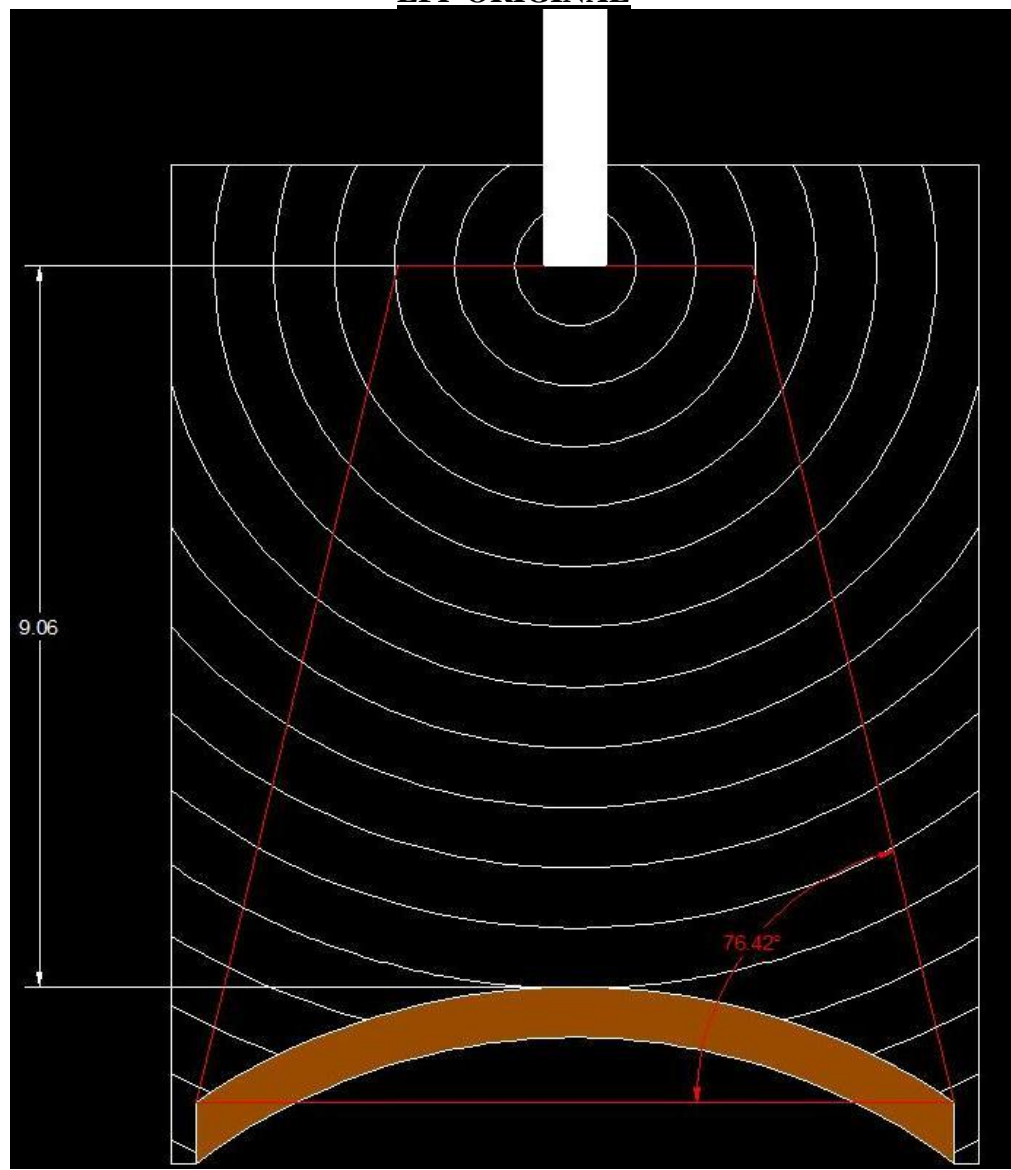
high-speed video along with an oscilloscope for more accurate velocity readings, a second velocity collection system, and better visualization of the projectile in flight. The oscilloscope method could also collect data from the EFP designs fired in the underground testing facility.

## **APPENDIX**

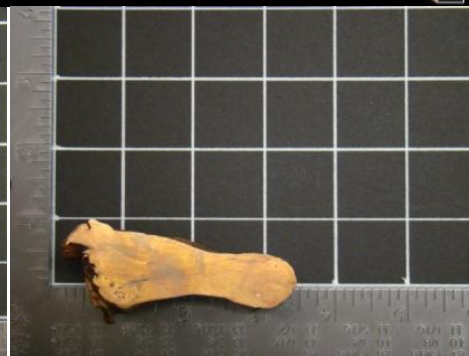
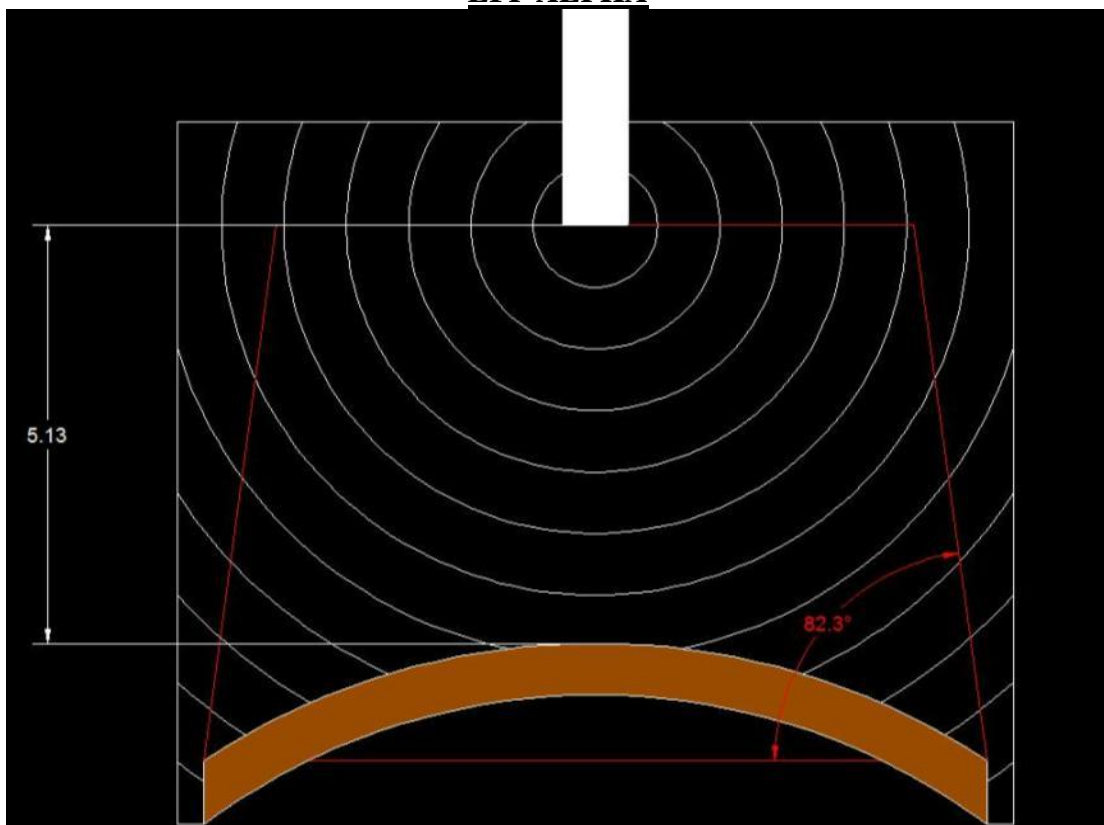
### **PERFORMANCE DATA**

This Appendix includes an AutoCAD drawing of each EFP design, a picture of the target showing the typical impact for each design, and a picture of the projectile or projectiles collected. Each AutoCAD drawing shows the detonation wave expanding through the EFP as a time-step function. Each step is one microsecond. The AutoCAD drawings also show the design's HH and ECW angle. The pictures of the projectiles are taken on a 2.54 cm grid, with the exception of the picture of India's projectile, which is taken with a centimeter scale in the picture. The penetration, velocity, dominant projectile, and kinetic energy data is listed in Section 5.

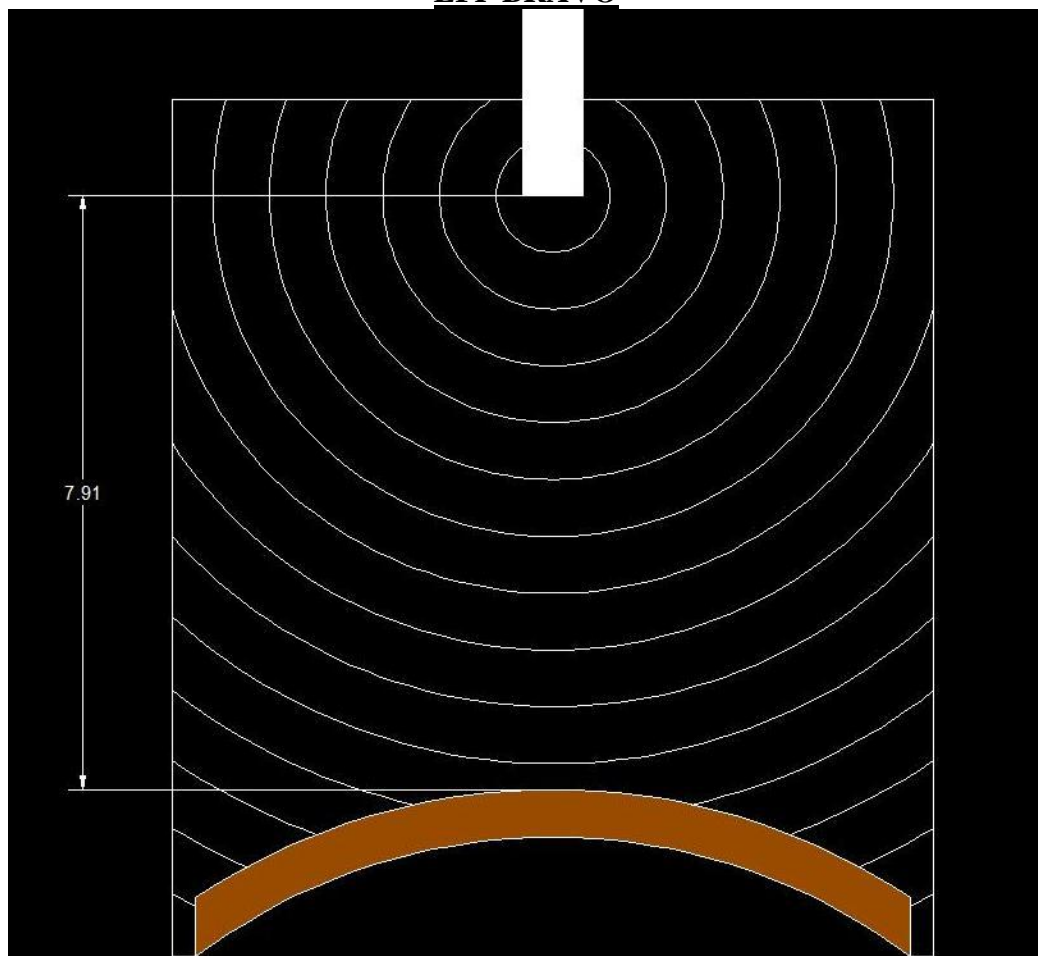
**EFP ORIGINAL**



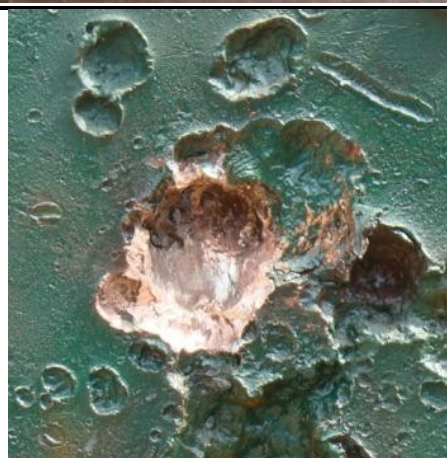
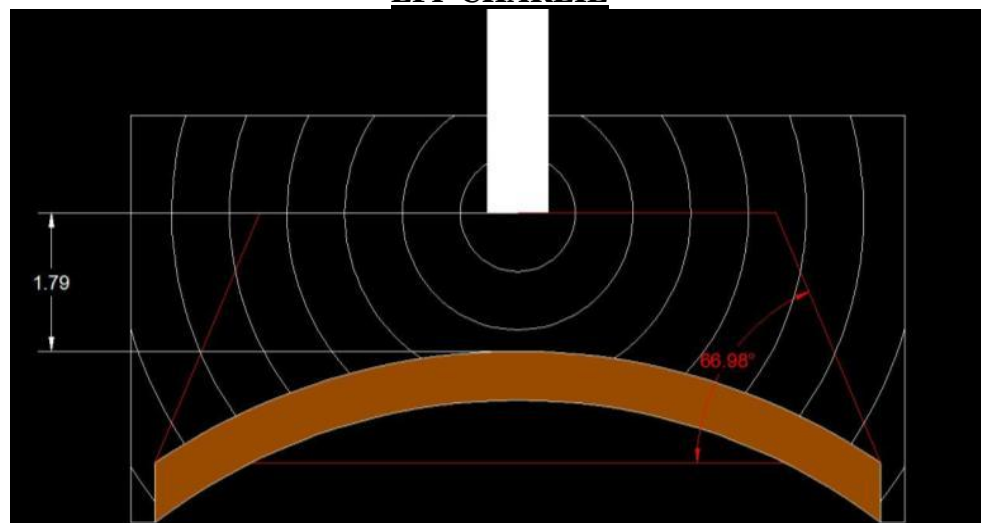
**EFP ALPHA**

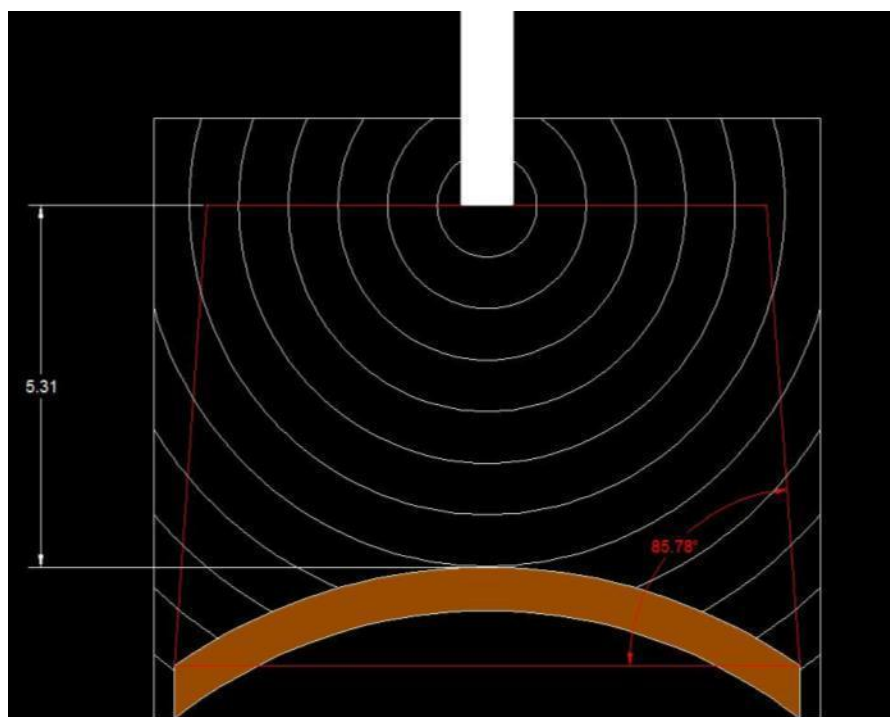


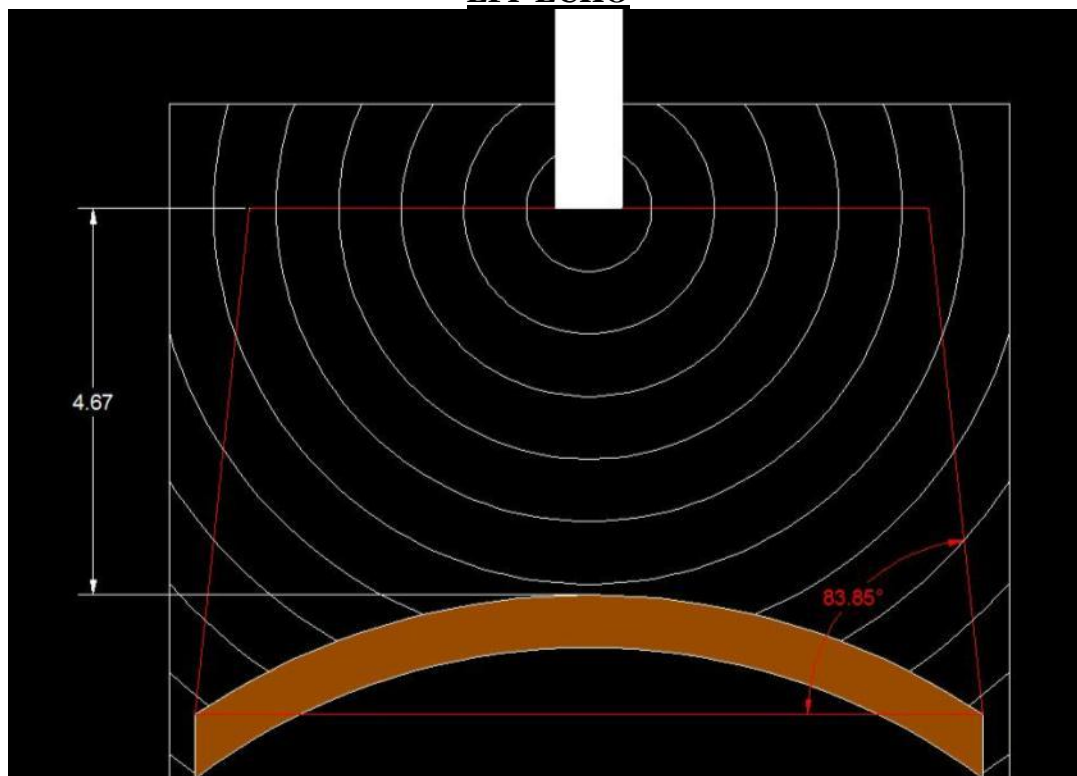
**EFP BRAVO**

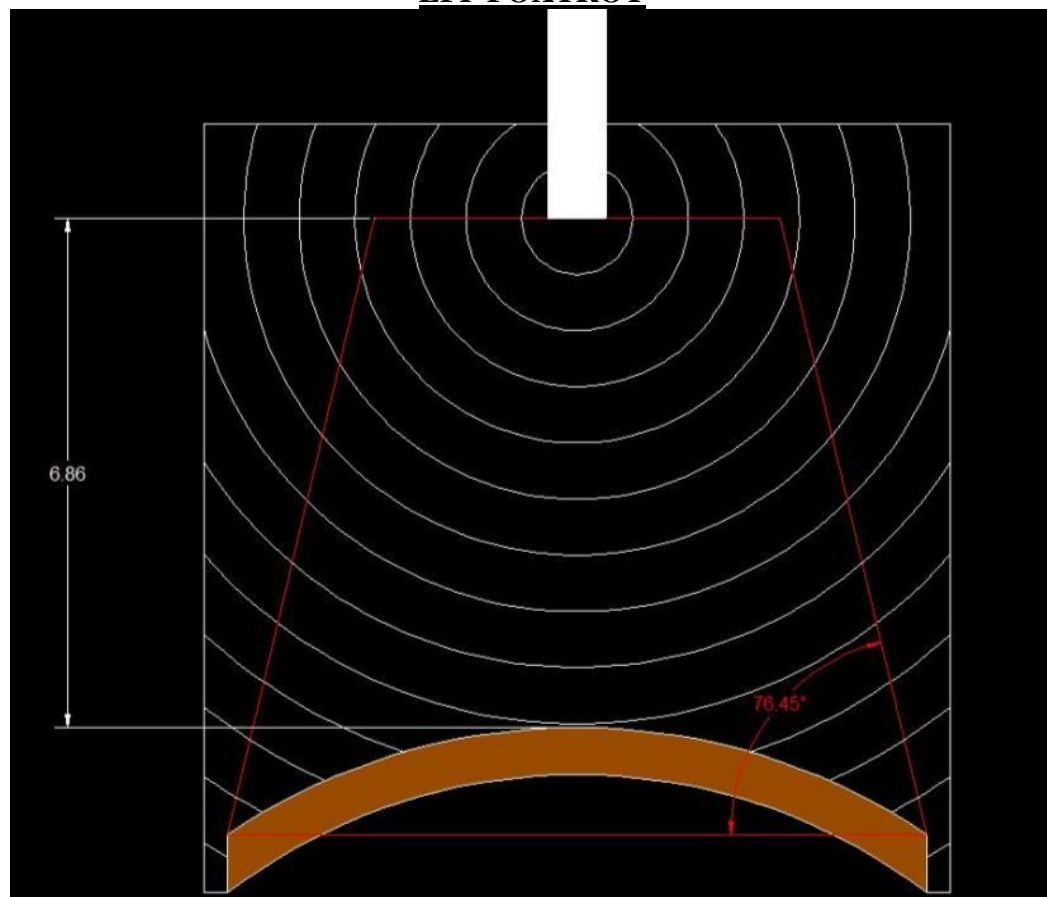




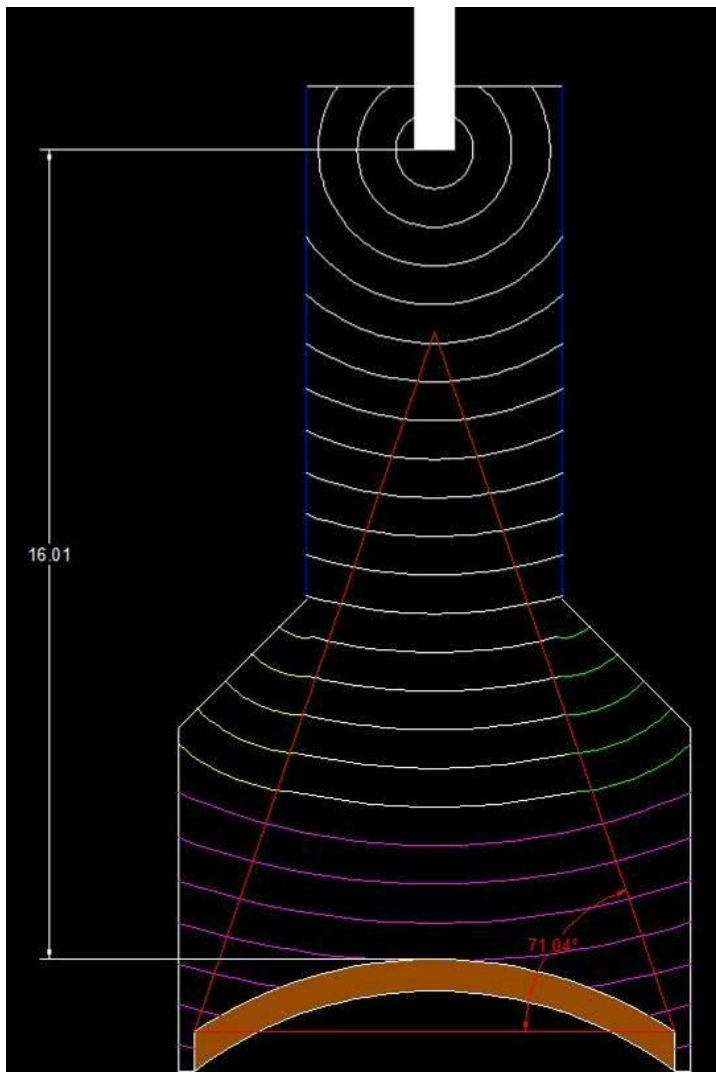
**EFP CHARLIE**

**EFP DELTA**

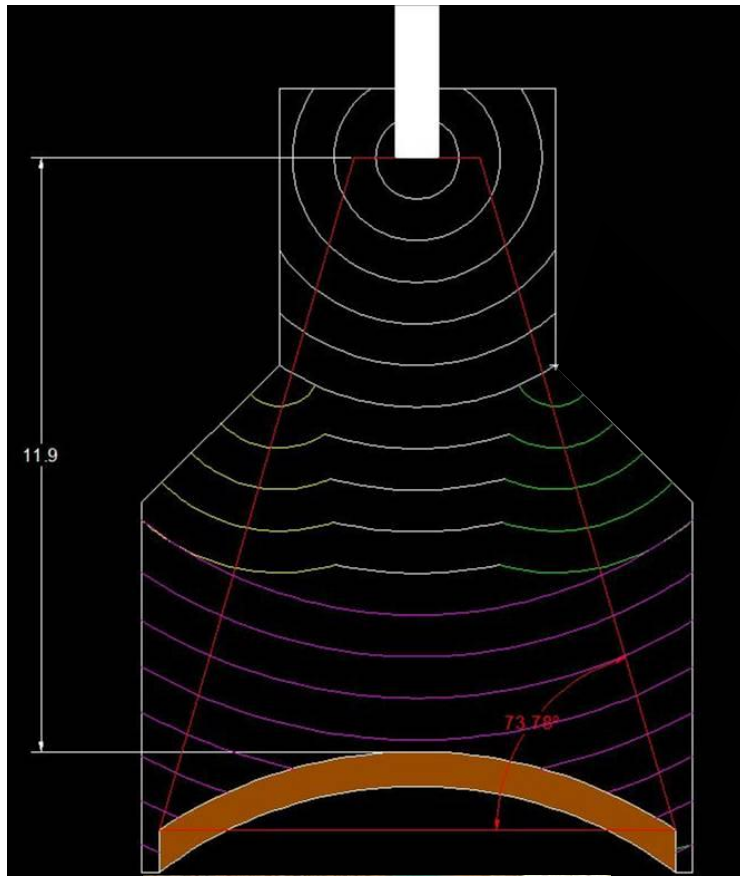
**EFP ECHO**

**EFP FOXTROT**

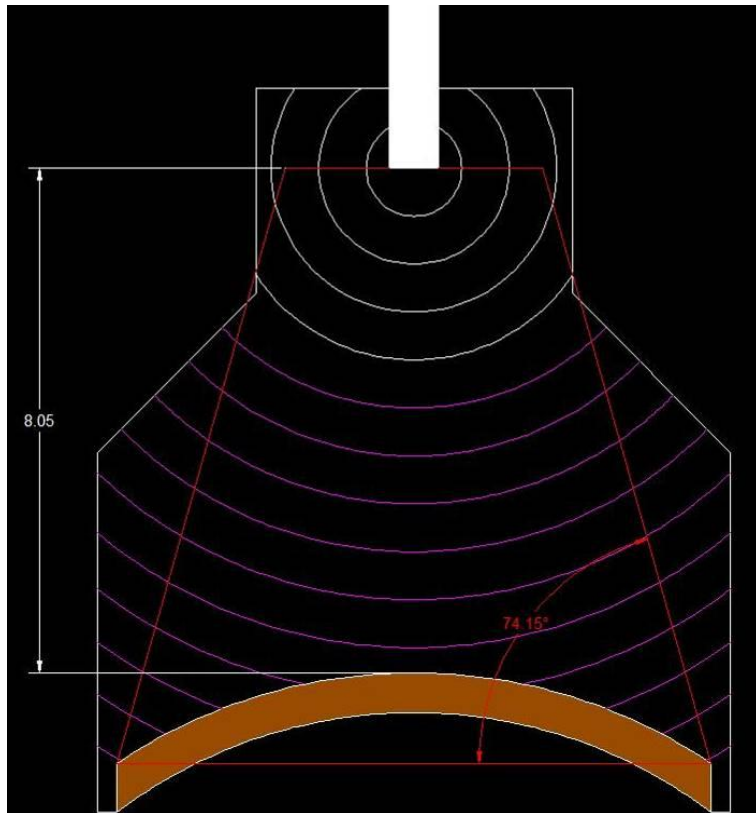
**EFP GOLF**



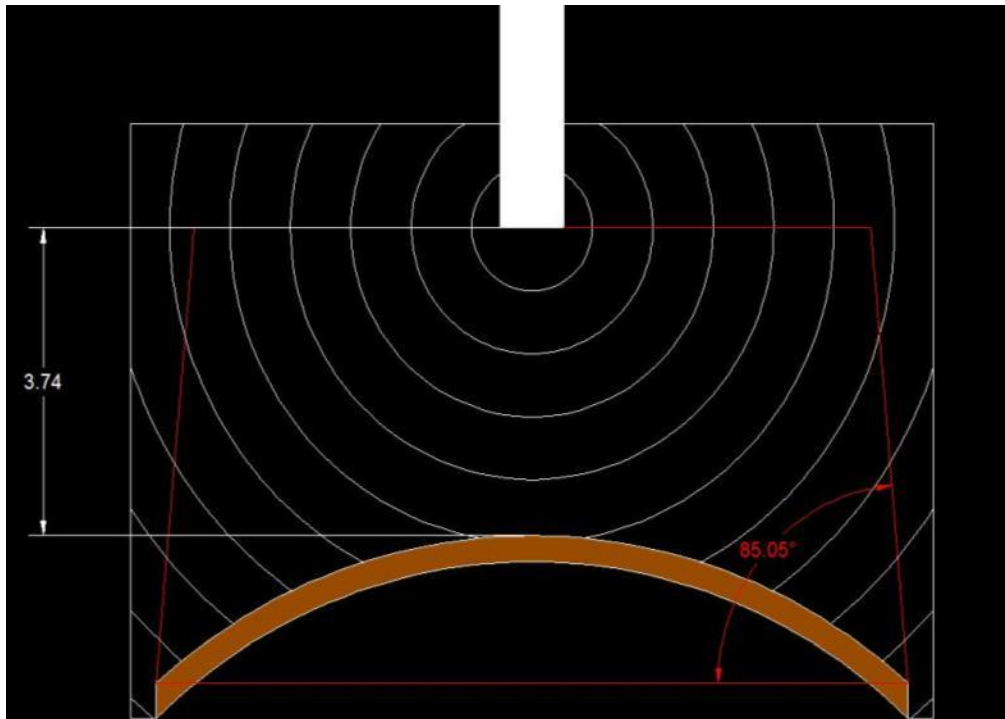
**EFP HOTEL**



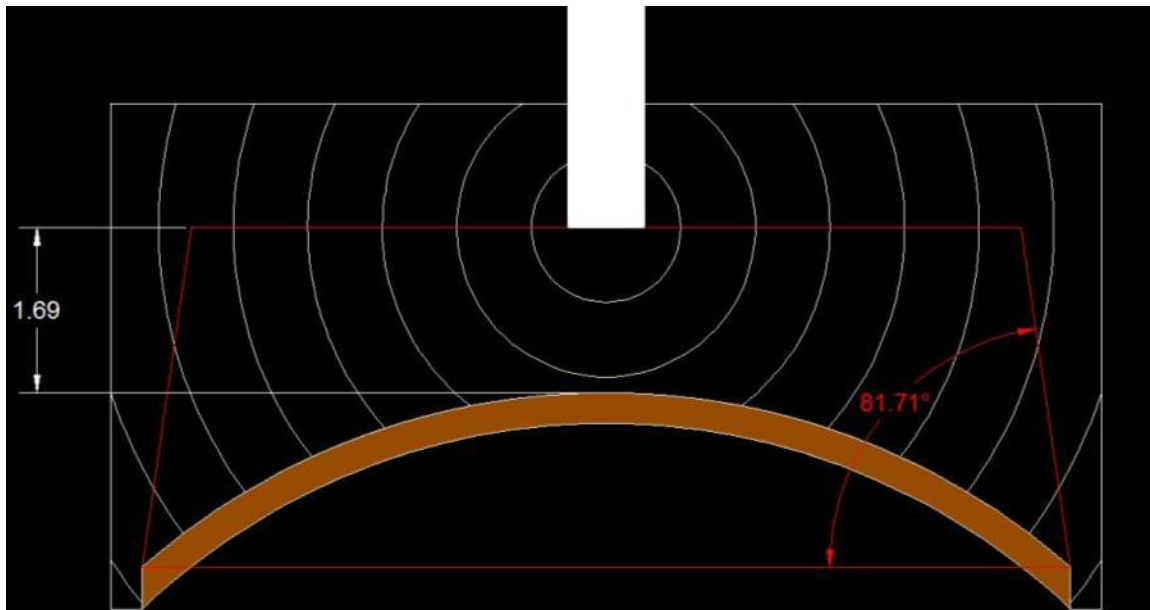
EFP INDIA



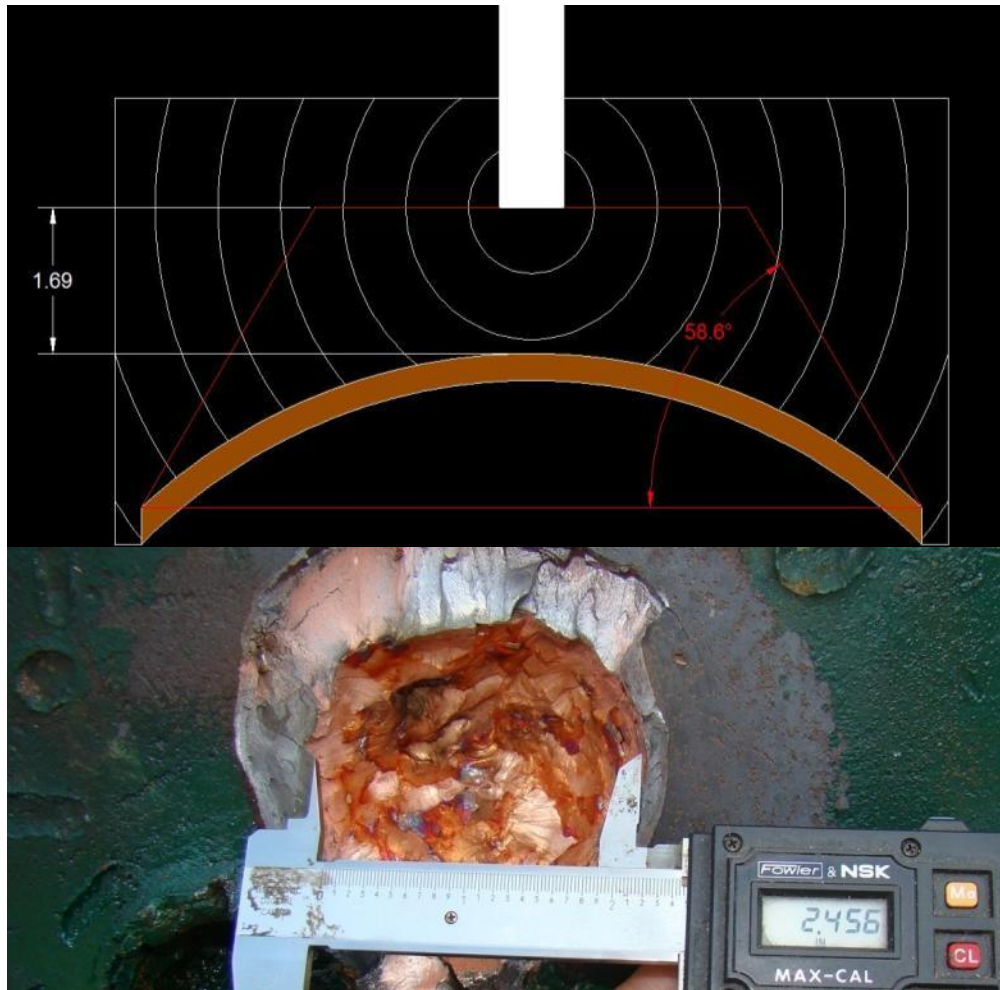
**EFP JULIET**



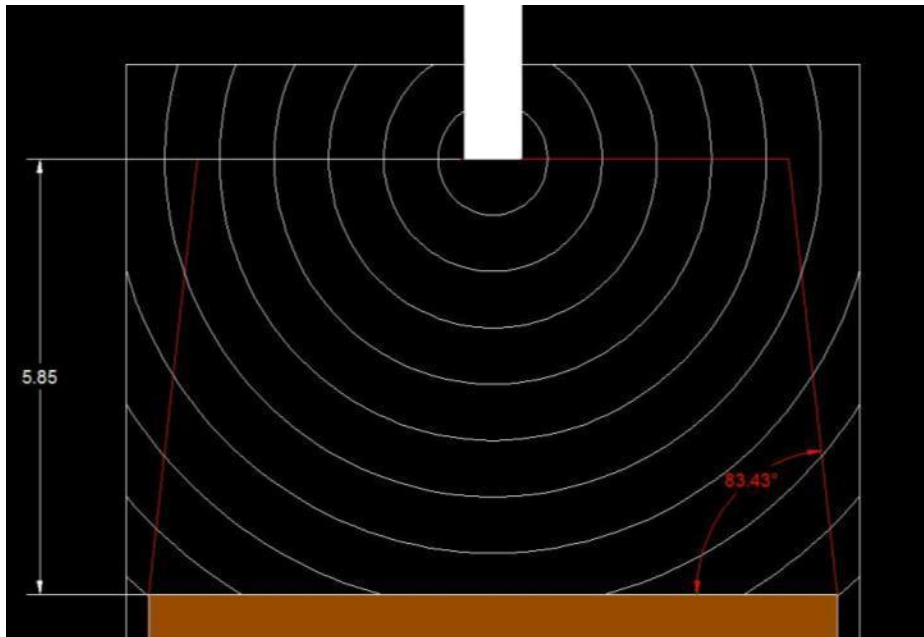


EFP KILO

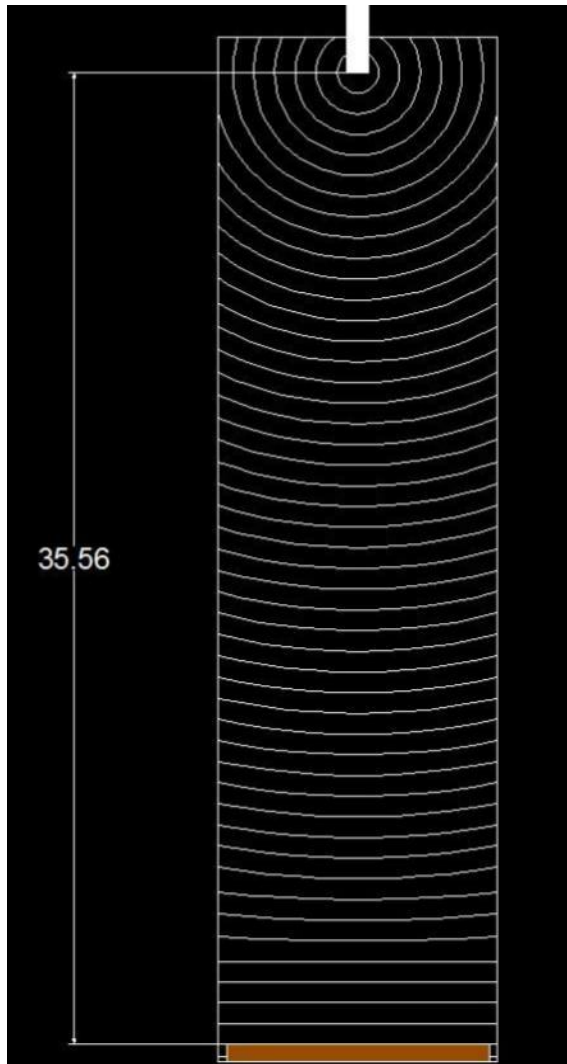
**EFP LIMA**

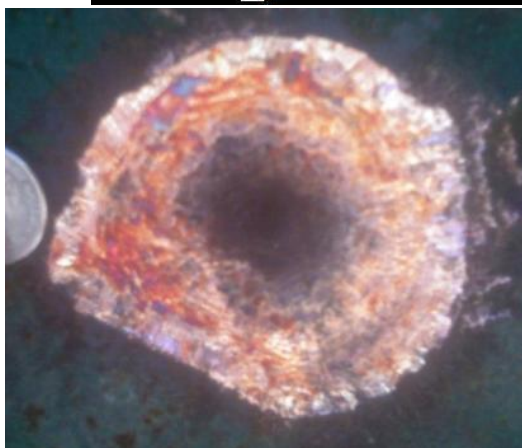
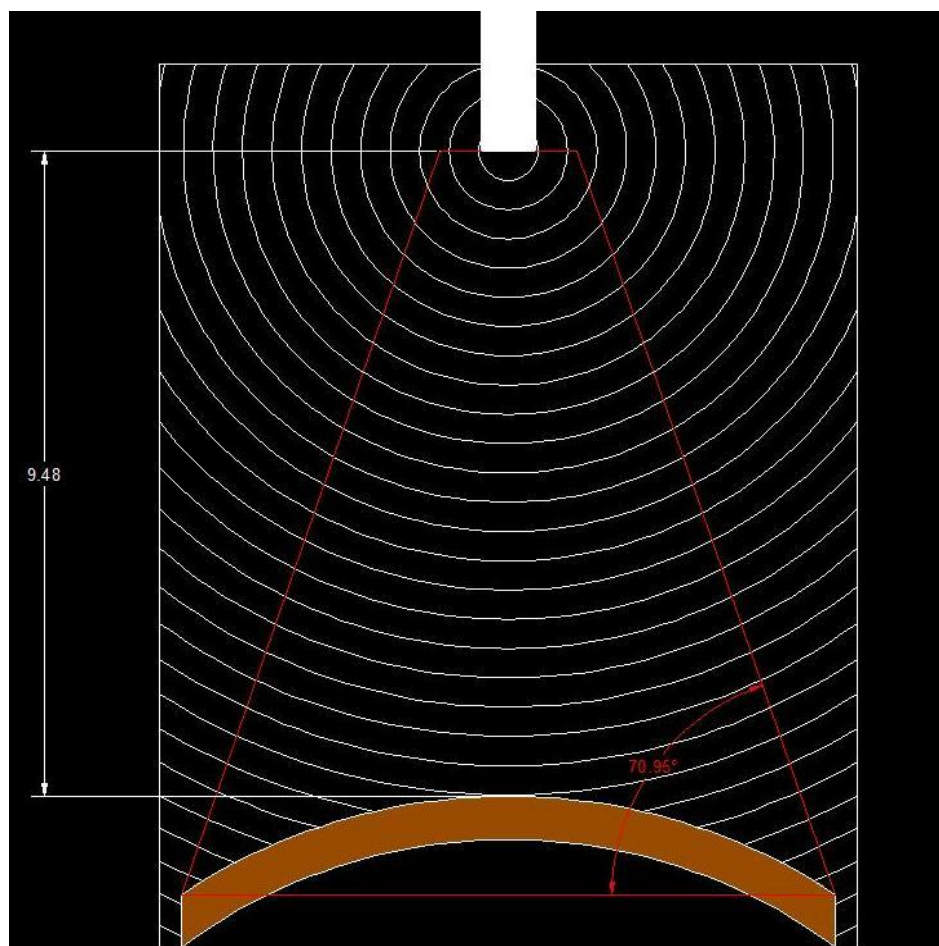


**EFP MIKE**

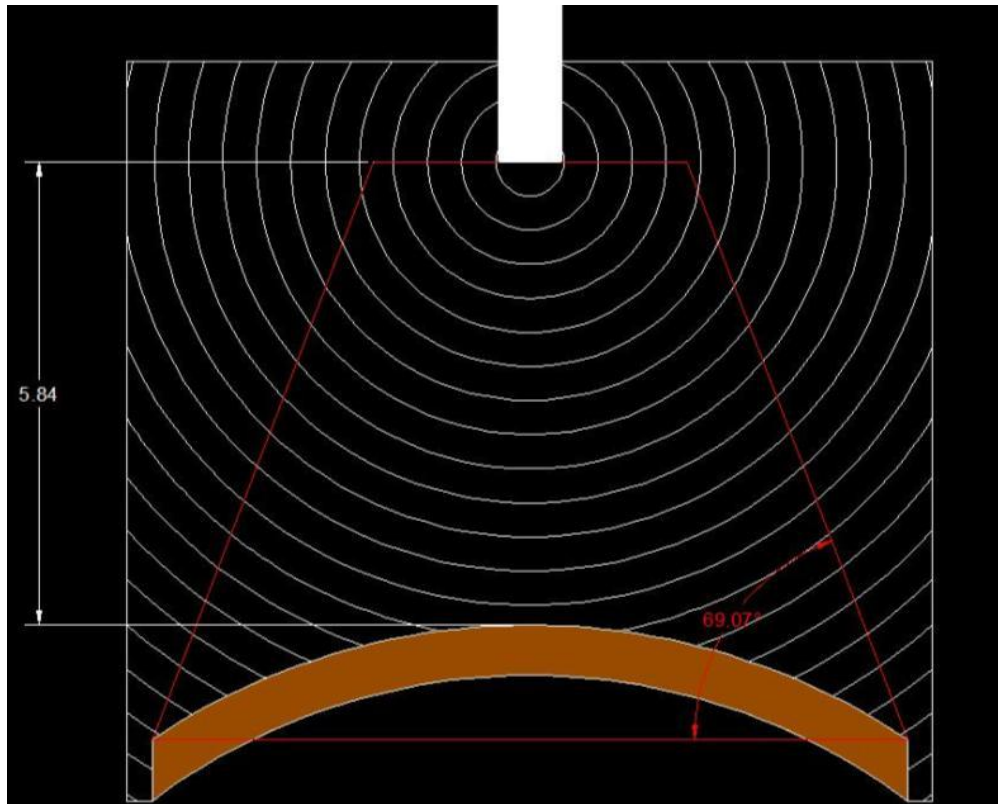


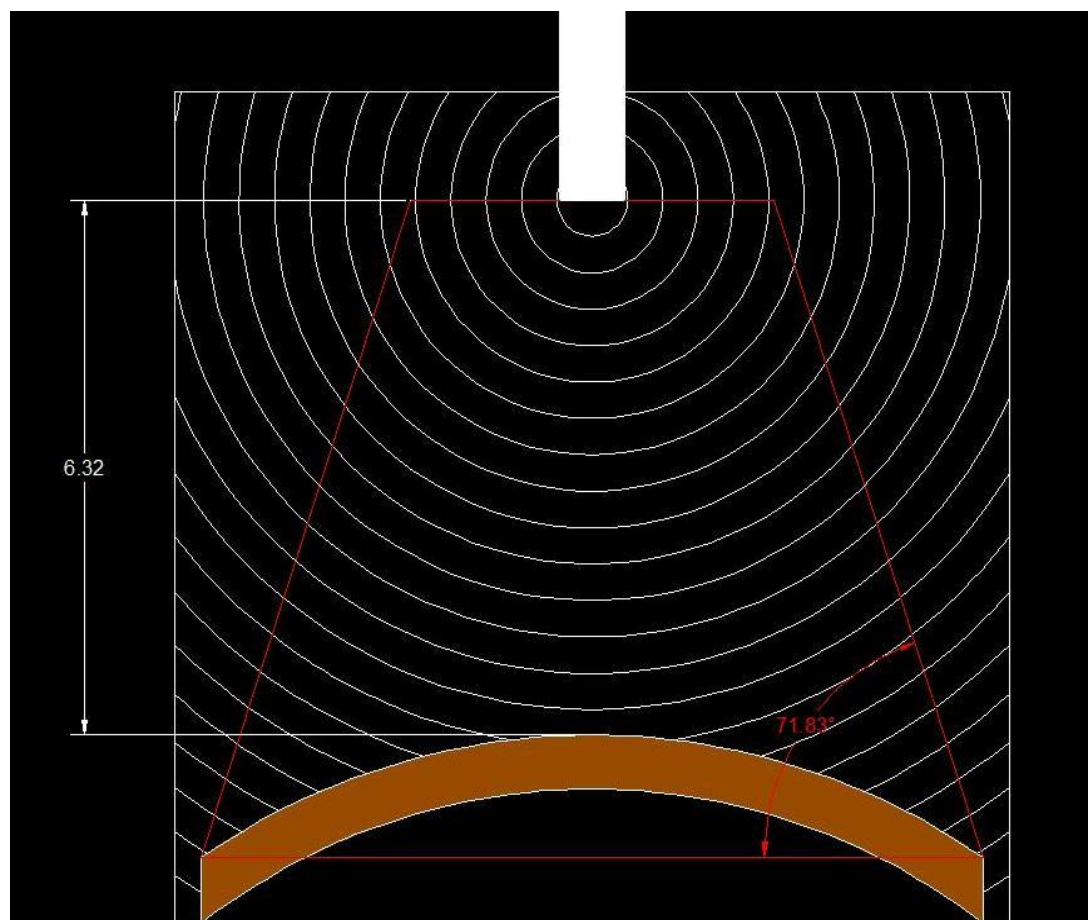
EFP NOVEMBER



EFP OSCAR

**EFP PAPA**



**EFP QUEBEC**

## BIBLIOGRAPHY

**2010.** Analyze Math. *Analyze Math*. [Online] Abdelkader Dendane, October 8, 2010. [http://www.analyzemath.com/Geometry\\_calculators/surface\\_volume\\_frustum.html](http://www.analyzemath.com/Geometry_calculators/surface_volume_frustum.html).

**B. M. Dobratz, P. C. Crawford. 1985.** *LLNL Explosives Handbook - Properties of Chemical Explosives and Explosive Simulants*. Livermore : U.S. Department of Commerce, 1985.

**Baird, Dr. Jason. 2009.** Detonation wave expansion through pipe reducer. 2009.

—, **2008.** EFP Research. 2008.

—, **2008.** Misznay-Shardin device. Rolla, Missouri : s.n., June 2008.

—, **2009.** Shock velocity. 2009.

—, **2008.** *Spalling*. 2008.

**C. Lam, T. Liersch and D. McQueen. 1997.** An Investigation into an Alternative Fragment Projector for Insensitive Munitions Qualifications. 1997.

**C. Lam; D. McQueen. 1998.** Study of the Penetration of Water by an Explosively Formed Projectile. s.l. : DSTO Aeronautical and Maritime Research Laboratory, 1998.

**Chris A. Weickert. 1998.** Explosively Formed Projectiles. [book auth.] Jonas A. Zukas and William P. Walters. *Explosive Effects and Applications*. s.l. : Springer, 1998, pp. 386-391.

**Cook, Melvin A. 1958.** *The Science of High Explosives*. s.l. : Robert E. Krieger Publishing CO. INC., 1958.

**Cooper, Paul W. 1996.** *Explosives Engineering*. s.l. : Wiley-VCH, 1996. p. 387. *Deformation of An Explosively Driven Flat Metallic Flyer During Projection*. **Lim, Seokbin. 2010.** 2010. International Society of Explosives Engineers. pp. 1-8.

**Dictionary.com. 2009.** Energy Density Definition. *Definition of Energy density at Dictionary.com*. [Online] Dictionary.com Unabridged. Random House, Inc., October 05, 2009. <http://dictionary.reference.com/browse/Energy+Density>.

**Dr. James N. Willson; Dr. David E. Lambert, and Mr. Joel B. Stewart. 2006.** *Explosively Formed Projectiles*. s.l. : Air Force Research Lab Munitions Directorate; Assessment and Demonstration Division; Computational Mechanics Branch, Eglin AFB FL, 2006.



**Eugene S Hertel, Jr. 1992.** A Comparison of the CTH Hydrodynamics Code with Experimental Data. September 1992.

*Experimental and numerical study on the flight and penetration properties of explosively-formed projectile.* **Wu, Jun. 2007.** 2007, International Journal of Impact Engineering, pp. 1147-1162.

**Fong, Richard. 2004.** *Advanced Warhead Technologies.* 2004.

**Gerber, SFC Jason T. 2009.** *Commonly seen EFPs by EOD specialist.* 2009.

**Giltner, Scott. 2009.** *Energy Equivalency of Unigel.* 2009.

**Henry S. McDevitt, Jr. 1997.** *Explosively Formed Penetrator Research.* Ft. Leonard Wood, MO : s.n., 1997.

*IED effects research at TNO Defence Security and Safety.* **Voort, Martijn van der. 2009.** 2009. 13th International Symposium of the Interaction of the Effects of Munitions with Structures. pp. 1-18.

**Nobel, Dyno.** Unigel Technical Information. *Dyno Nobel.* [Online] Dyno Nobel. <http://www.dynonobel.com/files/2010/04/Unigel.pdf>.

**Plunket, Dr. Jerry. 2009.** *Projectile Penetration.* 2009.

*Research and Development in the Area of Explosively Formed Projectiles Charge Technology.* **Weimann, Klaus. 1993.** 1993, Propellants, Explosives, Pyrotechnics, pp. 294-298.

**Rudolf Meyer, Josef Kohler, Axel Homburg. 2007.** *Explosives.* Weinheim : WILEY\_VCH Verlag GmbH & Co. KGaA, 2007.

**W. P. Walters, J. A. Zukas. 1989.** *Fundamentals of Shaped Charges.* 1989.

**Worsey, Dr. Paul. 2009.** *EFP research at Missouri University of Science and Technology.* Rolla, June 2009.

—. **2011.** *Shock of Unigel.* 2011.

—. **2008.** *Testing limits at Missouri S&T.* 2008.

## VITA

Phillip Russell Mulligan was born in Olin, IA. He attended elementary school in the Olin Consolidated School District in Olin, IA and graduated from Olin High School in June 2003. Phillip entered the University of Missouri, Rolla in August 2003. He received a degree of Bachelor of Science in Mining Engineering, with a minor in Explosives Engineering and Business, in June 2008. Phillip entered Missouri University of Science and Technology in June 2008 and is a candidate for the Masters Degree in Explosives Engineering, May 2011.

